ANL-7793

Argonne National Laboratory

INSTRUMENTATION SYSTEMS TO PROTECT LMFBR CORE INTEGRITY

by

W. C. Lipinski, C. E. Cohn, D. R. MacFarlane,
T. P. Mulcahey, D. Okrent, K. G. Porges,
W. C. Redman, J. B. van Erp, and R. H. Vonderohe

Printed in the United States of America
Available from
National Technical Information Service
U.S. Department of Commerce
5285 Port Royal Road
Springfield, Virginia 22151
Price: Printed Copy $3.00; Microfiche $0.95

ANL-7793
Reactor Technology

ARGONNE NATIONAL LABORATORY
9700 South Cass Avenue
Argonne, Illinois 60439

INSTRUMENTATION SYSTEMS TO PROTECT LMFBR CORE INTEGRITY

by

W. C. Lipinski, Reactor Analysis and Safety Division
C. E. Cohn, Applied Physics Division
D. R. MacFarlane, Reactor Analysis and Safety Division
T. P. Mulcahey, Engineering and Technology Division
D. Okrent, Office of the Director
K. G. Porges, Applied Physics Division
W. C. Redman, Applied Physics Division
J. B. van Erp, Reactor Analysis and Safety Division
R. H. Vonderohe, Applied Mathematics Division

March 1971

PREFACE

(by W. C. Redman)

During FY 1970 a small interdivisional and interdisciplinary group undertook a review and evaluation of the status of instrumentation systems intended to protect the cores of future liquid metal cooled fast breeder reactors. This study was one of several which considered various aspects of LMFBR core design. In addition to providing an independent assessment of the existing status of instrumentation systems for core protection, as an aid in evaluating the related portions of proposed LMFBR demonstration plants and 1000 MW(e) designs, attention was directed to how such systems might be improved, through extension of current technology in the areas of detectors, circuitry and information processing. The latter was considered necessary to insure that future developmental activities related to LMFBR instrumentation were optimized in terms of achieving the ultimate goal of reliable and economic fast reactor safety.

The primary goal of the study was to determine the potential for protecting LMFBR core integrity by appropriate instrumentation. The significant aspects of this problem were considered to be the following:

1. Accessibility for instrumentation with proposed primary system designs; other design concepts to improve instrumentation access.
2. Degree of core protection provided by available types of instrumentation.
3. The increase in protection which would be afforded by other types of instrumentation, if they could be developed and utilized.
4. The conflict between the need for fast, dependable scram and the adverse effects of spurious scrams, and the need for an analytical and experimental assessment of scram reliability.
5. The potential for more reliable (and/or different) bases for scram via rapid, on-line information analysis using multiple signals.
6. The relation between instrument capability, potential effects from fuel failure propagation, core resistance to deformations, and safety rod scram capability.

7. The conflict between the objective of fast reliable scram and good LMFBR economics; between fast reliable scram and mechanical access and space capabilities; and between redundant, diverse instrumentation and good LMFBR economics.

8. Redundancy requirements needed to achieve specified reliability.

9. Coincidence requirements needed to achieve specified reliability with periodic testing.

10. Modes of degraded performance.

11. Effect of long-term environmental factors on reliability and maintainability.

A study group, composed of the authors of this report, investigated the above problem areas, in a series of approximately twenty-five discussion meetings. The areas of specialization of the members of this group included detectors, circuitry, instrumentation systems, data processing, reactor kinetics and reactor accident analysis. The group's capabilities were augmented as required by participation of other staff members in specific discussions. Such contributors included Ira Charak (EBR-II), Raymond Goertz (deceased), Barton M. Hoglund (CES), Kenneth A. Hub (PRO), David H. Lennox (PRO), Donald E. Lutz (ETD), Thomas J. Marciniak (RAS), David A. Shaftman (AP) and Jack H. Tessier (RAS).

This report was prepared to provide a record of the significant information assembled and developed in and for these meetings. While a consensus existed on most of the major opinions and conclusions, the principal authors for each section have been identified in the Table of Contents in order to avoid an implication of complete unanimity among the participants. The chairman of the study group, W. C. Lipinski, served as editor for this report, with assistance from W. C. Redman.

TABLE OF CONTENTS

TABLE OF CONTENTS

TABLE OF CONTENTS

LIST OF FIGURES

LIST OF FIGURES

LIST OF FIGURES

LIST OF TABLES

INSTRUMENTATION SYSTEMS TO PROTECT LMFBR CORE INTEGRITY

by

W. C. Lipinski, C. E. Cohn, D. R. MacFarlane,
T. P. Mulcahey, D. Okrent, K. G. Porges,
W. C. Redman, J. B. van Erp, and R. H. Vonderohe

ABSTRACT

This report assesses the role of instrumentation systems in providing protection for cores of future liquid-metal-cooled fast breeder reactors. The existing status of instrumentation systems for core protection is reviewed and consideration given to how such systems might be improved, through extension of current technology in the areas of detectors, circuitry, and information processing. Credible types of accidents and malfunctions are considered, in order to establish the time scale required for instrument system response and action. Emphasis is given to the effectiveness of various types of detection systems in providing protection against localized abnormalities. An indication is given of the direction for future developmental activities in order to satisfy the dual requirements of reliability and economy in systems intended to insure fast-reactor safety.

I. INTRODUCTION

(by D. Okrent)

The high power density, the difficulty of detecting local anomalies, the difficulty of access for permanent instrumentation in or near the core, and the knowledge that fuel elements have melted in many reactors (including two fast reactors, Fermi and EBR-I) have lead to a general concensus that local fuel-element melting on a subassembly scale is an accident with a finite probability of occurrence.

Maintaining the integrity of fuel subassemblies and the capability to insert safety rods is one of the essential requirements for safe operation of sodium-cooled fast breeder power reactors (LMFBRs). Questions of possible reactivity insertion from either the voiding of core sodium or the reassembly of fissile material into a more dense configuration, as well as questions of capability of removal of decay heat from a core whose geometry has been appreciably disrupted, make it very important that gross failure or melting of several or most of the fuel pins in a subassembly not lead to damage to neighboring subassemblies or fail to be detected and timely protective action taken.

The potential propagation and possible effects of fuel failure have been the subject of several studies;[1-4] however, the definition of specific initiating events is difficult and complex phenomena are involved. Also, only limited experimental information is available. Among the more difficult questions to resolve are the probable sources, magnitudes and timing of strong local pressure pulses, and the ability of highly irradiated subassembly structural wrappers (or casings or cans) to absorb significant energy without failure. Sodium-bubble collapse, rapid boiling of reentrant sodium on very hot surfaces, or a very rapid heat exchange between sodium and molten fuel are potential pressure-pulse mechanisms receiving particular consideration.

The first large fuel-coolant interaction pressures were directly observed in the destructive reactivity excursion in the water-cooled SPERT ID core.[5] A pressure peak of about 3000 lb/in^2 was observed as a second pulse in this experiment and is attributed to coolant reentry and mixing with hot fuel. Similar pressures were later generated in the laboratory by rapidly mixing molten fuel and water.[6]

Large pressures did not occur during the EBR-I core meltdown[7] or the Fermi incident.[8] However, a pulse of several hundred pounds per square inch in a TREAT experiment is attributed to the intimate mixing of metallic fuel and sodium,[9] and much higher pressures have since been obtained during in-pile and out-of-pile experiments involving molten oxide and sodium.[10-14] These experiments have exhibited a rather low conversion efficiency of thermal energy to mechanical work; however, more work is required to be definitive about this important matter.

The potentially important role of instrumentation and information processing in detecting local core anomalies in LMFBRs has been examined by various groups.[15-20] Table 1[21] illustrates the diverse thinking of various design groups as presented at the 1968 Argonne Conference on Large Fast Reactor Design[18] and in concurrent papers.

Thinking has continued to evolve with regard to the appropriate instrumentation to protect core integrity against local anomalies. Particularly interesting studies have been reported by General Electric,[19-20] in which complete or partial flow blockage of a subassembly has been assumed and the course of events estimated assuming a lack of protection-system action, but nevertheless providing the probable times when sensors of diverse character, if available, might have been able to detect the event and initiate protective action. Flowmeters, thermocouples, pressure sensors, fuel-failure detectors, boiling detectors, and reactimeters each respond to a particular impetus. Each might provide some basis for protective action at a different specific time during the course of one particular postulated accident, but exhibit a different relative effectiveness for another set of anomalous conditions.

This report will examine the potential role to be played by instrumentation systems of various kinds with particular attention to sensing the local (or subassembly scale) accident, primarily by the use of illustrative transients and an examination of considerations of failure thresholds, stored heat, and the times required to generate significant molten fuel. The study of transients will be followed by a discussion of the status of various sensors, existing and potential, including considerations of reliability, accessibility, and potential failure modes of the sensors. The application of digital computers to protection of LMFBR core integrity will then be examined, and finally a comparative discussion of possible conclusions with regard to the choice of core instrumentation systems will be presented.

TABLE 1. Comparison of Some Safety Features for Eight Reactor Designs

	PFR	Phenix	SNR	AI	B and W	CE	GE	Westinghouse
Reactor power, MW(th)	600	~550	730	2400	2450	2500	2400	2600
Core								
Shape: H/D	Cyl.: 0.68	Cyl.: 0.61	Cyl.: 0.63	Cyl.: 0.51	Cyl.: 0.29	Cyl.: 0.2	Cyl.: 0.3	Modular: [a] 0.84 each of four modules
Fuel element	$(Pu,U)O_2$ in SS	$(Pu,U)O_2$ in SS	$(Pu,U)O_2$ in SS	$(Pu,U)O_2$ in SS	$(Pu,U)O_2$ in SS; vented to coolant	Na-bonded (Pu,U)C in SS; vented	$(Pu,U)O_2$ in SS; vented to coolant	Na-bonded (Pu,U)C in SS; vented to coolant
Added moderator?	No	No	No	No	No	Yes	No	No
Safety criteria on subassembly can wall	Capable of containing static pressure of 1500 lb/in^2	No	Integrity after sodium expulsion or recondensation pressure pulse	Can thickness adequate to prevent failure propagation	Can thickness adequate to prevent failure propagation	Can thickness adequate to prevent failure propagation	No	No can wall (or perforated can)
Core clamp	No	?	Yes	Yes	No(there is support top and bottom)	Yes	No (Hydraulically clamped by non-free-standing channels which expand against each other during operation)[b]	No (Relative thermal expansion at top of core is employed)

Table 1. (Continued)

	PFR	Phenix	SNR	AI	B and W	CE	GE	Westinghouse
Primary system System type	Pool	Pool	Loop	Loop	Pool	Loop	Pool	Loop
If loop, measures to deal with primary system leak	Not applicable	Not applicable	Double wall throughout	Double-wall vessel; elevated primary system	Not applicable	Independent secondary boundary in critical portions; siphon breakers	Not applicable	Siphon breaker; double-walled auxiliary cooling system
Reliance on double-(RH) wall vessel to keep core covered	Yes	Yes	Yes	Yes	Yes	Yes	Yes	Yes
Independent safety-(RH) rod systems	Two sets of rods provided. Also separate central rod	Yes	Yes	Yes	Multiple independent rod groupings	Yes	Yes	Yes
Diversity in safety-(RH) rod systems	Yes	?	Yes	No	No	Preferably	Yes	No
Worth of safety rod ($)	∿1	3.8	6	∿2.8	<1	∿1.1	<1.2	0.8
Worth of control rod ($)	∿2.5	-	1 1/2	∿1.4	<1	∿0.6	<1	0.2

Table 1. (Continued)

	PFR	Phenix	SNR	AI	B and W	CE	GE	Westinghouse
Instrumentation to protect core integrity[c]								
Thermocouple(s) in each core subassembly exit	Yes	Yes	Yes	Yes	Yes	Yes	Almost all	Not applicable
Reactimeter	Possibly	Yes	Yes	No	Yes	Yes	Yes	No
Delayed-neutron detector	Yes	Yes	Yes	Yes	Yes	Yes	Possibly	No
Boiling detector	Possibly	Not mentioned	Intended	No	No	No	Possibly	No
Subassembly flow	No	No	Intended	No	In eight selected subassemblies	No	Yes	Not applicable

Table 1. (Continued)

	PFR	Phenix	SNR	AI	B and W	CE	GE	Westinghouse
Containment and engineered safety features								
Double Containment	Yes	Yes	Yes	Yes	Yes (only outer containment is effective barrier to fission products)	Yes	No	?[d]
Primary containment to withstand blast	Yes	Yes	Yes	Yes	Yes	Yes	No	?[d]
If yes, how set criteria	Bethe-Tait calculation for unspecified ramp reactivity insertion	?	To handle thermal energy release of 2400 MW-sec, involving 60$/sec ramp at power	Loss-of-coolant flow without scram leading to sodium voiding and 2200 MW-sec of available work	60$/sec ramp leading to thermal energy generation of 15 000 MW-sec	100 MW-sec available work, based on on Bethe-tait analysis of core collapse	None	?[d]
Special features of blast protection	Designed on normal requirements. Blast resistance checked by model tests	Rotating plugs bolted down	Perforated immersed plate below top shield to suppress water hammer	Inerted strong dome over over plug; missile barrier for for control-rod drives and energy-absorbing hold-down for plugs.	Cover structure and plugs are held down	Conventional	None	?[d]

Table 1. (Continued)

	PFR	Phenix	SNR	AI	B and W	CE	GE	Westinghouse
How accomplish shutdown heat removal on loss of offsite power	Natural convection possible	Emergency power; possibly natural convection	Natural convection possible; emergency power	Natural convection	Diesel-powered pumps	Backup emergency cooling loop on emergency power natural convection	Diesel-powered pumps	Auxiliary coolant loop on diesel power
How accomplish shutdown heat removal from disrupted core	Specially cooled receptacle below core support plate but within reactor tank	Cooling coils outside reactor tank	Cooling of containment wall	Cavity liner cooling system	In the event of failure of the heat-exchange equipment in the pool, heat is removed through coils in the biological shield	Not established.	None	Normal and/or auxiliary coolant loops
Pressure criteria for secondary containment	20 in.w.g.	Low pressure	Sodium fire	Designed for 10 lb/in^{2}g; maximum acc. pressure of 2 lb/in^2 g.	Pool of burning sodium on top plug/or small plug out; 10/in^2 and 200°F	Unspecified sodium fire	None	?[d]

Table 1. (Continued)

	PFR	Phenix	SNR	AI	B and W	CE	GE	Westinghouse
Secondary containment inerted	No	No	No	No	No	No	No	No
Primary system containment inerted	Yes	Yes	Yes	Yes	Yes	Yes	Yes	Yes

[a] The Westinghouse presentation (Kelly 1968) at the Argonne Conference identified a cylindrical core as their alternate reference concept. Kelly at the AIF panel discussion (AIF-ANS Int. Conf. Constructive Uses of Atomic Energy, Washington D. C., November 10-14, 1968) stated that a cylindrical core would be used in the first Westinghouse "demonstration" reactor.

[b] Described in GEAP 5710.[20]

[c] In addition to full core flux and bulk coolant flow and temperature.

[d] Westinghouse has stated that "The credibility of a nuclear explosion in the Westinghouse 1000 MW(e) LMFBR has not been established. Additional work is being performed in this area, along with considerations of possible sodium fires, or other situations, which may require containment."

II. ANALYSES OF ACCIDENTS AND MALFUNCTIONS

(by D. R. MacFarlane and J. B. van Erp)

A. Scope of Study

The aim of the present chapter is not so much to give detailed analyses of the various accidents and malfunctions that can be postulated,* but rather to give a semiquantitative description of the chain of events and the accompanying phenomena (including the time scale). An attempt is made to determine the performance characteristics of the various sensors and measuring systems, to obtain an insight into the relative merits of the various possible instrument systems for preventing or minimizing core damage.

To achieve the above objective it was necessary to carry out some numerical evaluations.† As input for these studies, data were used pertaining to what was considered a typical present-day LMFBR design, having a core geometry of the "unspoiled" type, i.e., having been optimized for performance instead of for sodium-void coefficient of reactivity for the core region.

Some of the most important data regarding the LMFBR design on which the study is based are given in Table 2. It is believed, however, that the results of this study are not only applicable to the particular design for which they were obtained, but also have a general validity for present-day LMFBR designs.

Many relatively small accidents can, with sufficiently conservative assumptions, escalate into a major accident if corrective action

---

* In order to be able to perform such detailed analyses, one would need to have available a detailed core and plant design.

† Most of the numerical evaluations were performed by means of the SAS-1A Code[22] developed at Argonne National Laboratory and available through the Argonne Computer Code Center.

is not assumed to be forthcoming at some point of the chain of events. Design-basis accidents are not the concern of this report, so that the chain of events, for the accidents considered, is not pursued very much beyond the point where the slowest set of sensors was assumed inoperative.

Table 2. Parameters of Typical Oxide-fueled LMFBR Core*

a) General Parameters:

Height of Core Region	80 cm
Height of Axial Blankets (each)	40 cm
Height of Fission Gas Plenum	55 cm
Outer Diameter of Fuel Pellet	5.64 mm
Inner Diameter of Clad	5.86 mm
Outer Diameter of Clad	6.36 mm
Delayed-neutron Fraction, β	2.964×10^{-3}
Prompt-neutron Generation Time	4.728×10^{-7} sec
Doppler Coefficient $T \cdot \frac{dk}{dT}$ (no coolant voiding) (T in °C)	-6.7×10^{-3}
Doppler Coefficient $T \cdot \frac{dk}{dT}$ (coolant fully voided) (T in °C)	-4.1×10^{-3}
Subassembly Outlet Plenum Pressure	1.5 atm
Volume Fraction of Coolant	0.38
Number of Fuel Pins per Subassembly	265
Number of Subassemblies	265

* The data presented in Table 2 are predominantly those (apart from minor differences), pertaining to the 1000-MWe LMFBR Follow-On Study (Advanced Design), performed by the General Electric Co. for Argonne National Laboratory under AEC Contract No. 31-109-38-1997, and reported in Refs. 20, 23-25.

Table 2. (cont'd.)

Sodium-void Reactivity Effect

	Axial Nodes Number*	$\frac{\delta k}{k}$
Lower Blanket	1	-1.140×10^{-4}
	2	-2.401×10^{-4}
	3	-5.536×10^{-4}
	4	-5.064×10^{-4}
Core	5	2.760×10^{-4}
	6	1.108×10^{-3}
	7	1.783×10^{-3}
	8	2.157×10^{-3}
	9	2.157×10^{-3}
	10	1.783×10^{-3}
	11	1.108×10^{-3}
	12	2.760×10^{-4}
Upper Blanket	13	-5.064×10^{-4}
	14	-5.536×10^{-4}
	15	-2.401×10^{-4}
	16	-1.140×10^{-4}

* The axial nodes are numbered from inlet to outlet. Each axial node has a height of 10 cm, and is assumed to be voided completely over the entire cross section of the core and blankets.

Table 2. (cont'd.)

b) Hot-channel Parameters:

Temperature of Inlet Coolant to Lower Axial Blanket	432.0°C
Temperature of Inlet Coolant to Core	443.5°C
Temperature of Outlet Coolant from Core	603.7°C
Temperature of Outlet Coolant from Upper Axial Blanket	616.9°C
Mass Flow Rate of Coolant	8.92×10^{2} g cm^{-2} s^{-1}
Coolant Velocity (average)	10.7 m s^{-1}
Peak Linear Heat Rating	0.52 kW cm^{-1} (= 15.85 kW ft^{-1})
Peak Fuel Centerline Temperature	2718°C

B. Accidents or Malfunctions Affecting Localized Regions of the Core

1. Introduction

The class of accidents or malfunctions considered in this section is that which originates in local deviations from the normal operating conditions in the core. It is assumed that the core region involved is not large enough to affect strongly the overall reactivity, so that the power level remains essentially constant. Since the accidents considered here have only relatively small reactivity effects, it follows that identical accidents are less severe at a low power level (e.g., during startup) than during full-power operation. No separate analysis will therefore be presented for these accidents at low-power conditions.

2. Flow Reductions Affecting the Total Flow of One or More Subassemblies

General Aspects. This type of accident or malfunction results principally from flow obstructions, most often but not exclusively at the inlet of one or more subassemblies. The obstruction may be caused by foreign objects, gas bubbles, sudden movement of crud, etc. The flow reduction may be total or partial, instantaneous or rampwise, permanent or temporary.

The sensor types considered in connection with the detection of the accident or malfunction in its various stages of progress include flow sensors, temperature sensors, localized-boiling detectors, pressure-pulse (bubble collapse) sensors, anomalous reactivity detectors; and fuel-failure detectors.

The order in which the sensor types are listed does not necessarily reflect the time sequence in which they would detect the incident. This latter sequence depends on the type of incident and the sensitivity of the sensor.

Analysis and Detection of the Initial (Preboiling) Stage.

The sensor types most commonly considered for detecting a flow reduction in a subassembly in the preboiling stage are flow and temperature sensors. The former may be installed either at the inlet or at the outlet of the subassemblies; the latter are usually placed at the outlet of the subassemblies. It is therefore of interest to determine the relative merits of these two sensor types with regard to their capability of avoiding or minimizing fuel damage.

Most of the following analyses of localized core accidents or malfunctions are concerned with the hot channel, so as to evaluate the most severe case. If it is assumed that clad damage will occur for temperatures higher than approximately 800°C,* then the highest permissible reduction in the total subassembly flow which, for steady-state conditions, does not result in clad damage is easily determined:†

$$\frac{w}{w_o} = \frac{T_{e,o} - T_{i,o}}{800 - T_{i,o}} ,$$

where

w denotes the total subassembly flow;

w_o denotes the nominal value of the total subassembly flow;

$T_{i,o}$ and $T_{e,o}$ denote coolant inlet and outlet temperatures, respectively, at nominal conditions.

* The mechanical properties of stainless steel start to deteriorate rapidly with increase in temperature above 800°C. Obviously, there does not exist a uniquely defined threshold for clad failure, as this depends on fuel design, burnup, and the characteristics of the accident transient. However, since the present report is concerned primarily with trends, the assumed value for the failure threshold is not too important.

† The difference between the clad outside temperature and the average coolant temperature has, for the particular fuel design considered, a maximum value of ∿20°C at the core midplane for nominal values of the heat fluxes. In the following, all calculations use as threshold value for clad damage a coolant temperature of 800°C rather than a clad temperature of 800°C. This should not make much difference, as the threshold value of 800°C for initiation of clad damage is only an approximate value.

For $T_{i,o}$ = 432°C and $T_{e,o}$ = 616.9°C (see Table 1), one finds

$$w/w_o = 50.2\% ,$$

i.e., a reduction of the total subassembly flow by approximately 49.8% of nominal value is the highest permissible value which, under steady-state conditions, does not result in clad damage.

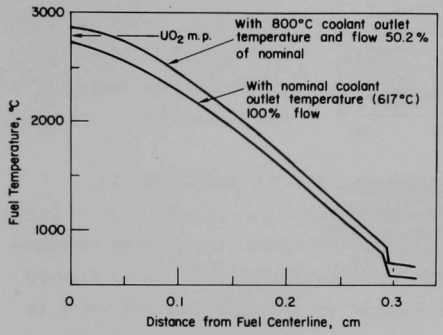

Fig. 1. Steady-state Radial Fuel-temperature Profiles in Midplane of Core when Operating at Nominal Power (peak rating = 15.85 kW/ft) and Inlet Temperature is Nominal (432°C).

Figures 1 and 2 give, respectively, radial temperature profiles in a fuel pin in the core midplane, and axial temperature profiles of fuel centerline and coolant, both for the case of nominal operating conditions and for the case of a coolant flow of 50.2% of nominal value. The latter case (which, as was seen above, results in a subassembly outlet temperature of 800°C), leads to a small degree of fuel melting (<6%) in the region of the core midplane. Possible effects on clad integrity, arising from prolonged operation at these higher than normal fuel temperatures, are not considered here.

Similarly, one can determine the highest permissible value for a reduction of the total subassembly flow for which sodium boiling would not occur under steady-state conditions. For this case the expression is

$$\frac{w}{w_o} = \frac{T_{e,o} - T_{i,o}}{T_{sat,e} - T_{i,o}} ,$$

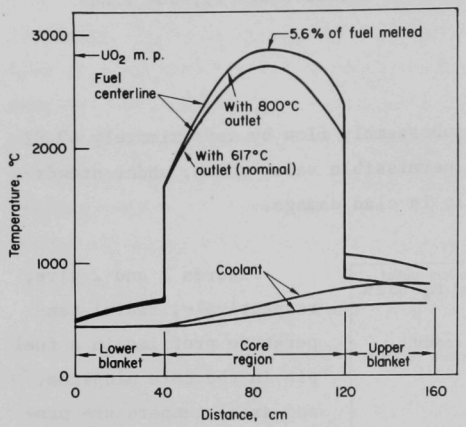

Fig. 2. Steady-state Axial Temperature Profiles of Fuel and Coolant in Core Hot Channel when Reactor is Operating at Nominal Power (peak rating = 15.85 kW/ft) and Inlet Temperature is Nominal (432°C).

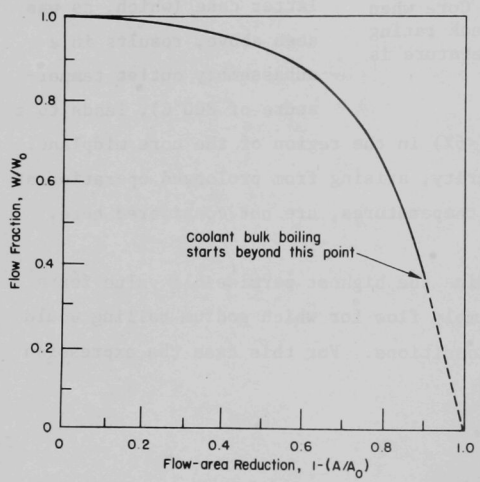

Fig. 3. Flow Fraction vs. Flow-area Reduction in Fuel Subassembly having Orifice-type Restrictions.[26]

where $T_{sat,e}$ denotes the saturation temperature of sodium at the outlet of the subassembly.

If the subassembly outlet plenum pressure is equal to ∿1.5 atm, one finds $T_{sat,e} \simeq 945°C$. Then with $T_{i,o} = 432°C$ and $T_{e,o} = 616.9°C$ (see Table 1), one finds

$$w/w_o = 36.2\% ,$$

i.e., a reduction of the total subassembly flow by 63.8% of nominal value is the highest permissible value which, under steady-state conditions, does not result in sodium boiling, all other operating parameters having their nominal values.

Figure 3 gives w/w_o as a function of the reduction in cross-sectional flow area, $1 - (A/A_o)$, of the subassembly for the case of an orifice-type restriction.[26] The point of the curve at which the dotted part starts gives the conditions for which,

under nominal operation, bulk boiling begins. The dotted part of the curve is only valid if boiling does not take place, i.e., for zero-power operation. It is thus noted that, in order to reach a coolant temperature of 800°C (w/w_o = 50.2%) or to reach coolant boiling (w/w_o = 36.2%), the flow-area reduction of the fuel subassembly has to be, respectively, 86% or 90%.

Having thus established the steady-state limits for flow reductions as regards clad damage and sodium boiling, it is now of interest to determine these limits for transient conditions, assuming a reactor trip to occur on either low flow or high coolant temperature at the subassembly outlet.*

In the following, the flow reductions are assumed to occur in the worst possible way (i.e., stepwise†) in order to determine the most limiting conditions. It is clear that, for the same terminal steady-state flow, rampwise flow reductions, followed by reactor trip, will result in lower temperatures for coolant and clad than will stepwise flow reductions.

The time delays relative to reactor trip were assumed as low as practical, but still within limits of relatively easy technical feasibility, in order to determine an upper limit for the magnitude of permissible stepwise flow reductions. The assumed values of these time delays are summarized in Table 3.

The reactor-trip margins# were assumed as follows:

---

* The fact that it will here be assumed that the reactor trip circuitry is actuated by sensors installed on individual subassemblies does not necessarily mean that this reflects the actual situation. The aim here is to determine the performance of such a system in order to be able to evaluate whether its actual installment would be advisable.

† It would seem fairly plausible that a flow reduction due to, e.g., a foreign object swept up by the flow, would occur in a near-stepwise manner.

Defined as the difference between the nominal value of a process variable and the setpoint for initiating reactor trip associated with that process variable.

Table 3

Time Delays Assumed for Reactor Trip Channels, Actuated by Subassembly Flow and Coolant Outlet Temperature

Time Delay	Reactor Trip on Flow (sec)	Reactor Trip on Outlet Temperature (sec)
Due to sensor	0.05	0.1
Due to safety circuitry	0.15	0.15
Due to safety-rod travel time in upper blanket*	0.1	0.1
Total for reactor trip†	0.30	0.35

* Based on safety-rod drive mechanisms delivering an acceleration of 3 g.

† This time delay is counted between the moment the process variable (flow or temperature) reaches the chosen setpoint value and the moment the rods start to introduce negative reactivity into the system.

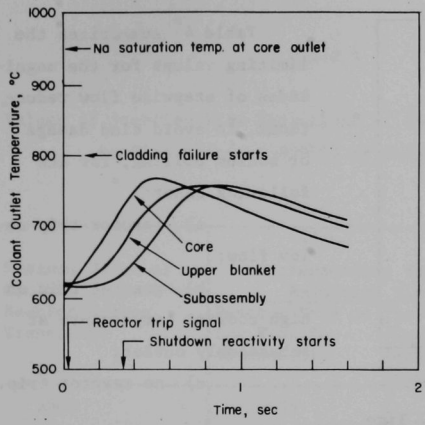

Fig. 4. Coolant Temperatures vs. Time after Sudden 60% Flow Reduction in a Single Subassembly. Reactor Trip at 90% flow; total trip delay 0.30 sec.

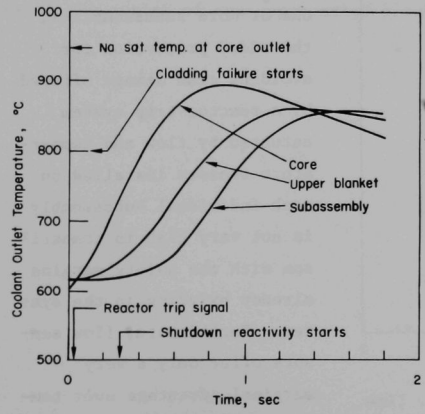

Fig. 5. Coolant Temperatures vs. Time after Sudden 77.5% Flow Reduction in a Single Subassembly. Reactor trip at 90% flow; total trip delay 0.30 sec.

a) For flow: A decrease of 10% of its nominal value.*

b) For outlet temperature: An increase of 30°C.

Figures 4 through 10 give typical transients of the coolant temperature in various locations for different values of stepwise flow reductions for the cases in which reactor trip occurred either on low flow or on high outlet temperature from the subassembly.

It is of interest to note that a 60% stepwise flow reduction (i.e., remaining flow is 40% of nominal value) results in maximum coolant temperatures of 770°C and 800°C for reactor trip on, respectively, low flow or high coolant temperature at the subassembly outlet. These temperatures are to be compared with the maximum coolant temperature of 800°C for a stepwise flow reduction of ∿50% without reactor scram.

* Since the flow reductions were assumed to occur stepwise, it is not necessary here to specify the reactor trip margin for flow. For completeness, however, a value is given.

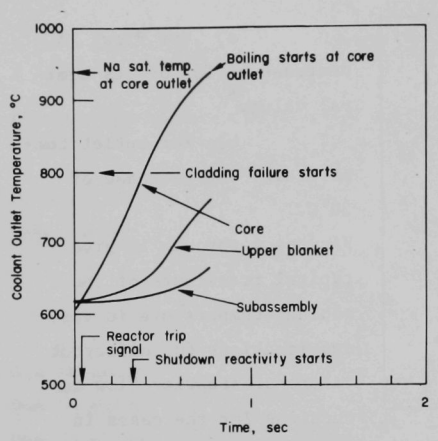

Fig. 6. Coolant Temperatures vs. Time after Sudden 83% Flow Reduction in a Single Subassembly. Reactor trip at 90% flow; total trip delay 0.30 sec.

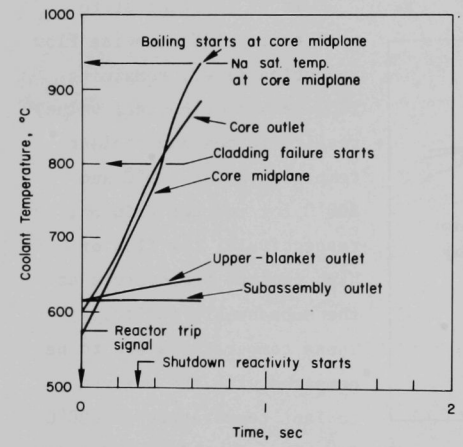

Fig. 7. Coolant Temperatures vs. Time after Sudden 99% Flow Reduction in a Single Subassembly. Reactor trip immediately; total trip delay 0.30 sec.

Table 4* summarizes the limiting values for the magnitudes of stepwise flow reductions, to avoid clad damage or sodium boiling, for the following cases:

a) reactor trip on low flow;

b) reactor trip on high coolant temperature at subassembly outlet;

c) no reactor trip.

From Table 4 it can be concluded that, for the class of accidents based on stepwise coolant flow reductions affecting the total flow of one or more subassemblies, the added protection for avoiding clad damage offered by a reactor-trip system actuated by flow and temperature sensors installed on each individual subassembly is not very high in comparison with the safety margins already existing in the system. Furthermore, flow sensors offer only a very marginal advantage over temperature sensors installed at the subassembly outlet for protecting against clad damage

* The results given in Table 4, which were obtained for an LMFBR having as main characteristics those listed in Table 2, are similar, but not identical, to the results reported in Ref. 27. Differences are due to differences in the plant designs studied.

Table 4

Values of Stepwise Flow Reductions of Coolant in a Subassembly Leading to Clad Damage (∿800°C) or Sodium Boiling (∿945°C)

Maximum Value of Coolant Temperature Reached During Transient* (°C)	Corresponding Value of Stepwise Coolant Flow Reduction (in % of nominal value) for:		
	Reactor Trip on Low Flow in Subassembly	Reactor Trip on Coolant Temperature at Subassembly Outlet	No Reactor Trip
⩾800	⩾∿65	⩾∿60	⩾∿50
⩾945	⩾∿80	⩾∿70	⩾∿64

*For flow reductions followed by a reactor trip, the maximum coolant temperature during the transient will occur at the outlet of the core region (except for the case of a total flow blockage, when the maximum coolant temperature will occur in the core midplane); for flow reductions without reactor trip, the maximum coolant temperature will be at the outlet of the upper axial blanket.

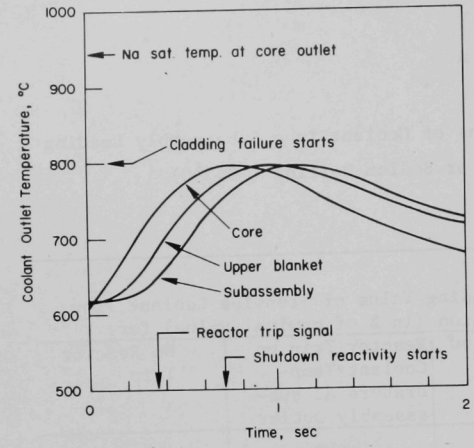

Fig. 8. Coolant Temperatures vs. Time after Sudden 60% Flow Reduction in a Single Subassembly. Reactor trip when coolant temperature at subassembly outlet rose 30°C; total trip delay 0.35 sec.

or sodium boiling (5% or 10%, respectively, for the difference of allowable stepwise flow reductions).

If temperature sensors could be installed at the outlet of the core region (i.e., at the inlet of the upper axial blanket), then the advantage of flow sensors over temperature sensors for a flow reduction accident would be even less evident.* Figure 10 gives the transients of the coolant temperature in various locations for a stepwise flow reduction by 80% of nominal value, followed by reactor trip on high coolant temperature at the core outlet. The maximum coolant temperature reached, 945°C, is identical to that reached in case of reactor trip on low flow for the same stepwise flow reduction (see Table 4).

The fact that so little is gained in added protection for the cases considered here is due, on the one hand, to the excellent heat-transfer properties of the coolant,† and on the other hand, to the substantial amount of heat stored in the fuel pins.

---

* This assumes that it is possible to obtain a representative measurement of coolant temperature at the outlet of the core. In view of the geometry in the region between core and upper blanket, this may not be easily obtainable, as mixing (swirling) devices could probably not be installed there. Furthermore, it would require the temperature sensor to be part of the fuel subassembly, which would entail considerable complications for refueling operations.

† The maximum values for local heat fluxes encountered in present-day LMFBR designs are much lower than the value of the critical heat flux. This situation - which is contrary to that existing for light water reactors (LWRs) - combined with the fact that coolant operating temperatures are, under nominal conditions, relatively far below the temperatures for clad failure and for sodium saturation, results in large safety margins against flow starvation for LMFBRs. See p. 55.

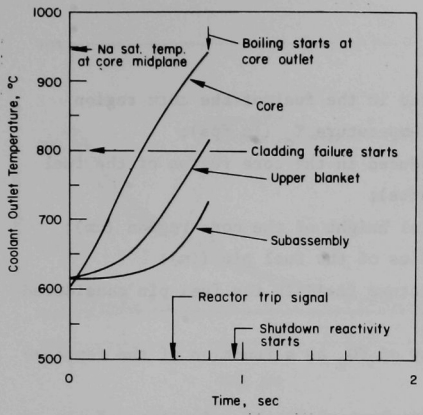

Fig. 9. Coolant Temperatures vs. Time after Sudden 77.5% Flow Reduction in a Single Subassembly. Reactor trip when coolant temperature at subassembly outlet rose 30°C; total trip delay 0.35 sec.

It is of interest, at this point, to investigate in more detail the amount of heat stored in the fuel. Figures 11 and 12, represent transients, respectively, for coolant temperatures and power (fission, as well as thermal) following a reactor trip with reactivity in the safety rods equal to approximately -$16. From these transients one finds through integration that the heat stored in the fuel of the core region, above the coolant inlet temperature of 432°C, is equal to 2.02 fps.*

An identical value for the heat stored in the fuel of the core region, above the coolant inlet temperature, was found from

$$E(T_o) = \frac{2\pi}{P} \int_{z=0}^{z=H} \int_{r=0}^{r=R} \int_{T=T_o}^{T=T(r,z)} r\, \rho(T)\, C_p(T)\, dz\, dr\, dT\,,$$

with

$$C_p(T) \simeq 1.2 \times 10^{-1} + (1.93 \times 10^{-4})\, T \quad (\text{in J g}^{-1}\,^{\circ}\text{C}^{-1})^{\dagger}$$

for 400°C < T < 2800°C.

* fps denotes full-power-seconds. One fps is equal to the energy produced in 1 sec at nominal power. The full-power-seconds considered here are relative to the average value of the power of the cooling channel under study rather than to the average value for the core.

† This analytical expression is derived, for the indicated temperature range, from Refs. 28 and 29.

Here

$E(T_o)$ denotes the heat stored in the fuel of the core region above the reference temperature T_o (in fps);

P denotes the power produced in the core region of the fuel pin considered (in Watts);

H denotes the total axial height of the core region (cm);

R denotes the outer radius of the fuel pin (cm);

$T(r,z)$ represents the temperature field in the fuel pin considered (in °C);

$\rho(T)$ represents the density of UO_2 as a function of the temperature (in g cm^{-3});

$C_p(T)$ represents the specific heat of UO_2 as a function of the temperature (in J g^{-1} $°C^{-1}$).

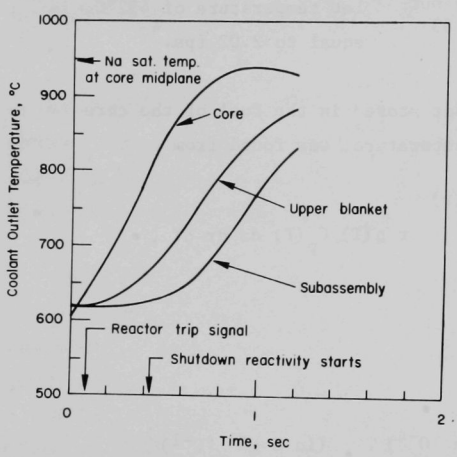

Fig. 10. Coolant Temperatures vs. Time after Sudden 80% Flow Reduction in a Single Subassembly. Reactor trip when coolant temperature at core outlet rose 30°C; total trip delay 0.35 sec.

Of interest also are the values of the heat stored in the fuel of the core region above the temperature at which cladding damage starts (800°C) and above the saturation temperature of the sodium at the subassembly outlet (945°C): 1.51 fps and 1.26 fps, respectively. Figure 13 gives the amount of heat stored in the core region of the fuel pin above the reference temperature T_o as a function of T_o.

In order to obtain a better feeling for the relative magnitude of this stored heat, the following reasoning is helpful. The average coolant velocity in the core-region is approximately 1070 cm sec^{-1}, from which follows a coolant transit time in the core region of $80/1070 = 7.45 \times 10^{-2}$ sec.

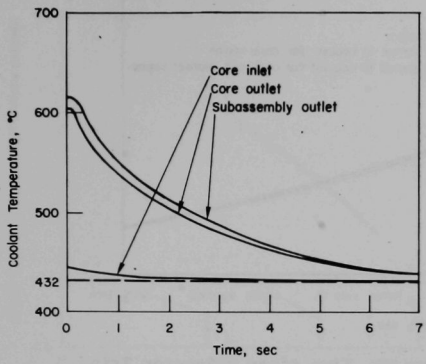

Fig. 11. Coolant Temperatures vs. Time after a Reactor Trip. Decay heat not taken into account.

This means that under nominal conditions all the sodium in the core region will be replaced by new sodium every 7.45×10^{-2} sec; in this time period the heat removed is, of course, 7.45×10^{-2} fps.

As was found previously, the heat stored above 800°C in the core region is 1.51 fps, which is equal to 20 times the heat removed during one time period for coolant transit. Now, if one were to reduce the flow by a factor of 2.22, then the coolant temperature at the outlet of the core region would rise to approximately 800°C after re-establishment of steady-state conditions. The new coolant transit time would then be 0.165 sec, and the heat removed during one new time period for coolant transit would be 0.165 fps. This means that the heat stored above 800°C in the fuel of the core region is enough to heat up, from 443.5°C to 800°C, an amount of sodium equal to ~9 times that contained at any instant in the cooling channel in the core region.

From the above it can be concluded that the heat stored in the fuel is relatively large with respect to the amount of coolant contained at any instant in the cooling channel. A consequence is that there will be some value (<100%) for the reduction in coolant flow for which sodium boiling and/or clad damage will occur, no matter how fast the flow reduction is detected, and no matter how fast the reactor trip system is actuated. This latter conclusion is, of course, in agreement with the results shown in Figs. 4 through 10 and reported in Table 4.

Analysis and Detection of the Boiling Stage. Previously, only flow sensors and temperature sensors were considered. Other types of

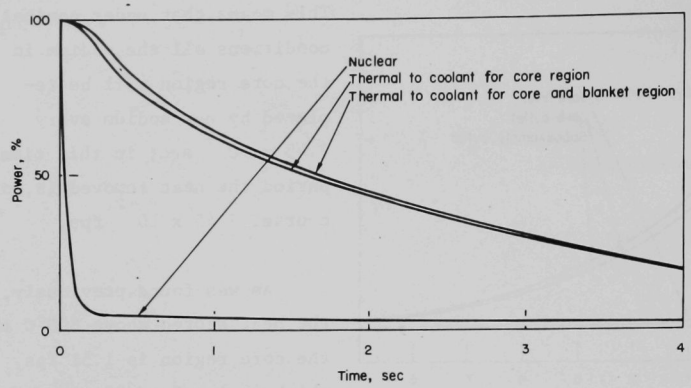

Fig. 12. Nuclear and Thermal Power vs. Time after a Reactor Trip. Decay heat not taken into account.

sensors become significant when the local core accident proceeds into the coolant-boiling stage.

To establish an upper limit for severity, a stepwise flow reduction will be assumed equal to 100% of the nominal value (total blockage). An attempt is made in the following at determining the time sequence of the events that follow a total blockage of a single subassembly.

To do this it is useful (a) to determine the heat required for melting the fuel, and (b) to study the temperature transients in a fuel pin following complete thermal insulation at full power. A solution for the first problem can easily be found by means of the following expression:

$$E_s = \frac{M}{P} \int_{T_o}^{2800} C_p(T)\, dT \quad \text{(in fps)}$$

with C_p for UO_2 given on p. 37 in J g^{-1} $°C^{-1}$ and where

E_s denotes the heat required (in fps) to heat the fuel from some reference temperature T_o (in °C) to 2800°C;*

* The melting temperature of UO_2 at near-atmospheric pressures is assumed to be 2800°C.

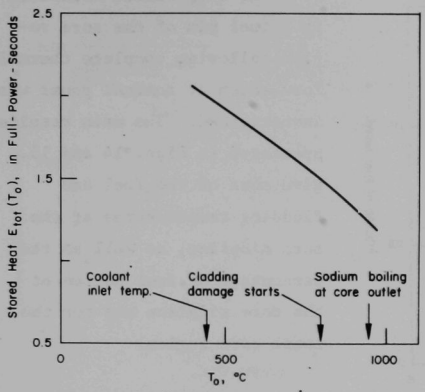

Fig. 13. Heat Stored in Fuel Pins above Reference Temperature, T_o.

M denotes the fuel mass (in g);

P denotes the nominal power (in W).

For a fuel pin of the core region, M = 2.65 g cm^{-1} and P = 5.2 x 10^2 W cm^{-1} (maximum linear heat rating in core midplane). Choosing T_o = 432°C (i.e., equal to the coolant temperature of the subassembly inlet), one finds

$$E_s = 5.2 \text{ fps} .^*$$

Furthermore, the heat required for transforming solid fuel at 2800°C into liquid fuel at 2800°C is found from

$$E_m = M\gamma/P \text{ (in fps)},$$

where γ denotes the heat of fusion. Taking a value of 270 J g^{-1} for γ, one finds

$$E_m = 1.38 \text{ fps} .$$

The total heat stored above 432°C in molten fuel (at 2800°C) in the core region is thus 6.58 fps.

As mentioned previously, the heat stored above 432°C in the fuel of the core region at nominal conditions is equal to 2.02 fps. Thus the heat required to bring that part of the central fuel pin at the core midplane from nominal operation to the fully melted condition at 2800°C is equal to 4.56 fps.

---

* The full-power-second values given in this section are relative to the maximum heat rating in the core midplane.

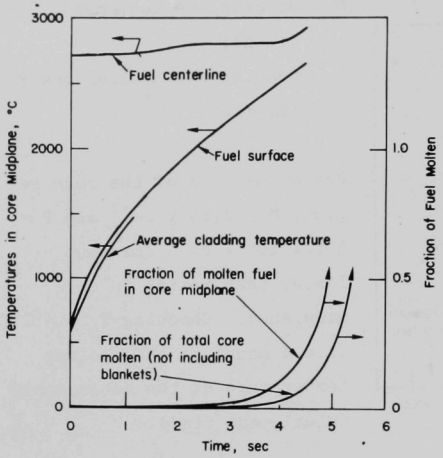

Fig. 14. Fuel Temperature and Fraction Molten vs. Time after Vapor Blanketing of a Fuel Pin.

The temperature transient in a fuel pin of the core region following complete thermal insulation at nominal power was investigated. The main results, presented in Figs. 14 and 15, give some of the fuel and cladding temperatures at the core midplane, as well as the percentage of fuel molten at the core midplane and for the total core region.

It is of interest to note that initially the centerline fuel temperature changes very little; all the added heat heats the outer concentric regions of the fuel pin. This is easily understood by considering that the system (i.e., fuel pin with peripheral heat sink) is perturbed initially only in the peripheral region by the change in heat-transfer coefficient. Figure 15 shows that initially the temperature profile in the center region of the fuel pin remains unaltered and the heat generated in that region flows outwards. The perturbation "propagates" relatively slowly towards the center region of the fuel pin, resulting eventually in a "flattened" temperature profile. It is not until t = 2.5 sec that the melting temperature is reached on the fuel centerline. After this time, some melting occurs on the fuel centerline, but still much of the heat continues to be stored in the colder peripheral fuel regions. However, once the radial fuel-temperature profile has been "flattened" (i.e., for t > 4.0 sec, approximately), rapid melting of the rest of the fuel occurs. Beyond 4.0 sec, some heating of the liquid fuel above the melting temperature of 2800°C occurs. This causes the moment at which 100% fuel melting is reached in the core midplane to be slightly later than the 4.56 sec calculated previously for the quasi-stationary case.

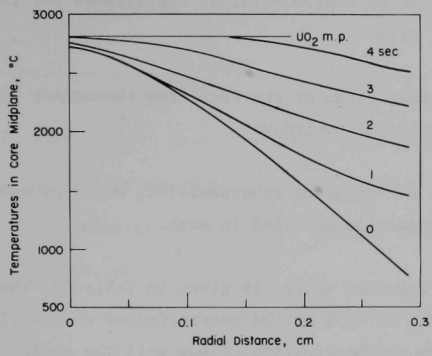

Fig. 15. Radial Temperature Profiles in Fuel Pin at Various Times after Vapor Blanketing.

From the foregoing, the following conclusions can be drawn: (1) The same material properties of UO_2 which result in a considerable amount of heat being stored in the fuel at nominal conditions (2.02 fps) also require considerable heat to be stored in the fuel in order to achieve fuel melting. (2) For the extreme case of a sudden and complete insulation of the fuel at nominal power, it takes approximately 4.0 sec for 10% fuel melting to occur in the core midplane; for t = 4.0 sec the fraction of molten fuel in the total core (blankets not considered) is less than 3%. (3) For the case of a sudden and complete thermal insulation of the fuel at nominal power, the clad-failure temperature of 800°C is reached relatively fast in the midplane, i.e., in approximately 0.2 sec, whereas the clad melting temperature is reached in approximately 1.0 sec.

With this background information, an attempt will now be made to determine the chain of events, including its time scale, subsequent to a total flow blockage in a single subassembly, primarily for the purpose of illustration and without claim to great accuracy.

The following assumptions are made:

1) Stepwise coolant flow reduction in a single subassembly by 100% of nominal value (total flow blockage).

2) Failure of all reactor-trip circuits, except those actuated by detectors of anomalous reactivity due to fuel slumping. Reactor-trip signals generated by pressure pulses due to

coolant expulsion or sodium-void collapse, [30,31] or by reactivity effects due to sodium voiding, are assumed not to result in reactor trip.

3) Complete thermal insulation of the fuel from the moment boiling starts until fuel meltdown.

4) Distortion of all six adjacent subassemblies, which causes a stepwise flow reduction of > 64% in each.

The chain of events, with its time scale, is given in Table 5. The times are, of course, approximate in view of the uncertainties that still exist. One uncertainty pertains to the question of how well the solid fuel pellets will remain in place after some or most of the cladding has melted. Perhaps the pellet fragments will in part be "coughed" out during the "chugging" phenomenon due to sodium reentry.

However, notwithstanding the various uncertainties, it is felt that the events pictured, as well as the time-scale given, appear to be relevant for estimating the probable role of protection instrument systems.

Table 5. Sequence of Events

Following Total Flow Blockage of a Single Subassembly

Event	Time (sec)
1) Stepwise total blockage of single subassembly.	0.0
2) Flow sensors fail to detect; no reactor trip.	0.0
3) Boiling is reached in core midplane.*	0.65
4) High-sensitivity localized boiling detectors fail to detect; no reactor trip.	0.65
5) Cladding fails and melts; partial release of fission gas.	0.65-2.5
6) Upper half of subassembly is voided; sodium vapor bubbles collapse in upper plenum.	0.85
7) Pressure-pulse (vapor-collapse) sensors fail to detect; no reactor trip.	0.85
8) Lower half of subassembly is voided; continued collapse of large sodium vapor bubbles in upper plenum.	0.85-1.5
9) Sensors of subassembly coolant outlet temperature fail to detect; no reactor trip.	0.95
10) Reactivity effects of voiding of subassembly ($< \sim 10¢$) is not detected; no reactor trip.	0.85-1.5
11) Sodium reenters, is heated, and is expelled. Interaction between coolant and molten cladding material. Outside fuel surface is now approximately 1500°C in hottest locations.	1.5-2.0
12) Pressure-pulse sensors fail to detect; no reactor trip.	2.0

*See Fig. 7

Table 5 (cont'd)

Event	Time (sec)
13) As 11). Interaction between coolant and molten cladding material. Outside fuel surface is now approximately 1800°C in hottest locations.	2.0-2.5
14) Pressure-pulse sensors fail to detect; no reactor trip.	2.5
15) As 11). All clad is now molten, and clad debris is expelled from the subassembly. Outside fuel temperature is now approximately 2000°C in hottest locations. Centerline of fuel starts to melt (molten fuel fraction in core midplane < 2%).	2.5-3.0
16) Pressure-pulse sensors fail to detect; no reactor trip.	3.0
17) As 11). but now all cladding material has been expelled. Molten fuel fraction in core midplane <2%. Fraction of molten fuel total core <1%. Outside fuel temperature is now approximately 2200°C in hottest locations.	3.0-3.5
18) Pressure-pulse sensors fail to detect; no reactor trip.	3.5
19) As 11). Molten fuel fraction in core midplane <5%. Fraction of molten fuel in total core <1%. Outside fuel surface temperature is now approximately 2400°C in hottest locations.	3.5-4.0
20) Pressure-pulse sensors fail to detect; no reactor trip.	4.0
21) The "chugging" phenomenon (11 through 19) is continued until a sufficient amount of fuel is molten to cause some degree of fuel-coolant interaction.	4.0-5.5
22) Fraction of molten fuel in core midplane ∿50%. Fraction of molten subassembly fuel in core region ∿20%.	5.5

Table 5 (cont'd)

	Event	Time (sec)
	Fuel-coolant interaction, causing relatively small pressure pulse (as energy content of molten fuel is only approximately 330 cal g^{-1}).	
23)	Six adjacent subassemblies are distorted, causing a flow reduction > 64% in all.	5.5
24)	Pressure-pulse sensors fail to detect; no reactor trip.	5.55
25)	The "chugging" and pressure-pulse generation (points 11 through 22) continue until a substantial part of the fuel of the subassembly is molten and the fuel starts to slump; 100% melting of the fuel in the core region of the subassembly occurs at approximately t = 6.0 sec. The reactivity effects may be either positive or negative, but are assumed to be sufficiently large to be detected.	6.0
26)	A reactor-trip signal is generated from either power level or anomalous reactivity effects.	6.0
27)	The six adjacent subassemblies reach boiling in the core midplane.	6.15
28)	The cladding of the six adjacent subassemblies fails and melts; partial release of fission gas.	6.15-onwards

Table 5 (cont'd)

Event	
29) Safety rods introduce negative reactivity*	6.25-6.45
30) Molten fuel starts to melt subassembly can wall. It would take between 10 and 15 sec to melt through to the cooling channels of the adjacent subassemblies. However, since the fission power is drastically reduced after the reactor trip there will probably be no melt-through, under the assumptions made.	6.3-onwards
31) The upper parts of the six adjacent subassemblies are voided; large sodium vapor bubbles collapse in upper plenum.	6.35
32) The lower parts of the six adjacent subassemblies continue to be voided.	6.35-onwards
33) Stored heat in hot fuel of affected subassembly is removed by "chugging."	6.45-onwards
34) Sodium may reenter the six adjacent subassemblies, heat up, and be expelled.	7.0-7.5
35) As 34). This "chugging" may continue until the major part of the stored heat is removed. Then decay heat is removed by means of remaining flow or natural circulation. No further propagation.	7.5-onwards

* A crucial point in this chain of events is that neither core nor scram system have, up to this moment, been distorted to the extent as to make insertion of the scram rods impossible, except perhaps for rods in the immediate vicinity of the affected subassemblies.

From the chain of events presented in Table 5 conclusions may be drawn:

1. The sequence of events following a total flow blockage of a single subassembly is relatively slow compared to the technically feasible speed of response of sensors and reactor-trip systems. Though clad damage and clad melting occur relatively fast, considerable time is needed for any substantial degree of fuel melting. The times subsequent to the occurrence of the total flow blockage at which the various sensors would be able to give a signal are given in Table 6.

2. The accident develops relatively slowly because, on the one hand, local core accidents have small reactivity effects (so that, in the initial stages, the power level remains essentially unaffected); on the other hand, a considerable amount of heat is needed to obtain any substantial degree of melting of the fuel.

3. A massive and violent fuel-coolant interaction with high pressure pulse, involving molten fuel having a high energy content,* may be quite improbable, since the relative "slowness" of the accident would tend to preclude attainment of high energy contents, and since the conversion factor[32] for heat to mechanical work appears to be small for 330 cal g^{-1}. The maximum rate of heating, corresponding to a peak linear power rating of 15.85 kW/ft, is 47 cal g^{-1} s^{-1}. In order to attain an energy content of, say, 600 cal g^{-1}, the molten fuel would have to remain thermally insulated for an additional 5.7 sec.

4. Even under the conservative assumption that many levels of protection instrumentation fail, and the reactor is tripped only because of anomalous reactivity effects due to fuel-slumping, the propagation of fuel damage should stop before spreading beyond the seventh subassembly, assuming that the first subassembly would damage only its immediate neighbors.

---

* By "high" is meant >>330 cal g^{-1}; 330 cal g^{-1} corresponds to just molten fuel at 2800°C.

TABLE 6. Approximate Times Required for Various Sensor Types to Generate a Signal Subsequent to Total Flow Blockage of Single Subassembly

Sensor Type	Approximate Time (sec)
Flow sensor	∿ 0.05
Localized-boiling detector	∿ 0.7
Pressure-pulse (bubble-collapse) sensor	∿ 0.85
Temperature sensor at subassembly outlet	∿ 0.95
Anomalous-reactivity detector (high sensitivity)*	∿ 1.0-1.5
Anomalous-reactivity detector (low sensitivity)	∿ 6.0
Fuel-failure detector	∿15.0-upwards

*High- or low-sensitivity anomalous-reactivity detectors are defined, for the purpose of the present report, as detectors capable of detecting the reactivity effects caused by, respectively, sodium voiding or fuel meltdown of a single subassembly.

5. Regarding the comparative merits of the various sensors, the following can be said:

a) The time delay subsequent to a total flow blockage for a temperature sensor installed at the outlet of the subassembly to give a signal is $\sim$ 0.95 sec, i.e., $\sim$ 0.90 sec larger than that for a fast-response flow sensor. During this 0.95 sec prior to the generation of a reactor-trip signal, there is a lower rate of heat transfer from the fuel in the region of the core midplane over a period of at most 0.3 sec, because cooling remains close to normal until boiling starts in the core midplane. If one assumes a total delay time for reactor trip of 0.25 sec (counted from generation of the reactor-trip signal until insertion of negative reactivity starts), and furthermore assumes conservatively complete thermal insulation of the fuel from the moment boiling starts, then the fuel in the region of the core midplane could be thermally insulated only for 0.55 sec prior to shutdown of the neutron chain reaction due to reactor trip on subassembly coolant outlet temperature. It is seen from Fig. 15 that complete thermal insulation for 0.55 sec does not lead to any fuel melting.

If reactor trip were initiated by a low-flow signal generated by fast-flow sensors, then sodium boiling could still not be prevented for an accident in which the flow reduction is greater than 80% (see Table 4). Thus, terminating the accident by means of a reactor-trip signal from either low flow or high subassembly outlet temperature would not make much difference, since both cases would result in sodium boiling and substantial clad damage, but not in fuel melting, prior to shutdown of the neutron chain reaction.

It may thus be concluded that, for the accident due to total (or near total) flow blockage, the advantage of flow sensors over temperature sensors is marginal.

b) Pressure-pulse sensors installed in the upper plenum and sensing the collapse of sodium bubbles in the subcooled sodium of the upper part of the subassembly or the upper plenum, are expected to give a

signal in 0.85 sec following a total flow blockage of a subassembly. The advantage of fast-acting flow sensors over pressure-pulse (bubble-collapse) sensors is thus even less than that over temperature sensors installed at the subassembly outlet. Bubble-collapse detectors furthermore have the very attractive feature of being "whole-core" sensors, i.e., sensors not required to be installed in each individual subassembly. Pressure-pulse sensors might also later sense a larger signal due to a fuel-coolant interaction or rapid sodium boiling due to interaction with very hot steel.

c) Localized-boiling detectors have, for this type of accident, only an advantage of 0.15 sec as regards time delay if compared to bulk boiling (bubble-collapse) detectors. Even this advantage may be illusory. Since the signal-to-noise ratio for localized-boiling detection is probably rather low, it may not be feasible to use them in connection with the reactor-trip circuitry.

d) Anomalous-reactivity detectors of high sensitivity (capable of sensing sodium voiding) have, for the same reasons as presented under item (a), only a relatively small disadvantage in comparison with fast flow sensors, since a signal is produced in from 1 to 1.5 sec following the total flow blockage. However, it may not always be easy to obtain a sufficiently dependable signal, so that the reactor-trip margin may have to be increased so as to give a reactor-trip signal only following substantial fuel melting and slumping. In that case the time delay could be as high as 6.0 sec. A reactor-trip system with such a delay might still be of interest as a backup system.

e) Fuel-failure detectors are slow and thus do not have great usefulness in terminating an accident due to total flow blockage through reactor trip.*

* The fact that the fuel-failure detectors are not very useful in the context of the accident considered here (stepwise total flow blockage) does not at all mean that they are of no importance; quite to the contrary. Most slowly developing localized fuel failures inside a subassembly can only be detected in the early stages by means of fuel-failure detectors. See also p. 61.

3. Accidents or Malfunctions Affecting Localized Regions Inside a Single Subassembly

General Aspects. This type of accident or malfunction is due primarily to:

a) Foreign objects lodged in between fuel pins, or fuel distortions (e.g., local bulging of cladding and fuel-pin bowing) causing localized flow starvations or localized flow blockages inside the subassembly, and

b) Rupture of fuel-pin clad, causing release of gaseous fission products into the coolant, possibly followed by further clad damage to other fuel pins due to gas blanketing or coolant flow reduction.

In order to evaluate the type of accident or malfunction resulting from the former, it is of interest to determine first the safety margins against flow starvations and flow blockages that exist inherently in the system, by making a comparison between LMFBRs and LWRs. Subsequently, the possibility and means for early detection will be investigated again with the aim of comparing the merits of the various possible sensors.

Safety Margins against Flow Starvation and Flow Blockage in Localized Regions of a Subassembly. LMFBRs have a very compact packing of the fuel pins compared to LWRs, so that the probability for the occurrence of local flow starvation or flow blockage would seem to be higher for the former than for the latter. On the other hand, the heat-transfer characteristics of the liquid metal coolant relative to those of water tend to compensate to some extent for this disadvantage.

As is well known, burnout occurs in LWRs whenever the local heat flux exceeds the local value for the critical heat flux. This latter value depends on the local values of enthalpy, flow, and pressure. Burnout can take place even if the bulk temperature in the coolant channel is still below saturation; in fact, the phenomenon appears to be most violent

under those circumstances.

In LMFBRs of present-day design burnout is not dependent on a local critical heat flux value.* All that is required to avoid "burnout" is to avoid boiling. Since the coolant saturation temperature is relatively far removed from the highest nominal operating temperature of the coolant in an LMFBR, a larger safety margin against localized flow starvation is available than for LWRs.

In the following, the safety margin against localized flow starvation will be determined first. Only a very qualitative evaluation will be presented here, the primary objective being not so much to provide results of high accuracy, but rather to gain a feeling for the magnitude of the safety margins available.

It is assumed that a flow starvation of a certain severity exists in a localized region inside a subassembly, extending over a certain axial height. The evaluation is here limited to the case in which the flow starvation extends radially over a limited part of the cross-sectional area of the subassembly, so that the overall subassembly flow does not change much.

It is conservatively assumed that no flow mixing takes place along the length of the flow-starved region (i.e., no coolant from surrounding colder regions enters the flow-starved region), and furthermore, that no radial heat transfer through conduction from the flow-starved region into the colder surrounding regions occurs. By neglecting, in this way, all radial heat transfer, the radial dimensions of the flow-starved region do not enter the results (provided, as mentioned above, that the overall subassembly flow is not changed much).

The expression giving the dependence between the flow in the flow-starved region and the allowable axial height of the flow-starved

---

* As mentioned before, at much higher heat fluxes than encountered in present-day LMFBR designs the concept of a "local critical heat flux" would need to be considered also for liquid metal coolants.

region, which would just not lead to sodium boiling, is

$$\Delta H = \left(\frac{G}{G_o}\right) \frac{T_{sat} - T_o}{(dT/dH)_o} \qquad (1)$$

where

ΔH denotes the axial height (cm), of the flow-starved region measured from the point where the starvation occurs in the direction of the flow;

G denotes the specific flow in the flow-starved region ($g\ cm^{-2}\ s^{-1}$);

G_o denotes the nominal value of the specific flow ($g\ cm^{-2}\ s^{-1}$);

T_{sat} denotes the coolant saturation temperature at the downstream end of the flow-starved region considered (°C);

$\left(\frac{dT}{dH}\right)_o$ denotes the mean value of the axial coolant-temperature gradient under nominal conditions in the region considered ($°C\ cm^{-1}$).

In order to get a feeling for the magnitude of the various quantities, a calculation is presented below using the data from Table 1, namely,

Height of core region	$H = 80$ cm
Coolant temperature at core inlet	$T_i = 443.5°C$
Coolant temperature at core outlet	$T_e = 603.7°C$

For a rough evaluation, the heat flux is assumed to be uniform over the core height, so that

$$\left(\frac{dT}{dH}\right)_o = \frac{160.2}{80} = 2.0°C\ cm^{-1}$$

The flow-starved region will be assumed to occur close to the outlet of the core. The sodium saturation temperature at the outlet of the core region under nominal conditions is found to be 1059.1°C. One then finds

$$\Delta H = \left(\frac{G}{G_o}\right) \frac{1059,1 - 603,7}{2,0} = 227.6 \left(\frac{G}{G_o}\right)$$

For a flow starvation with $(G/G_o) = 0.1$, one finds $\Delta H = 22.8$ cm, i.e., a localized flow-starved region close to the outlet of the core, in which the flow is reduced to 10% of its nominal value, can thus extend over an axial height of 22.8 cm without leading to boiling.

At the inlet of the core, due to the lower coolant temperature and the higher sodium saturation temperature (= 1138.0°C), the safety margin against boiling would be larger: a localized flow-starved region in which the flow is reduced to 10% can extend, at the inlet of the core region, over an axial height of 34.7 cm without leading to boiling.

Similarly, the safety margin against clad damage at the core outlet can be determined. For this T_{sat} in the previous equation is replaced by T_{cf}, the clad failure temperature, which will be assumed to be 800°C. One then finds

$$\Delta H = \left(\frac{G}{G_o}\right) \left(\frac{800 - 603.7}{2.0}\right) = 98 \left(\frac{G}{G_o}\right)$$

A flow-starved region close to the core outlet, in which the flow is reduced to 10% of its nominal value, can thus extend over an axial length of 9.8 cm without exceeding the temperature at which clad damage starts. The corresponding value at the core inlet would be 17.8 cm.

Having thus determined qualitatively the safety margins against flow starvation, an attempt will now be made at obtaining an estimate of the safety margins against flow blockages. The foregoing considerations have shown that increasing the severity of the flow starvation leads to decreasing permissible axial heights of the flow-starved region. In the limit, a completely blocked region would be allowed to have zero axial height. This, however, is not true, because the radial heat transfer by means of conduction and convection is not at all negligible. A completely

flow-blocked region can have a non-negligible geometric extension, before boiling or clad damage does occur. Of course, as soon as radial heat transfer is taken into account the radial dimensions of a flow-blocked or flow-starved region have to be considered.

McWethy et al.[19] carried out a study in which two cases were considered: (a) blockage of a single coolant channel, and (b) blockage of multiple coolant channels. A coolant channel is defined as the shaded area in Fig. 16. Figures 17 and 18 (reproduced from Ref. 19) give the time response of the sodium temperature for a single-coolant-channel case and for the multiple-coolant-channel case, respectively, with the axial height as parameter. These analytical results agree well with those found by Fontana et al.[33] Experimental programs in this area are underway at ORNL and at ANL, and should produce results soon.

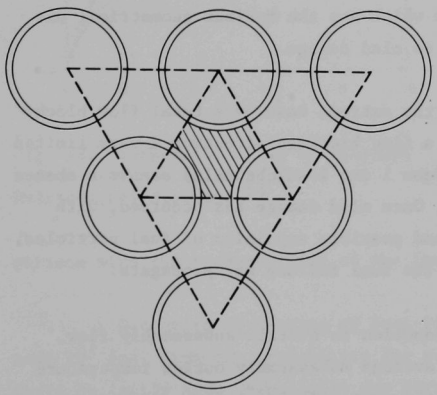

Fig. 16. Blockage of a Single Coolant Subchannel.[19]

As is seen for the single channel blockage, the temperature rise, even for a blockage extending over 30 cm, would lead to a maximum temperature increase of only ∿200°C, which would presumably not result in major clad damage and definitely not result in boiling. For the multichannel case, there is little or no radial heat transfer, so that a stagnant region of only very limited height would not cause trouble (heat transfer in the axial direction is taken into account).

In summary, the following conclusions may be drawn: (1) LMFBRs appear to have relatively high safety margins against clad damage and sodium boiling, as caused by localized flow starvation inside a subassembly; (2) for localized flow blockages, the region of stagnant

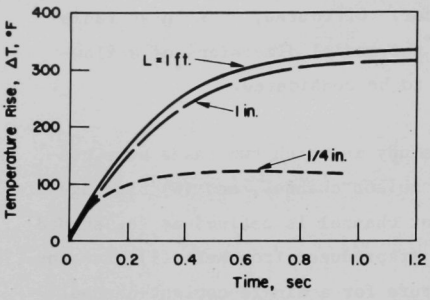

Fig. 17. Temperature Rise of Stagnant Sodium at Three Axial Heights, for Single-channel Blockage.[19]

sodium has to extend radially beyond a single cooling subchannel in order to cause clad damage (according to Ref. 19).

Detection of Flow Starvations and Flow Blockages in Localized Regions of a Subassembly. It was shown previously that localized flow starvations or flow blockages inside a subassembly need to have a certain geometrical extension (axial and radial) before sodium boiling and/or clad damage follows. The obvious question to ask is whether it is possible to detect a flow starvation or flow blockage which has the maximum geometrical extension that does just not lead to clad damage.

Limiting the evaluation to the extreme case of a total flow blockage, then it is noted that only a flow blockage affecting a very limited number of subchannels (say, between 1 and 4 subchannels) stands a chance of not leading to clad damage.* Once clad damage has occurred, with subsequent fission gas release and possible expulsion of fuel particles, the blocked area may extend and the fuel failure may propagate.

In order to obtain a 10% reduction in overall subassembly flow, corresponding to an increase in average subassembly outlet temperature of ∿18.5°C, the blocked part of the cross-sectional flow area of the subassembly has to be 54% for orifice-type blockages (see Fig. 3), i.e., affecting some 290 subchannels. Obviously, if such a large number of subchannels are blocked, localized sodium boiling would occur, which might affect both flow and outlet temperature of the subassembly to a

* This does not take into account considerations regarding the probability of the occurrence of a complete flow blockage extending over a cross-sectional area of several adjacent subchannels. In reality, the probability of occurrence of a flow blockage of such relatively large size may be very low, as it would require debris of certain dimensions (that could be strained out fairly easily) to be lodged in adjacent subchannels at approximately the same height.

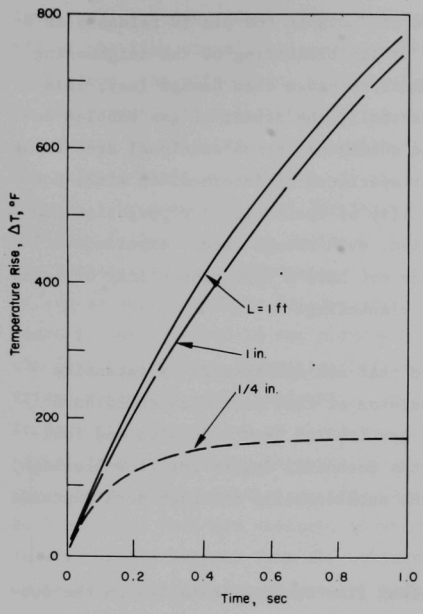

Fig. 18. Temperature Rise of Stagnant Sodium at Three Axial Heights, for Multichannel Blockage.[19]

much larger degree than would be the case solely as a consequence of the reduced cross-sectional area of the flow passage.

It appears unlikely that a localized flow blockage can be detected, before clad damage and boiling occur, by means of flow or temperature sensors installed on the subassembly.* Once boiling does take place, detection by means of high-sensitivity boiling detectors, if feasible, may be just as fast as flow or temperature sensors. When clad damage has taken place, a fuel-failure-detection system would be of great importance, particularly if the rate of fuel-failure propagation is small in comparison with the response time of the fuel-failure-detection system.

Detection of Rupture of Fuel-Pin Clad. In cores containing some 10^5 fuel pins the probability for rupture of the fuel-pin clad could be fairly high, especially for burnups of 100,000 MWD/ton or more.

Judd[2] presented plausible arguments that ruptures of fuel-pin clad releasing fission gas (and not fuel particles, which could lead to subchannel blockages) may have a relatively low probability of leading to fuel-failure propagation. If the aperture of the rupture is large, the

* Some authors suggest that noise analysis of the subassembly flow and/or outlet coolant temperature could perhaps give an earlier signal. This matter is, however, still conjectural; furthermore, it may not be possible to use such an early signal in the reactor-trip system because of reliability requirements.

total inventory of gaseous fission products in the pin is released in a short time. This could only lead to gas blanketing of the neighboring fuel pins for a time period too short to cause clad damage (say, less than 0.3 sec). If the aperture is small, the stream of gas bubbles occupies too small a fraction of the subchannel cross-sectional area to be able to cause gas blanketing. For apertures of intermediate size, however, there may still be a possibility of fuel-failure propagation due to gas blanketing and flow reduction, even though recent experiments[34] indicate that adjacent fuel pins do not have a high probability of being damaged by overheating due to gas blanketing.

Ruptures of the fuel-pin clad that are accompanied by extensive clad deformation and possible expulsion of fuel particles could have serious consequences in that they may lead to flow blockages and fuel-failure propagation. In view of the potential danger for flow blockage, it would be desirable to locate the subassemblies in which such ruptures did occur.

Some authors have suggested that flow sensors installed on the subassemblies would be capable of detecting fission gas released into the coolant subsequent to the rupture of a fuel pin. In the following an attempt will be made to determine whether or not flow sensors might be useful in this respect.

One gram of fuel will, at 10% burnup, produce approximately 12 mg of gaseous fission products. If a uniform burnup of 10% is assumed in the core region, the volume of the fission gas produced in one pin would be approximately 760 cm^3 at the coolant outlet temperature of 617°C and at the subassembly outlet pressure of 1.5 atm.

The total volumetric coolant flow of the subassembly is approximately 4.4×10^4 cm^3 s^{-1}. Thus, if all gaseous fission products were to be released in 1 sec, then the gas volumetric flow would be 0.25% and 1.75% of the total flow at the inlet and at the outlet of the subassembly, respectively. This small flow disturbance of short duration could probably not be detected in view of the relatively high "noise"

level, which, under ideal laboratory circumstances, was found to be ~5% of the flow signal, measured peak-to-peak.[35] Under actual reactor conditions, the noise level would probably be considerably higher, due to the presence of a large number of parallel channels and the probable occurrence of relatively large-scale vortices in the lower plenum. If the release times are shorter, or if a number of pins fail simultaneously, the possibility of distinguishing the flow disturbance from the flow "noise" would be improved. The sensitivity of detecting fuel-pin failures by using flowmeters may be better than indicated above if it can be experimentally demonstrated that the "noise" caused by gas release is concentrated in one portion of the frequency spectrum. Even if the reliability of a flowmeter-fuel-failure-detection system is not satisfactory enough to be included as part of the reactor protection system, it may still have value as a system for fuel-failure location if the signal from a flowmeter is correlated with a subsequent signal from a gross fuel-failure monitor system. Alternatively, in order to be able to locate the fuel-pin rupture, it would be necessary to draw continuous (small) sample streams from the outlets of each individual subassembly, or to resort to tagging or coating techniques.

4. Accidents or Malfunctions Caused by Errors of Fuel Enrichment

General Aspects. This type of accident is not limited to LMFBRs, but may occur with LWRs. In either type of reactor, fuel zones of different enrichment may be used to flatten the radial neutron-flux profile and thus improve the overall core performance. It has been argued, however, that enrichment errors are potentially more dangerous in LMFBRs because of the possibility of positive reactivity effects that could accompany fuel movement.

Two types of enrichment errors should be distinguished: (1) enrichment errors involving an entire fuel subassembly, and (2) enrichment errors in which one or more fuel pins of a certain enrichment are installed in a fuel subassembly of lower enrichment. Type (1) is in most cases caused by a fuel-loading error, in which a subassembly with a certain enrichment is placed in a core zone of lower enrichment, whereas type (2) constitutes an error in fuel-subassembly fabrication.

It is possible to reduce the possibility of loading errors involving entire fuel subassemblies by providing subassemblies of different enrichments with certain mechanical features so as to make interchange impossible. This, however, may affect unfavorably the flexibility of the overall fuel cycle. It will, therefore, here be assumed that such loading errors can take place. Obviously, the primary defense against the occurrence of such loading errors is a very strict administrative control during the refueling process. However, once a loading error of this type has been made, means should in principle be available for detecting it at low power during the startup procedure before fuel damage ensues. This should not be too difficult. A loading error involving an entire subassembly should show up at low power level, and under known flow conditions, as a high (or low) reading of the temperature sensors installed at the subassembly outlet, in comparison with subassemblies that should have the same power. Also, a loading error of this type may show up as an anomalous reactivity effect prior to criticality. Since adequate detection means are thus available, this type of enrichment error will not be further examined in this report.

In the case of the enrichment error involving a limited number of fuel pins, detection prior to the occurrence of an incident is very difficult, primarily because the effect on either reactivity or coolant outlet temperature would be very small. The following treatment is limited to this type of error.

Analysis. Present-day LMFBR designs have a comparatively large safety margin against flow starvations. As was shown previously, the flow in the hot channel may be reduced to ∿50% of its nominal value before the coolant outlet temperature reaches 800°C at which clad failure initiates. The same safety margins do not obtain for overpower conditions: for overpower, the operational limit reached first is not the clad temperature, but the fuel centerline temperature and the percentage of molten fuel in the cross section of a fuel pin at the core midplane. An overpower of 30% of nominal value results in ∿17% of the cross-sectional area of the fuel pin being melted in the midplane of the core region. Figures 19 and 20 give, respectively, radial temperature

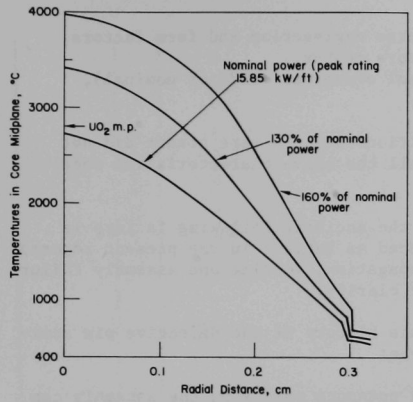

Fig. 19. Steady-state Radial Temperature Profiles in a Fuel Pin at Various Powers. Coolant inlet temperature = 432°C.

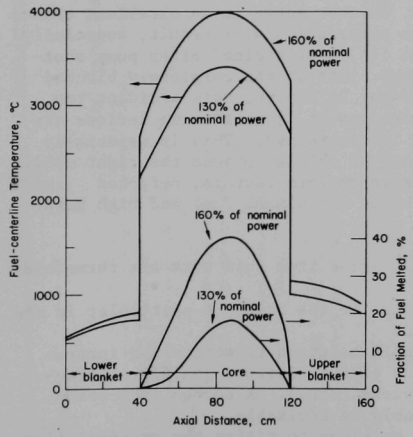

Fig. 20. Axial Profiles of Fuel Temperature and Percentage of Molten Fuel at 130 and 160% of Nominal Power.

profiles at the core midplane and axial temperature profiles of the centerline temperature, as well as axial profiles of the percentage of melted fuel at power levels of both 130% and 160% of nominal value.

A number of mechanisms have been suggested by which molten fuel in the centerline region of a fuel pin could result in clad damage. One postulates that the molten UO_2 from the centerline region seeps through cracks suddenly formed in the pellets, thus coming in direct contact with the clad. Obviously, the possible damaging effects of molten fuel on the cladding depend on the fuel pin design and on the previous history (burnup, etc.) of fuel.

P. L. Wattelet *et al.*[36] analyzed an accident due to an enrichment error, involving a limited number of fuel pins of a subassembly. Their results are reproduced here:

> "A fuel pin in which the cladding is defective in strength due both to a fabrication flaw and subsequent irradiation induced embrittlement is

found to fail* only under certain simultaneous adverse conditions. The fuel pin is:

1. the 'hot' pin having adverse engineering and form factors,
2. defected just above the core center,
3. operating at 120% of normal overpower (138% of nominal),
4. irradiated to 5% burn-up.

"Cases studied in which conditions 3 and 4 were absent did not fail, but a fuel pin having all the above characteristics does fail.

"The chronological record of the accident following failure is given in Table 3.1-1 (reproduced as Table 7 in the present report) in which fuel pin failure propagation, voiding and assembly failure propagation are separated for clarity.

"The main uncertainties in this history of the defective pin accident lie in the following areas:

1. Effect of voidage induced pressure pulses on the assembly can and especially on neighboring assemblies.
2. Mode of propagation from pin to pin (here taken to be radial).
3. The reactivity changes arising from the slumping assembly.
4. Exactly when shut-down is achieved to alleviate can melt-through.
5. Whether significant heat inputs can be achieved into the second assembly before shut-down.

"The main conclusion, however, is that there is an excellent chance that no inter-assembly failure propagation will result, especially if a somewhat higher flow than 10% is maintained after pump shut-down. Indeed it would seem that, just as the completely blocked assembly accident can be ruled out by design, this accident too should not lead to drastic consequences if monitoring devices are adequate and if adequate flow is maintained. This is especially true in view of the unlikelihood of obtaining just the right conditions for failure to occur, (adverse form factors, defected cladding at the right point, wrong enrichment fuel and high burn-up).

"The main recommendations which arise from this work are threefold:

1. That further study be devoted to the case, in particular in the areas of uncertainty noted.
2. That further attention should be given to monitoring instrumentation for the detection of fuel failure (sniffers, reactivity meters, noise analyzers, etc.). A sooner indication than a high flux signal would be advisable.
3. That consideration should be given to sizing the residual flow following pump shut-down according to the need for protecting a damaged assembly rather than for merely removing normal core

* Failure is defined as the point at which the cladding stress reaches the reduced hoop yield strength.

TABLE 7

Defective Fuel Pin

Reproduced from Ref. 36

TIME	FUEL BEHAVIOR	VOIDAGE	POWER AND FLOW
(Sec.)			
	A hot defected fuel pin at 5% burn-up is subjected to local overpower on being loaded into a lower enrichment zone and the reactor being brought to power		Local power at 120% of 115% of nominal power. 100% flow in all assemblies.
0.0	Fuel cladding attains yield stress and fails.		
0.9	Fuel ejection due to internal pressures - also fission product gases.	Sodium voiding due to fuel/sodium heat transfer.	
0.902		Peak pressures of 800 ± 300 psia Assembly can yields as pressure waves strike - may crack if embrittled.	
0.91		1.3' of channel voided, pressures are down to 670 ± 250 psia.	
0.95		Voided channel - significant external condensation, pressures small	Power decreasing due to -5¢ from voidage.
	Fuel blocks channel and slumps.	Vapor and fission gas blanket next row of pins.	
4.5	Cladding of peak rod in first row fails.		
5.4	Fuel ejects from peak rod of first row together with fission product gases		Slow power decrease counteracted by addition of reactivity due to slumping.

TABLE 7 (Cont.), reproduced from Ref. 36

TIME	FUEL BEHAVIOR	VOIDAGE	POWER AND FLOW
(Sec.)			
5.7	Cladding in second row pins fails.		
6.6	Fuel ejects from second row pins together with fission gas.		
6.9	Cladding in third row pins fails.		
7.8	Fuel ejects from third row pins. First hot pin completely slumped.		
10.5	Cladding of fourth to eighth row pins fail very rapidly as sufficient vapor is produced for full blanketing		δk due to voiding + 8.2¢
		ASSEMBLY FAILURE PROPAGATION	
11.4	Fuel ejects from rows 4 to 8. Fuel starts to contact the assembly can.		
12.3	First row of pins completely slumped.		δk > 2¢ from slumping.
12.4		Assembly can at hot spot fails due to high temperature	
13.5	Second row of pins completely slumped		δk > 5¢ from slumping
14.4		Fuel contacts adjacent can at local point of failure	
14.7	Third row of pins completely slumped.		δk > 10¢ from slumping.

TABLE 7 (Cont.), reproduced from Ref. 36

TIME (Sec.)	FUEL BEHAVIOR	ASSEMBLY FAILURE PROPAGATION	POWER AND FLOW
16.3		Heat input into adjacent assembly may peak at 2.10^6 Btu/hr ft^2 if enough slumped fuel reaches the can wall before shut-down. If so, adjacent wall may reach melting.	$\delta k > 30¢$ from slumping Power on a 20 sec. period.
18.3	Last rows 4 to 8 completely slumped. Fuel in full contact with assembly can wall.	Fuel in contact with assembly wall reaches 6100°F (Pvap = 200 psi).	$\delta k = 60¢$ from failed assembly. Power reaches 110% overall reactor scrammed.
19.3	Fuel in center of slumped mass reaches 6100°F (Pvap = 200 psi).		Pumps tripped - flow in adjacent assembly coasts down.
24.3			Flow in adjacent channel down to 45%.
28.0	Pressure in slumped assembly high (in range 100-1400 psia).	Heat input into adjacent assembly slowly rising ($\sim 0.4.10^6$ Btu/hr ft^2). Adjacent can wall average 1300-1400°F. Adjacent can wall maximum 1700-2000°F. (Cooled after shutdown.)	Residual flow in adjacent channel

TABLE 7 (Cont.), reproduced from Ref. 36

TIME	ASSEMBLY FAILURE PROPAGATION	POWER AND FLOW
(sec.)		
	No Propagation*	
500.0	Heat flux into adjacent assembly approaches $0.5.10^6$ Btu/hr ft.^{2} Adjacent can wall average at core outlet = 1600°F - if adjacent flow is 12.5% (If, however, the adjacent flow is 10%, then the maximum sodium temperature there is 1660°F and above boiling.)	Flow of 12.5%

*Propagation is defined by the failure of the second assembly which is imminent following sodium boiling. Therefore, no propagation is defined as the avoidance of boiling sodium temperatures in the adjacent channel.

decay heat. This could be achieved by scramming the pumps by stages separated by an appreciable delay for reassessment of the current condition of the core."

According to the foregoing analysis, the local core accident, which was initiated by the failure of a single fuel pin due to a fuel enrichment error, is terminated, without propagating beyond the affected subassembly, by scramming the reactor at t = 18.3 sec on overpower (110%). The overpower is caused by a reactivity increase of approximately $0.60 due to fuel slumping. No credit was taken for in-core instrumentation.

Detection of Accidents Caused by Fuel-enrichment Errors. It is of interest to evaluate what in-core instrumentation might be able to do to mitigate the consequences of the accident considered, especially since it may be relevant to question, with respect to the analysis presented in Ref. 36, whether the power-level control system might not have counteracted the reactivity effects due to fuel slumping, so that a reactor trip on overpower would not have occurred. In the following, the course of the incident as presented in Ref. 36 is assumed to be valid for the purpose of evaluating the capabilities of the various types of in-core sensors (no attempt was made at reanalyzing the incident):

(1) Anomalous-reactivity Detector. Rather than relying on a reactor trip caused by high neutron flux, it might be considerably better to use anomalous-reactivity detectors for generating a reactor-trip signal. Since the anomalous-reactivity detectors account for changes in the position of the control rods, the danger of not detecting an anomalous reactivity due to compensating action by the control system is eliminated. As was mentioned previously, it is useful to distinguish two levels of sensitivity with respect to anomalous-reactivity detectors, i.e., high sensitivity (capable of detecting reactivity effects due to sodium voiding of a single subassembly) and low sensitivity (capable of detecting fuel movement in a single subassembly).

According to Table 7, anomalous-reactivity detectors of high sensitivity could detect the accident at t $\approx$ 10 sec, whereas those of low

sensitivity could provide a reliable signal at t $\approx$ 18 sec.

(2) Pressure-pulse Sensors. According to Table 7, immediately after the injection of molten fuel from the first failed fuel pin into the coolant, pressure pulses between 500 and 1100 psia are generated within the subassembly. Thus there exists, provided that such pressure pulses can be detected with sufficient reliability by sensors in the upper (or lower) plenum, the possibility for terminating the accident earlier (with substantial reduction in overall damage to the core) than if detected from reactivity effects.

It is not clear at what point in time pressure-pulse sensors could give a reliable signal regarding the occurrence of bulk boiling. This would depend on sodium bubbles rising into the upper part of the subassembly or into the upper plenum and subsequently collapsing. According to Table 7, this might occur at t $\approx$ 10 sec.

(3) Localized-boiling Detectors. As a means for detecting single fuel-pin failure due to a fuel-enrichment error, localized-boiling detectors of high sensitivity might be equally fast as pressure-pulse sensors, capable of sensing the first pressure pulse, since boiling would presumably occur to a substantial degree following the injection of melted UO_2 into the coolant.

(4) Flow Sensors. Flow sensors installed on each individual subassembly conservatively cannot be expected to generate a reliable signal before a 10% flow change has taken place. According to Fig. 3, this might occur when 54% of the cross-sectional area of the coolant passage is affected, or when the fuel failure has propagated to the 6th or 7th row of fuel pins. This might be, according to Table 7, at t $\approx$ 10 sec.

(5) Temperature Sensors. Sensors measuring the coolant temperature at the subassembly outlet would presumably be somewhat slower than flow sensors. The difference would, however, be small. According to Table 7, one might expect a signal at t $\approx$ 10 sec.

(6) Fuel-failure Detector. The delay in obtaining a signal from fuel-failure detectors based on detection of fission products is due, in this case, exclusively to the sampling and detection method used, since fission products are released to the coolant at the very instant the accident is initiated. A fast scheme for detection of fission products, based on sampling streams taken from the outlet of each subassembly, might provide a signal in $\geq$ 15 sec following the rupture of the first fuel pin.

A summary of the results of the above considerations is given in Table 8.

C. Accidents or Malfunctions Affecting the Whole Core

1. Introduction

The class of accidents or malfunctions to be considered in this section is characterized by the fact that from the beginning they affect the whole core, or at least a very large fraction. The problems encountered in the study of this class are therefore of a different nature than those found for the accidents or malfunctions affecting a localized region of the core (as treated in Sect. B). For the localized accident, the main problem is how to obtain as early as possible a dependable signal in order to avoid a power excursion and to limit core damage by corrective action. For the whole-core accident, however, the problem is not so much how to get a dependable signal within acceptable time limits, since this is obtained usually without much difficulty, but rather to limit, through proper design of core and primary cooling system, the highest rate of reactivity insertion due to the accident in question, so as to be able to offset reactivity with a technically feasible and reliable reactor-trip system.

The main accidents or malfunctions of this type are the following:

1) Loss-of-flow accidents, as caused by:

TABLE 8. Approximate Times Required for Various Sensor Types to Generate a Reliable Signal, Subsequent to Failure of a Single Fuel Pin due to a Fuel-enrichment Error

Sensor Type	Approximate Time (sec)
Pressure pulse (fuel-coolant interaction)	1
Localized-boiling	1
Flow	10
Temperature at subassembly outlet	10
Pressure-pulse (bubble collapse)	10
Anomalous reactivity (high sensitivity)	10
Fuel failure	$\geq$15
Anomalous reactivity (low sensitivity)	18

a) Loss of power to, or malfunction of, one or more primary cooling pumps, or

b) Locked rotor of a single primary cooling pump, or

c) Rupture of a pipe in the primary circuit.

2) Reactivity accidents, at full power and at reduced power (e.g., at startup), as caused by:

a) Control-system malfunction or

b) Gas entrainment.

2. Loss-of-flow Accidents

As was pointed out on p.31 , LMFBRs of current design have relatively large safety margins against flow reductions. A flow reduction of ∿50% of nominal value will just raise the outlet coolant temperature to the temperature of clad failure, 800°C; a flow reduction of ∿65% will just lead to sodium boiling at the subassembly outlet. Furthermore, as long as sodium voiding is prevented, there are no reactivity problems, since the combined reactivity effects of the temperature increase of fuel and coolant is small and generally negative. It is only in the subsequent stages of a loss-of-flow accident that reactivity effects may become positive due to sodium voiding of the central core region and possibly due to fuel melting.

The most common cause of a total loss-of-flow accident is reactor trip (or turbine trip) accompanied by loss of off-site power. In that case all power to drive the main primary pumps is lost. The primary pumps will coast down due to their inertia and that of the coolant. It is important that, during the coastdown, sufficient flow be maintained to remove the heat stored in the fuel, while keeping the coolant outlet temperature well below the clad-failure temperature. In order to achieve this it may be desirable to increase artificially the inertia of

the pumps, e.g., by means of flywheels. Once the coastdown transient has passed, sufficient cooling must be provided to remove the decay heat. This may be done by natural convection, by means of smaller emergency cooling pumps, or by pony motors attached to the main pumps and driven from an emergency energy supply (diesel-generators).

Partial loss-of-flow accidents (e.g., loss of a single pump) are usually less severe than the total loss-of-flow accident. However, two types of partial loss-of-flow accidents warrant further attention, i.e., the locked-rotor accident affecting a single pump, and the guillotine rupture of a pipe of the primary circuit between a pump and the inlet to the lower plenum. In the former accident the flow in one loop is assumed to suddenly reduce to zero, whereas in the latter accident the coolant provided by the pump in the affected loop is assumed to be lost, and at the same time coolant from the lower plenum partly bypasses the core by flowing through the ruptured pipe.

For none of these accidents is there any problem in obtaining a signal, because flow sensors on the loop, as well as tachometers, voltmeters, wattmeters, etc., on the pumps should be able to provide, within acceptable time limits, a command signal to trip the reactor.* In this respect, the problems of protection instrumentation for LMFBRs for loss-of-flow accidents are not much different from those for LWRs.

Figures 21 and 22 give coolant temperatures in various locations of the cooling channel subsequent to, respectively, a total loss-of-flow accident and a locked-pump-rotor accident (the latter for a two-loop plant) in a typical LMFBR (see Table 2), with reactor trip on excessive outlet temperature. For both cases, reactor-trip command signals derived from sensors installed on the pumps (tachometer, voltmeter, etc.) would obviously have been much faster than those derived from outlet temperature, and the resulting maximum values of the coolant temperatures would have been lower. However, even for reactor trip on outlet temperature, the coolant temperatures remain well below the 800°C threshold value for clad damage.

* Compounded accidents, in which loss of flow is combined with a failure to trip, will not be dealt with here. In that case, what would otherwise be a small accident not resulting in any core damage may develop into a major accident of the class of a DBA because of the accompanying reactivity effects, if a back-up reactivity-insertion system has not been provided.

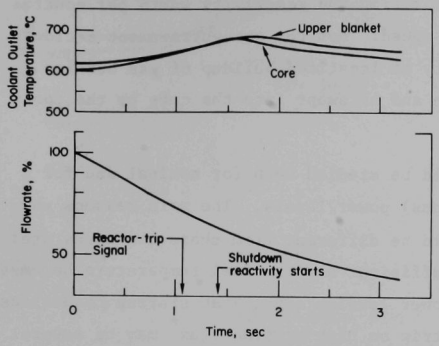

Fig. 21. Coolant Temperatures and Flowrate vs. Time for Pump-coastdown Transient (Total Loss-of-Flow Accident).

It can thus be concluded that protection against this type of accident does not constitute any great problem as regards instrumentation, with respect to both obtaining a timely reactor-trip command signal and avoiding core damage.

3. Reactivity Accidents

Only those accidents that start as reactivity accidents are treated here. Primary sources of direct reactivity insertions are, as mentioned before, malfunction of the control-rod system and the passage through the core of a large quantity of entrained gas. For the latter, voiding of the core region could add ∿$3.6 in reactivity (see Table 2). A void occupying some 28% of the central core region could thus result in a prompt critical excursion.

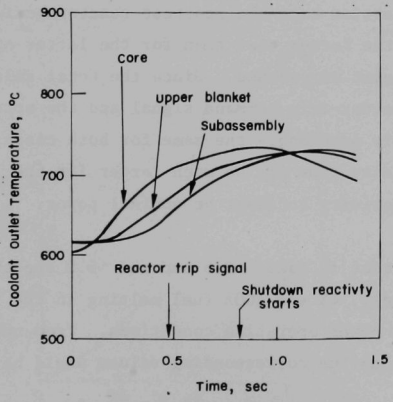

Fig. 22. Coolant Temperatures vs. Time for Sudden 50% Flow-reduction Transient due to Locked Pump Rotor.

Obviously, the solution to these reactivity accidents is to attempt to minimize, by proper design, the maximum possible rates of reactivity insertion, so as to be able to compensate them with that of the reactor-trip system. In the case of an accident due to malfunction of the

control-rod system this means limiting the reactivity worth per control rod as well as the control-rod speed. For the gas-entrainment accident one has to avoid the possibility of localized buildup of gas bubbles that could suddenly break loose and be swept into the core by the coolant flow.

Reactivity accidents should be studied both for nominal and for reduced (e.g., startup conditions) power levels. The main reasons why the course of the accident could be different from these two cases are: (a) the negative reactivity coefficient for the fuel temperature becomes effective more slowly at low power levels, and (b) at startup conditions the nearest point for reactor trip on high neutron flux* may be several decades removed from the level at which the accident starts, whereas at nominal power conditions the set point for reactor trip on high neutron flux is at most some 20% above the nominal neutron-flux value. It is primarily because of this latter difference that the startup accident can be considerably more dangerous than the reactivity accident at power, since for the same reactivity insertion rate the shortest reactor period attained may be much shorter for the former case than for the latter at the moment the reactor-trip set point is reached. Since the total delay time between generation of the reactor-trip command signal and the actual insertion of negative reactivity is presumably the same for both cases, the energy released during this delay time may be much larger for the startup accident than for the reactivity accident at nominal power.

From Fig. 14 it can be seen that it takes ∿3.5 sec and ∿5.0 sec at nominal power to reach, respectively, 4% and 100% fuel melting in the core midplane, starting from full-power operating conditions. From near-zero power at hot-standby conditions the corresponding values would be ∿5.5 sec and 7.0 sec.

The energy released in a reactivity accident can be evaluated very approximately as follows

---

* In many, if not most, present-day power reactors the period trip has been eliminated in favor of a source-range and an intermediate-range trip, because the period trip has proven to be a potential source of spurious reactor trips.

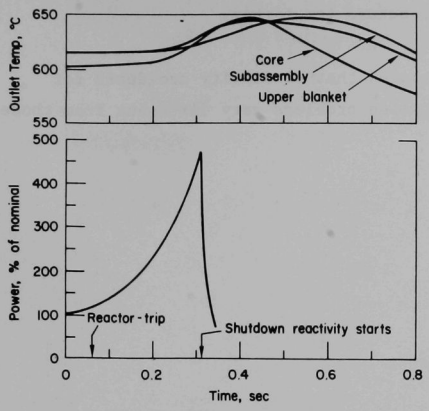

Fig. 23. Coolant Temperatures and Reactor Power vs. Time for \$3/sec Reactivity-insertion Transient.

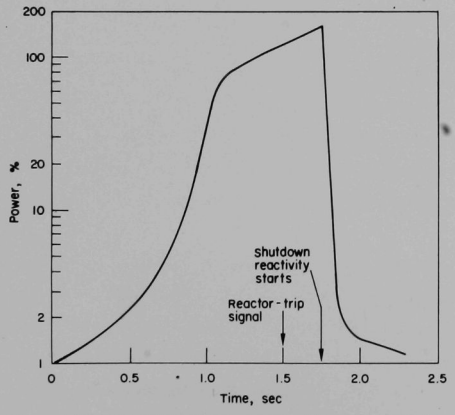

Fig. 24. Reactor Power vs. Time for \$1/sec Reactivity Insertion from 1% of Nominal Power.

$$E = \frac{1}{2} \hat{P} \tau_s \quad ,$$

where $\hat{P}$ is the power peak expressed as a multiple of full power and τ_s the reactor-trip delay time.

Assuming reactor trip to occur on power-range high neutron flux, and assuming τ_s = 0.25 sec, one finds $\hat{P}$ = 28 and $\hat{P}$ = 44 for the peak power levels to be reached during a reactivity accident, in order to result in 4% fuel centerline melting in the core midplane, respectively, for accidents starting from nominal operating conditions, and for accidents starting from zero-power hot-standby conditions.

As examples, Figs. 23 and 24 illustrate effects of reactivity accidents, respectively, at 100% and at 1% of nominal power, at nominal coolant inlet temperature, and with reactor trip on high neutron flux at 120% of nominal power. The reactivity-insertion rates are, respectively, 3 and 1\$ s^{-1}. The maximum values of the power reached are, respectively, 470% and 157% of nominal. These values are much lower than those calculated previously to result in fuel-centerline

melting, so that no fuel damage occurs for either.

In conclusion, it can be stated that reactivity accidents for LMFBRs do not entail instrumentation problems very different from those encountered with LWRs.

III. SENSORS AND MEASUREMENT SYSTEMS

(by W. C. Lipinski, T. P. Mulcahey and K. Porges)

A. Introduction

The environmental requirements for sensors are determined by application, i.e., whole-core measurements vs individual-subassembly measurements. In general, the environmental conditions are more severe under in-core conditions of individual-subassembly measurements. In addition, in-core sensors must be as small as possible so as not to cause significant perturbations in the variable being sensed. Space limitations and accessibility must be considered in the overall problem of transmitting information from the sensor to outside of the core of an LMFBR, and in the installation and maintenance of the sensors, cables, and connectors.

In general, sensing a particular variable represents the first step in a protective chain. In the simplest case, the measured variable is compared to a limiting value in a comparator circuit; if the measured value is outside of limits, i.e., high coolant outlet temperature, low subassembly flow, etc., protective action ensues. In other cases, circuits in addition to a comparator circuit may be required to process the information obtained from a sensor, i.e., reactivity meter, and the sensor and circuits are more appropriately classified as a system.

The overall reliability of a protection system is directly related to the reliability of the individual components. The failure modes of the individual sensors are of paramount importance. Unsafe failures require periodic testing to uncover a sensor failure or, alternately, more advanced methods must be used to program high and low limit values on the sensor output throughout the plant operating range.

Due to inherent random variations around the mean value of a measured variable, limitations are imposed as to how close a trip limit may be set with respect to the mean value of a variable. Similarly,

any errors in calibration, or sensor or circuit drift can influence trip-limit settings.

The instrumentation and control portion of the LMFBR Program Plan describes the state-of-the-art and outlines the development work which remains to be done for sensors, components, circuits, and systems in support of the LMFBR safety program.[37] The specific tasks relating to safety instrumentation are:

Task		Priority
4-3.3.	Systems for the Detection and Location of Failed Fuel	1
4-3.4	Systems for the Detection of Incipient Boiling in Sodium	1
4-4.2	Applications for Computers	1
4-5.1	Multiplexing for Transmission of In-core Signals	3
4-5.3	Cable for Electrical Transmission	1
4-5.4	Connectors for Electric Signal Transmission	1
4-6.1	Metals for Sensors and Cables	1
4-6.2	Electrical Insulators for Sensors and Cables	1
4-7.1	Sensors for the Detection of Neutrons In and Near the Core	1
4-7.3	Temperature Sensor for General Use	1
4-7.5	Sodium Flow Sensors for Use on Fuel Assemblies	1
4-7.7	Pressure Sensors for Use In or Near Core	1
4-7.10	Sodium Level Sensors	1

The LMFBR program plan includes a comprehensive list of references and a bibliography which documents prior work. Therefore, no attempt has been made to duplicate the material of the program plan in all its detail, but a brief review of TREAT, SEFOR, and EBR-II, and some of the latest developments in safety instrumentation are described. Areas requiring future development are indicated. In order to obtain a better comparison with respect to the measurement of a specific variable, the experiences at facilities for each variable are grouped according to the specific measurements.

Boland[38] has discussed the general aspects of in-core instrumentation for thermal and fast reactors. He gives operating principles of in-core systems, accompanied by schematic diagrams.

B. Sensors

1. Neutron Detectors

Introduction. Whole-core as well as local-flux probes have a number of different safety missions, each requiring certain performance characteristics (see p. 73). In particular, prevention of a startup accident calls for a fast-acting flux probe which senses the whole core; loading errors or flux tilt due to other causes can be detected by local probes, etc. These problems are, to be sure, familiar ones in power-reactor instrumentation; however, LMFBR plants, in comparison with conventional water-cooled reactors, imply considerably less favorable detection conditions and more severe environmental conditions.

To cope with these problems, one may choose a conservative or an innovative approach. Conservative design would aim at the maximum exploitation of instruments which have a demonstrated reliability with a minimum number of changes required to meet stricter specifications; this not only takes advantage of established performance, but also makes use of maintenance personnel training, two important safety considerations. At the same time, a consistently conservative policy must eventually lead to a situation in which further adaptation produces unsatisfactory results at considerable expense. When this stage in development of an instrument channel is reached, it is well if a certain investment in new and different possibilities has meanwhile uncovered an alternative system. An innovative instrumentation policy thus must necessarily take the long view, bearing in mind that safety-instrument innovation can defeat its basic purpose if the new system yields only marginal improvements in performance while presenting maintenance personnel with new problems which inevitably generate some psychological resistance. To merit intensive investigation, new approaches must offer substantial prospects of improvement, whether such improvements involve increased

stability and durability of sensors, reduced calibration and maintenance requirements, or considerably enhanced performance parameters, such as sensitivity, speed or reaction, and background discrimination. These remarks apply especially to flux-sensing channels; a number of new sensing and processing methods have been proposed in recent years, while it is increasingly difficult to make do with conventional methods. In the following, we shall consider both conventional and unconventional methods, and attempt to assay the adaptability of each approach.

Whole-core Flux-level Sensing. Flux-level sensing during startup requires a fast response to the level and its rate of change. The hostile environment, as well as the mechanical design, of LMFBR cores militates against detectors of adequate sensitivity being located in the core itself. Thus, a fairly large number of flux sensors, located peripherally at a certain distance, is called for by various design studies for a 1000-MW LMFBR plant. The sensors specified in these plans are conventional, if radiation-hardened, fission chambers; electronic processing of signals is not described in detail.

The preference for fission chambers over other flux sensors is dictated by their very considerable capability to reject γ-ray input in the pulse-counting mode, which is largely a matter of mean fission track ionization versus Compton electron ionization; during startup of an aged core, intense gamma radiation from long-lived fission products and other induced activities calls for the most efficient discrimination possible by any means.

Estimates of the degree of discrimination available from conventional fission chambers vary, partially because the gamma background is usually measured in R/hr, a unit which does not reveal the energy spectrum of the incident radiation on which the counter pulse-height spectrum necessarily depends. In principle, gamma background results largely from Compton electrons released in the counter wall and other surfaces, whence counter geometry and gas pressure must be expected to have a strong influence on the mean pulse height; the intensity increases with the atomic number of wall materials. Further considerations

of this nature, such as pileup, are discussed in Appendix A of Ref. 39. The fission-to-gamma pulse-height ratio for typical commercial counters is very roughly 10^3,[40]; this can be somewhat improved by closer plate spacing as described in Appendix B.

Although this degree of gamma rejection is probably adequate for startup in an LMFBR core, three difficult problems remain which have not thus far been solved in a convincing manner. The first is convenient readout over a range of more than 10 decades; another, connected with the first, is counter deterioration, in particular, due to burnup of fissionable coatings; third, also intimately connected, optimal siting of detectors with respect to the core. A number of studies[40-44] have shown that signals from a single, necessarily highly efficient fission chamber can be processed in such a way as to secure flux and period sensing over the full range.

Such a fission chamber, however, is rapidly depleted if located where it has the necessary sensitivity for startup purposes. Typical full-power fission rates in counters possessing an effective area of 10^3 cm^2 and 200-μg/cm^2 coating thickness come to 4×10^8 fis/sec-cm^2 or 1.2×10^{16} fis/yr-cm^2. The coating thickness of 200 μg/cm^2 is near the upper limit of usable coatings and corresponds to 3×10^{17} atoms uranium/cm^2, which implies a depletion of the order of 4%/yr.

With several detectors, maintenance problems are magnified, but siting can be flexible. A further solution adapted at several ORNL reactors of water-cooled design is a servo-feedback system through which a single counter is withdrawn into a region of attenuated flux,[45] whence this counter can span the whole power regime while maintaining its calibration for a time comparable to the life of the plant. The problem of calibration would become considerably easier if a calibration channel, essentially immune to deterioration, could be provided to check other detectors. A channel of this sort is under development. It is based on Cherenkov light sensing of prompt gamma radiation in a gaseous medium; by adjusting the gas pressure, one can, in principle, discriminate against the softer decay radiation.[46-48] Flux-level sensing through

gamma detection at intermediate and full power has been discussed by several authors.[48-51] In the absence of a calibration channel, fission chambers must be calibrated periodically against irradiated foils,which implies considerable problems; such calibrations can be supplemented by burnup calculations. Finally, burnup can be ameliorated by breeding. Deterioration of insulation, filling gas, and even metal components of fission chambers suggest, at any rate, a policy of frequent replacement.

These problems are to some extent common to systems both with a single sensor and with a number of sensors of different sensitivity. However, the latter type of system admits at least the possibility of withdrawing those counters which have the highest sensitivity after their job is done to a milder environment, where both their fissionable coating and physical structures are not significantly deteriorated. Counters for the intermediate and power range may be located at greater distance from the core or shielded, whence their life is extended. This strategy implies certain switchover problems,[44] which can be ameliorated by providing adequate overlap between operating ranges. This question is evidently closely connected with the means chosen for extracting flux-level information from the signal delivered by sensors of various types. Pulse counting in the source range, and mean-square-current readout in the intermediate and power ranges have been discussed. Further remarks on the mean-square readout technique are presented in Appendix A. Where several detectors are used to span the range, one can build a certain amount of gamma rejection into the detectors for the higher power ranges; such "compensated" chambers deliver current signals only and are thus most directly exploited by dc-current amplification, although Campbelling may also be used if a further increase of the operating range is desirable. On the other hand, special pulse chambers may be employed to obtain digital operation over the whole range from startup to full power. Considerations of statistics require that a given counter run at some 10^3 cps when another counter is reaching its saturation limit. For that reason, conventional fission chambers and electronics, which develop several microseconds of deadtime per event, are hardly adequate: four or more separate detectors and three or more switchovers would be required to span the whole power range. With current pulse equipment,

however, the same range can be covered with two sensors; a third may then be inserted to smooth switchover through extended overlap. Current pulse operation, discussed in Appendix B, is also likely to improve the performance of a Campbelling channel for similar reasons. Practical performance criteria of various means of spanning the whole operating range are presented in Table 9.

Enlarging on the entries of that table, it may be stated that analog systems such as a "Campbelling" channel may not achieve the long-range stability of a digital system, even when the utmost is done to stabilize their performance. With regard to noise, the large number and variety of noise sources within a wide range of frequencies which one finds at a reactor plant site again appear to favor a digital solution. Thirdly, pulse-counting channels can be readily maintained at a desired operating point by pulse-injection techniques;[52] in contrast, a Campbelling channel can be checked out only by interrupting normal operation and injecting a test signal. Finally, on-line digital computation, which is likely to be provided in the future for startup as well as for other chores, is directly compatible only with a digital system, but evidently requires an additional ADC for analog readout systems; the ADC, in turn, must be regulated somehow against drift. It may further be added that switchover problems, which are sometimes cited as a distinct disadvantage of digital, multicounter systems, pertain only for the most primitive, count-and-dump scheme of obtaining the mean channel count rate and its derivative. Digital hardware techniques[53,54] have been described which smooth that particular problem.

The single sensor system, with pulse counting in the lower and mean-square measurement in the upper power range, has been recently developed into operational systems[55,56] which will be extensively tested in the next few years. The pulse-counting channel is made slow because this is believed to provide the best compromise between the different requirements of the mean-square-current and pulse readout. The resultant deadtime of the order of 2 μsec limits pulse counting to 2×10^5 at 10% error. A self-correcting count-rate meter[56] can, however, be employed to reduce this error to less than 1%. If

TABLE 9. Comparative Evaluation of Three Systems of Power-level Sensing

System a.	Pulse counting throughout range, employing two or three sensors (special fission chambers and cables) with 200-MHz current-pulse amplification and fast logic.
System b.	Single sensor, sensitivity adequate for source range; pulse counting in source range, mean-square-current readout in intermediate and power ranges.
System c.	Single sensor, sensitivity adequate in source range, servo-actuated withdrawal.

A. Construction and Installation

1. Siting and Hardware
   a. Requires a number of channels, cables, and other hardware.
   b. Single channel and cable.
   c. Single channel and cable, but requires access for withdrawal system.
2. Mechanical Problems
   a. No special problems unless withdrawal is used (see Item 3).
   b. No special problems.
   c. Considerable mechanical complexity with several peripheral sensors; single centered channel may be possible.
3. Durability
   a. Favorable if most sensitive detectors can be withdrawn.
   b. Unfavorable; single counter must be sensitive for source range, thus depletes strongly in power range.
   c. Favorable; even, low depletion.

B. Electronics (Signal Processing)

1. Stability
   a. Favorable, largely digital.
   b. Less favorable; considerable stabilization of analog circuitry required.
   c. Favorable.
2. Switchover and Matching
   a. Problems with two detectors, only marginal problems with three detectors, provided that suitable electronics are used.
   b. Does not apply.
   c. Does not apply.
3. On-line Testability
   a. Pulse-injection testing can maintain constant performance; immediate failure detection.
   b. Surveillance interruption required for testing; hence, failure detection depends on test interval.
   c. Same as Item a.

Table 9 (Contd.)

4. Computer Compatibility
   a. Directly compatible; constant-statistics readout of power level and period at minimum delay through computer or hardware digital calculator possible over entire range.
   b. Not directly compatible; requires several analog circuits, including ADCs.
   c. Same as Item a.

5. Noise Sensitivity
   a. Favorable, only input stage is noise-sensitive; considerable immunity to noise below MHz frequency range.
   b. Relatively sensitive to noise throughout analog paths.
   c. Same as Item a.

---

difficulties should be experienced with gamma pileup, it should still be possible to reduce the pulse width through the preamplifier and introduce any desired integration at the mean-square channel input; in fact, the prevailing gamma background may well call for a system which employs wideband techniques for the pulse regime and thus can deliver up to 10^7 cps, as discussed below. It is evident that the extension of the overlap region to a higher decade results in a commensurate improvement in statistics as well as benefiting background subraction; at the same time, of course, reduction of the pulse length has a very marked influence on pileup.[39] Tests in a representative gamma background can best determine whether wideband pulse techniques are called for; in this survey, it is opportune to point out that highly reliable amplifiers and logic circuits with nanosecond risetimes, routinely employed in nuclear and high-energy physics for the past several years, are commercially available at modest cost.

To sum up, whole-core flux sensing for a LMFBR implies a number of problems resulting from higher backgrounds, wider power ranges, and stricter performance requirements in comparison with conditions typical for thermal-flux power plants. Several possible solutions to these problems, involving both hardware development and electronics development to a varying degree, have been surveyed. The case for digital techniques has been stressed somewhat more strongly, because such techniques, familiar in experimental physics, are still not widely applied in reactor instrumentation.

In-core Neutron Detectors: Monitoring of in-core neutron flux in reactor plants is chiefly required for purposes of control, which falls outside of the specific area of interest of the present survey. Safety considerations come into play, however, in connection with the detection of loading errors and similar possible causes of local flux distortions, as well as in the detection of delayed neutrons--one of several methods through which cladding failure can be detected. The latter topic is discussed elsewhere; in this section, only neutron detectors potentially suitable for local flux detection are considered.

Such detectors must be physically small, possess a very considerable degree of radiation and environmental insensitivity, and also must develop a signal which can be conveyed through long cables without substantial attenuation or distortion. Typically, a neutron-flux sensor may be incorporated in a capsule or dry well provided for temperature sensors; such temperature test points are planned for some LMFBR designs in every subassembly flow channel and will be attached to the upper grid structure. Neutron sensors potentially capable of meeting these stringent specifications include mainly two types: self-powered detectors and miniaturized fission detectors. Since self-powered detectors have some design features which make them particularly resistant to radiation and temperature, this type of sensor appears to be of considerable interest and warrants a thorough discussion with a view of assaying its potential application in a fast-neutron spectrum and large gamma background. This survey attempts such an assay, concentrating on aspects which have not been thoroughly covered in a growing number of publications on the subject.[66,75]

Self-powered detectors, in brief, directly collect the charge developed by a conductor embedded in an insulating medium, when this arrangement is immersed in a large flux of nuclear radiation.

As the voltage developed across the insulation is very low, the quality of insulation (which inevitably deteriorates due to radiation damage) is far less important than for high-voltage devices such as ionization chambers. Consequently, a thin layer of insulation suffices,

which allows the device to be made very small. The neutron-sensing element is usually a foil or wire, which can be readily combined with a thermocouple junction.[66] Differential readout of two detectors allows a certain degree of background subtraction.[66-75] Inherent background discrimination is secured through choice of materials, with consideration of neutron capture cross sections as well as other cross sections, beta-decay half-lives, and decay energies, as discussed in detail in the following. The presence of beta decay implies a certain equilibriation time for the readout. The specific use of these detectors for neutron-flux monitoring appears to have been first considered by Mittelman et al.,[67] although the observation that cables immersed in a radiation flux deliver weak dc currents was made considerably earlier.[68] Tests of self-powered detectors in water-cooled plants[69] have established their performance in relatively mild gamma backgrounds; the small size of the sensing head makes this type of sensor very useful for flux plotting.[66] The very low detection efficiency* is a clear advantage in measuring correspondingly large flux levels; gradual depletion of the sensing element under continuous exposure can be coped with through calculations or periodic recalibration.

A major question remains, however, concerning the ability of this type of sensor to discriminate against large gamma backgrounds encountered in LMFBR plants, and even larger backgrounds in LMFBR plants with vented fuel. In water-cooled plants, self-powered detectors owe much of their performance quality to the choice of electrode materials with relatively large thermal-neutron capture cross sections; this advantage is again absent in typical fast-breeder neutron spectra. It thus appears that self-powered detectors suitable for use in LMFBR plants may well require somewhat different choices of materials and possibly other changes as well to achieve adequate performance. To consider this question, a somewhat more detailed discussion of the basic mechanisms through which charge is transferred between different

*Typically, 0.1 $\mu A/10^{14}$ (thermal) neutrons/cm^2/sec

media immersed in a neutron and gamma flux appears to be pertinent. Other aspects of self-powered detector design have been thoroughly covered.[66-75]

In this discussion, we neglect heavy-charged-particle emission or recoil as contributing only negligibly to charge transfer; we further neglect slow electrons, which do not have sufficient range, and concentrate attention on fast electrons. Such electrons are generated directly by beta emission and internal conversion, as well as indirectly by various processes involving hard gamma radiation. For heavy elements, Auger electrons following K-shell internal conversion or photoelectric gamma absorption also have sufficient energy to contribute a certain charge-transfer current. The rather complex history of events leading to electron emission can best be coped with by considering certain case histories in conjunction with their mirror images or obverse histories. Integration over the appropriate coordinate space, and over electron range distributions and other variables, yields partial currents proportional to differences in certain averaged macroscopic cross sections. This affords at least a qualitative picture of the dependence of signal and background currents on the choice of materials and geometry.

We shall first apply this treatment to beta decay and internal conversion, and then to electrons resulting from local neutron capture, followed by local gamma-to-electron conversion processes. To simplify discussion, parallel slab geometry is assumed. A <u>beta decay</u> at some interior point P_1 in the detector slab, with the emitted electron coming to rest at some point P_2 in the surrounding insulator, has the obverse process of a beta decay at P_2, with the electron stopping at P_1, if one may neglect for the present actual differences in beta-range distributions. With the further assumption that the slab is thin compared to the mean beta range, one thus obtains a net electron loss from neutron capture processes leading to beta activation in the whole slab, and a net gain from neutron captures activating nuclei in the surrounding medium up to a distance amounting to the mean electron range. The net charging rate or current due to beta emission should

thus be directly proportional to the difference between macroscopic cross sections only:

$$i \sim \phi_n(\Sigma_{nE} - \Sigma_{nS}), \qquad (1)$$

where ϕ_n is the neutron flux, Σ_{nE} the macroscopic capture cross section of the detector electrode medium, and Σ_{nS} the macroscopic capture cross section of the surrounding insulating medium; cross sections and flux are understood to be appropriately integrated. Consideration of electrons whose ranges are short in comparison to detector slab thickness leads to essentially the same result.

Internal conversion (**IC**), usually followed by additional electron emission through the Auger process, may be either prompt (in connection with neutron capture) or delayed (in connection with beta decay). Much as the case of beta decay just treated, it involves only a single coordinate integration. Let P_E = IC overall probability for electrode nuclides (formed by capture and/or decay) and P_S = IC overall probability for surrounding nuclides; then the signal current contribution amounts to

$$i \sim \phi_n(\Sigma_{nE}P_E - \Sigma_{nS}P_s). \qquad (2)$$

Small conversion probabilities are, as mentioned, partially compensated through the generation of several electrons per event; these electrons can contribute to charge transfer to the extent to which their generally modest ranges permit them to escape from the electrode. This consideration suggests very thin electrodes, which, however, still must have adequate conductivity to prevent the buildup of a local field opposing electron transfer. Equations 1 and 2 further point to the importance of choosing a large activation cross section, consonant with the requirement that the electrode must be a good conductor and tolerate high temperatures, and the further requirement of fast decay i.e., short half-life for the neutron capture product. The insulator must contrariwise have a small cross section, in which case insulator decay is relatively unimportant. Unfortunately, strong differences in capture

cross sections are available only for thermal capture. Thus, the net current contribution due to direct beta emission is strongly reduced in a fast-neutron spectrum; moreover, the decay of any activity induced in the insulation will inevitably influence the equilibration time. Certain insulators, such as quartz (with a 2.6-hr half-life for ^{31}Si), are therefore clearly undesirable; even alumina (2.3-min ^{28}Al) or magnesia (9.5-min ^{27}Mg) may make the response too slow. Beryllia (2.7×10^6-yr ^{10}Be) appears most suitable, considering further that this material has a very soft beta emission which tends to reduce the second term in Eqs. 1 and 2, and thus improves the net current. A final remark may be added: the presence of activities featuring electrons of relatively high energies and therefore large range in the coolant requires shielding of the electrode by a sufficient thickness of insulator; the detector thus cannot be arbitrarily small.

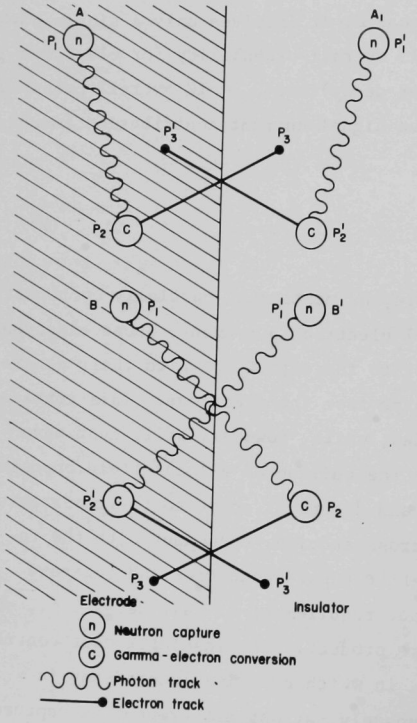

Fig. 25. Charge-transfer Histories

Turning now to the more complex cases of electrons generated by external conversion of gamma rays, a schematic diagram may be helpful: such a diagram, depicting two charge-transfer histories and their obverse histories, is presented in Fig. 25. The history labelled "A" involves neutron capture at internal point P_1, accompanied by gamma emission. The gamma photon subsequently generates a fast electron, say through Compton scattering, at internal point P_2; the electron penetrates the electrode surface and comes to rest at external point P_3. The obverse process, A´,

starts at the image point P_1' and proceeds by analogous stages to P_3'. Another history which leads to charge transfer, Case B, has an internal starting point P_1, external conversion point P_2 and internal end-point P_3; whence, an electron is gained by the electrode slab. The obverse history, from P_1' through P_3', takes away one electron. Again, integrating over all pertinent coordinates, one readily finds a net charging rate

$$i \sim \phi_n(\Sigma_{nE} + \Sigma_{nS})(\Sigma_{\gamma E} - \Sigma_{\gamma S}), \tag{6}$$

where $\Sigma_{\gamma E}$ and $\Sigma_{\gamma S}$ are mean conversion cross sections which include Compton scattering and photoelectric conversion, but not pair production. We note, further, that gamma-ray emission in all these processes may be connected directly with neutron capture or else indirectly following beta decay. The net current contribution is considerably smaller than any contribution from beta decay, since two coordinate integrations are involved; this is, however, made up for to some extent by the multiplicity of gamma radiation.

This exhausts the list of processes for which mirror image or obverse cases can be found, and which therefore are necessarily confined to a distance of the order of the electron range. From further away, only processes which are analogous to histories A′ and B′ contribute to charge transfer: gamma rays emitted by neutron capture anywhere (or, for that matter, following beta decay anywhere) may reach the detector region and thereby cause an electron to pass across the electrode-insulator interface in either direction. The current due to these events is given by

$$i \sim \phi_n'\Sigma_n'(\Sigma_{\gamma E} - \Sigma_{\gamma S}), \tag{7}$$

where Σ_n' is the macroscopic cross section for neutron absorption, averaged over various materials situated in various neutron fluxes ϕ_n' and adjusted for solid angle, as well as attenuation.

Combining all currents, we obtain a net charge-transfer rate

$$i \sim \phi_n \left\{ \left[\Sigma_{nE}(1 + P_E) - \Sigma_{nS}(1 + P_s) \right] + A(\Sigma_{nE} + \Sigma_{nS})(\Sigma_{\gamma E} - \Sigma_{\gamma S}) \right\}$$

$$+ B\phi_n' \Sigma_n' (\Sigma_{\gamma E} - \Sigma_{\gamma S}). \qquad (8)$$

The constant A represents mainly another integration over the coordinate space defined by the mean electron range; constant B represents integration over the whole external space, solid angle, and attenuation. Increasing detector size thus only affects the relative magnitude of the second term in comparison with the other two terms, which approximately scale with size. The third term, of course, contains the main background due to that component of the gamma flux which arises from long-lived activation and fission products (short-lived decays as well as capture and fission gamma flux may be considered as contributing to the signal). The objective of designing a detector responsive to the neutron flux with a short equilibration time is to make the third term small in comparison with the other two. Since this is indeed very difficult to achieve for a fast-neutron spectrum, there remain only the alternatives of devising a subtraction, or else to attempt to make $\Sigma_{\gamma E} - \Sigma_{\gamma S}$ as small as possible, which will also eliminate the second term. The latter stratagem implies materials of comparable density and atomic number for insulator and electrode, with, however, entirely different neutron absorption properties. One possible approach would be the use of different isotopes of the same element, which would make such a detector, assuming it could be constructed to meet other specifications, rather costly. Subtraction would only require two electrode media of very different neutron absorption and similar gamma absorption, or electrode and insulating media with arbitrary but different properties. Let such a choice result in the equality

$$A\left[\left(\Sigma_{nE_1} + \Sigma_{nS_1}\right) + B\left(\phi_n'/\phi_n\right)\Sigma_n'\right]\left(\Sigma_{\gamma E_1} - \Sigma_{\gamma S_1}\right) = \alpha\left[A\left(\Sigma_{nE_2} + \Sigma_{NS_2}\right) + B\left(\phi_n'/\phi_n\right)\Sigma_n'\right]\left(\Sigma_{\gamma E_2} - \Sigma_{\gamma S_2}\right), \qquad (9)$$

where subscripts 1 and 2 refer to the two detectors, respectively, while α is a scale constant; then current subtraction with proportional scaling yields a net difference current

$$i \sim \phi_n \left\{ \left[\alpha \Sigma_{nE_1} \left(1 + P_{E_1} \right) - \Sigma_{nE_2} \left(1 + P_{E_2} \right) \right] - \left[\alpha \Sigma_{nS_1} \left(1 + P_{S_1} \right) - \Sigma_{nS_2} \left(1 + P_{S_2} \right) \right] \right\} . \qquad (10)$$

It must further be considered that proportional subtraction rather than direct subtraction will result in incomplete removal of charge-transfer effects in the cable, which therefore must be subtracted beforehand; this calls for a design with two heads and four cables.

In sum, the design of self-powered neutron sensors for LMFBR safety applications involves a number of difficult problems for which possible solutions, suggested here, still remain to be tried. A final design would then further require extensive testing for reliability and endurance.

These problems lend some emphasis to alternative devices, such as fission counters, which will now be briefly considered. The design of practical fission counters, particularly counters available from commercial sources, reflects the principal market for these counters in reactor control. Accordingly, design has centered on large, highly efficient detectors which deliver linear output over a very wide range of neutron flux. Such detectors also require a relatively large collecting voltage, which implies insulation-noise problems. It may be pointed out, however, that miniaturized counters with a uranium wire electrode and correspondingly small volume can develop an adequate collecting field with much smaller applied voltages; sufficient gas ionization can be maintained by raising the pressure. Detection efficiency in a fast-neutron spectrum, as well as depletion rate, can be designed to have values representative of self-powered detectors. Background discrimination, on the other hand, would be representative of other fission counters, if operation in pulse-counting mode is possible. For

that purpose, the connecting cable must be somewhat more massive than required for self-powered devices; further, the cable must be dimensioned to have an impendance which can be matched by a common-base input amplifier in order to take advantage of the excellent background-discrimination capability of wideband current-pulse amplification. Problems resulting from filling-gas deterioration and fission product buildup may be solved by occasional gas renewal through a gas flow channel in the cable.

Yet another possibility in providing neutron sensing with particularly good gamma discrimination lies in the employment of miniature corona-spark counters with a fission source. The voltage required for such counters, to be sure, is relatively high, but the available signal, pulses of more than 50 V, can be easily distinguished against any channel noise. Spark counters have the lowest gamma sensitivity of any known nuclear detectors and deliver signals which require no amplification. On the other hand, the endurance of these detectors is unknown, while the maximum count rate and therefore the flux range over which linear readout is obtained are limited by considerable deadtime. In designing a suitable device, considerable experience is available from the development and operation of similar devices designed for somewhat different purposes, such as flux plotting.[76]

2. Temperature Sensors

In reports by Popper and Knox,[77] Hochheiser,[78] and Shepard,[79] current practice and problems in temperature measurement are summarized.

Of the base-metal thermocouples, chromel-alumel is preferred for nuclear reactor service because it is relatively immune to thermal-neutron transmutation and because in-service experience has been accumulated at various reactor installations. For longtime service, the upper useful temperature is about 1100°C, which corresponds to the expected sodium outlet temperature during a transient. Commercially fabricated 1/8-in.-OD, stainless steel-sheathed, MgO-insulated, type K (chromel-alumel) thermocouples with insulated junctions provide better than 0.5%

accuracy up to 900°C and have time responses as fast as 0.5 sec for a step change in temperature.[79]

More accurate temperatures can be obtained with resistance thermometers, and under ideal conditions temperatures to within 0.01°F can be measured. Long-term thermal-cycle tests to 800°C at Oak Ridge National Laboratory are now demonstrating drift stability within 1% for commercial, ceramic-insulated, metal-sheathed, platinum resistance thermometers. Further development might produce a temperature sensor for use in fast reactors, if problems of nuclear transmutation, high-temperature insulation leakage, sensor size, and slow thermal response can be overcome.[79]

TREAT Experience. Thermocouple measurements of transient coolant temperatures have been made using stainless steel-sheathed thermocouples of 0.10-cm OD. The time response of the thermocouple for flowing sodium was estimated to be about 0.023 sec.[80]

SEFOR Instrumented Fuel Assembly. The coolant thermocouples consist of chromel-alumel junctions (0.012-in.-diameter wire), MgO insulation, and Inconel sheathing (0.062-in. OD and 0.009-in. wall thickness). The time constant is less than 0.1 sec.

EBR-II Instrumented Subassembly. All coolant thermocouples are of swaged construction, with chromel-alumel thermoelements, alumina insulation, and Type 304 stainless steel sheaths. This type of thermocouple has performed reliably in environments similar to those of the EBR-II core region.

Subassembly inlet-coolant temperatures are monitored by a thermocouple of either 0.04- or 0.0625-in. diameter attached to the lower end of the lead conduit. This thermocouple extends up through the conduit to a point above the bulkhead, where it is attached to flexible chromel-alumel lead wires. Outlet-coolant temperature is monitored by an identical thermocouple attached to the upper end of the conduit.

The results for the XX01 instrumented subassembly have been reported and the actual measured values were very close to the projected values.[81,82]

New Developments

Thermoelectric Method. A temperature-measuring device which offers the additional feature of locating the position of peak temperature along the transducer is offered for special measurement problems. The "Magic Wire" transducers of Continental Sensing, Inc., available in three diameters; 0.15, 0.20, and 0.225 cm, can measure temperature in the range from 93 to 1093°C with an accuracy of ± 1% calibration.

The location range is 93 to 760°C, and only the largest wire also has the location feature. Magic Wire consists of a thermoelectric pair plus a third, insulated conductor having a negative temperature coefficient, all uniformly compacted into a metallic sheath.

As the temperature reaches a maximum at some point, the shunt impedence is lowered, and an output emf equivalent to the standard millivolt output is generated at this point. If several nonequal peaks are located along the length of the transducer, the output emf will correspond to the highest temperature. The third wire is used in an ac bridge to determine the location of the peak temperature.

The time response of temperature measurements using this device is not much different from thermocouples of similar dimensions and materials. The speed of response of the determination of the position of peak temperature is not available and should be determined. If out-of-pile and in-pile tests are performed, they should use complete systems.

Acoustic Method. An acoustic method of measuring high temperatures, based on the temperature dependence of sound velocity in solid sensors, has been used in several applications, and is now under development for application to fast reactors in measuring fuel, cladding,

and coolant temperatures.[83,84]

The system is basically comprised of four parts: transducer, lead-in, sensor, and an electronic instrument. The transducer consists of a coil wound around a suitable magnetostrictive wire. The coil is pulsed, producing an elastic deformation in the wire. An axial wave then propagates along the wire, and is reflected according to the materials and geometric configuration of the line. On return to the coil reflected waves generate a signal due to an inverse magnetostrictive effect. A single thin wire, of ∿1-mm diameter, occupies less space than any practical thermocouple pair.

The time interval between reflections emanating from the beginning and end of the sensor is a measure of its average temperature. This time interval can be automatically measured and displayed on an oscillograph or a commercially available device such as the "Panatherm" produced by Panametrics, Inc. Since extensional and torsional waves propagate at velocities proportional to the square root of Young's modulus, E, and the modulud of rigidity, G, respectively, it is necessary to consider all the possible mechanisms by which the environment may affect these moduli.

The effect of reactions of sensor materials with oxide or carbide fuel materials, absorption or rejection of poorly bound alloying agents such as carbon, nitrogen, or chromium from unstabilized stainless steels used as claddings, and the oxygen, carbon, nitrogen, and other dissolved impurities in the coolant must be considered before confidence in this technique is justified. Radiation effects are estimated to be small.

Candidates for sensor and lead-in materials have been narrowed to W, Re, Ta, Mo, and their alloys for high temperatures and also to stainless steel for temperatures below 870°C. The velocity-temperature characteristics of these materials determine the accuracy of the temperature measurement in conjunction with the sensor length. For example, assuming a time resolution of 0.1 μsec, the length of a rhenium sensor required to yield an accuracy of ±1% at 2500°C is one inch.

Tests performed with empty prototype cladding of the type used in EBR-II fuel demonstrated the feasibility of using the tube itself as an ultrasonic sensor to measure its own average temperature. The effects of the fuel the fuel and sodium bond, however, remain to be investigated. Further, the use of the spiral spacing wire as a sensor was also demonstrated for possible use in measuring coolant temperature external to the clad. Sodium immersion tests performed at Argonne National Laboratory demonstrated that the ultrasonic thermometer can work in sodium. Also, a rhenium sensor was tested at temperatures up to 2760°C.

This application of ultrasonics shows great promise, but much additional development is necessary to realize the potential. The time response is about 100 msec, but this can be decreased by using larger sampling frequencies. Problems arise from spurious echos due to kinks and fastenings.

3. Flowmeters

The quantitative measurement of coolant flow through individual subassemblies or channels in a liquid-metal-cooled fast reactor requires a sensor which is reasonably accurate, has a short time constant, and can reliably operate at temperatures up to 1400°F in a fast-neutron and gamma flux environment. Sensors examined for this application include: permanent and electro-magnet flowmeters, eddy-current flowmeters, and turbine flowmeters.[85] The mechanical configuration of the megnetic or eddy-current flowmeter can be of either the flow-through or probe type.

A transit-time flowmeter employing analysis of thermocouple temperature variations by noise techniques has been proposed, but additional development is required to achieve the required accuracy and transient response.[86-87] Other methods of measuring assembly flow such as differential pressure (Venturi type) flow meters, vortex generators, impact measurements, and sonic techniques, have also been proposed.

The principle of magnetic-flowmeter operation is based upon Faraday's law of induced voltage.[88] As the conducting liquid flows through a tube positioned in a stable magnetic field, a potential is developed across the tube and at right angles to the field in a flow-through type of flowmeter. This potential is proportional to the volumetric flow rate of the liquid and the magnetic flux density. In the probe-type assembly, the magnets are enclosed in a tube and sodium flows past the outer surface of the tube. Successful application of the magnetic flow meter depends on developing magnets capable of producing a stable magnetic flux at temperatures up to at least 1200°F in the presence of nuclear radiation.

The electromagnet flowmeter operates under the same principle as the permanent-magnet flowmeter, except that a coil is used to produce the magnetic flux. The electromagnet flow meter has the following disadvantages: a large amount of power and current is needed to produce a modest flux, the power is not easily transmitted to the meter through reasonable sized leads, and the coils are relatively large.

The eddy-current flowmeter consists of ac-operated primary and secondary sets of coils electromagnetically coupled to a conducting fluid whose flow is to be measured. The coil system is balanced such that, with an ac current in the primary winding and with the fluid stationary, there is no induced voltage in the secondary winding. When the fluid moves, the pattern of the induced currents in the fluid is distorted and the condition of balance no longer exists. The resulting induced secondary voltage serves to measure the fluid velocity.[89] Successful application of the eddy-current flowmeter depends on developing coil assemblies capable of withstanding the high temperature, rates of change of temperature, and nuclear radiation.

Turbine-type flowmeters have been used successfully to measure flow rates in fuel subassemblies of many water-cooled reactors and have also been used, with limited success, to measure sodium flow rates in out-of-

pile loops operating at temperatures up to 1500°F. Successful application of the turbine flowmeter depends on developing bearings for operation in the high-temperature sodium and high-temperature sensing coils capable of withstanding nuclear radiation.

TREAT Experience. Electromagnetic flowmeters have been used routinely in the TREAT loop experiments.[80] Their response is essentially limited by that of the recording oscillographs used for transient data (∿3000 cps, or higher, depending on the galvanometers). In addition, during a severe loop meltdown with seven EBR-II pins, the loop flowmeter detected the flow of molten uranium.[90]

SEFOR Instrumented Fuel Assembly. A permanent magnet flowmeter, mounted on the bottom of the instrumented fuel assembly, consists of an Alnico VI cylindrical magnet canned on the inside and outside with 0.020-in.-thick stainless steel tubes. The meter has an overall length of 7 in. and an outside diameter of 1.84 in. The inside diameter of the test model was 1.20 in., but other throat sizes are used to conform with the orificing pattern across the core radius. The design flow rate is from 12 to 72 gpm. The meter was tested in a sodium flow loop at temperatures up to 1000°F. At 72 gpm, the meter generated a signal of 12.5 mv. The measured strength of the magnet was 648 G.

EBR-II Instrumented Subassembly. A permanent-magnet flowmeter was selected to sense coolant flow rates in the prototype subassembly. This selection was based upon successful operation of a similar unit for over 2000 hr up to 1000°F.[91-92]

The following design criteria have been established:

Geometry	Hexagonal
Distance across flats, in.	1.728
Overall length, in.	9.188
Flow conduit ID, in.	0.625
Maximum flow rate, gpm	60
Pressure drop at 53 gpm, psi	12.5
Integral extension lead wire	
Wire size	24 AWG
Wire length, in.	82
Sheath diameter, in.	0.125

Based upon the expected magnetic flux density and conduit inside diameter, a sensitivity of 0.325 mV/gpm is anticipated at a sodium temperature of 800°F, or about 10.5-mV output at the maximum flow rate (60 gpm).

The results for the xx01 instrumented subassembly were very close to the projected values.[81,82]

New Developments: In support of FFTF, probe-type flowmeters are being developed. In order to circumvent the problems encountered with magnets at high temperatures, effort is focused on flowmeters using the eddy-current principle.[93]

4. Pressure Measurements

The pressure-measuring techniques used in liquid metal systems measure the displacement of an elastic member or the amount of force necessary to restore the elastic member to an undisplaced position. The displacement of the elastic member as a result of applied pressure may be measured directly by means of a transducer contacting the elastic member, or indirectly by measuring the change in volume of a cavity which includes a diaphram or bellows on one side, a capillary, and a measuring elastic member connected to a transducer. Several systems have been used in which the capillary is functionally replaced by a push rod.

The displacement of the elastic member may be measured by a wide variety of transducers:

a) Differential transformer
b) Strain gage
c) Variable inductance
d) Potentiometer
e) Null balance
f) Oscillator
g) Capacitor
h) Photoelectric
i) Ionization
j) Magnetostrictive
k) Thermionic

The major problems encountered in measuring pressure in liquid metal systems are the high temperatures and the damaging effects of liquid metals on the materials used in the sensor portion of the transmitter. Of the above listed transducers, the ones that may be reasonably expected to function in high-temperature liquid metal systems are the first three listed. A discussion of the individual advantages and disadvantages of the listed transducers has been given by Slocomb.[94] An evaluation of potential pressure measurement instruments for sodium service in FFTF was given by Crocker.[95]

TREAT Experience. Pressure transducers exposed to the high transient radiation fields in TREAT respond to both reactor power and integrated power.[96] Power sensitivity has been essentially eliminated by use of certain variable-reluctance transducers or by means of a balancing circuit. For the miniature strain-gauge units used, signals proportional to integrated power have been as high as ∿15% of full scale. (This sensitivity appears as a smooth "zero change" and has been tolerated.) A variable-reluctance unit has been shown to have greatly decreased sensitivity to integrated power. Because of the relatively high dynamic range predicted to be necessary for ceramic experiments in which pin failure may be followed by rapid thermal mixing between coolant and fuel at ∿2500°C, these transducers have been adapted for service in advanced TREAT integral loops.[97] This device is similar to the transducer selected in an independent study as most suitable for the SNAPTRAN-2 transient pressure measurements.[98,99]

5. Core Vibration Sensor

A comprehensive review of the different types of high-temperature accelerometers has been made by Michels, Wilson and Wiegand.[100]

The ANL program on piezoelectric accelerometers currently centers on evaluation and use of a particular accelerometer with an advertised range of 1150°F, Gulton Industries model number 4972. This type of accelerometer has been used with separate flexible cable (asbestos insulation), separate semirigid cable (1/8-in. stainless steel sheathed), and integrally welded semirigid cable (120 ft long, 1/8 in. in diameter, and stainless steel sheathed). This accelerometer was first used at the Core Components Test Loop (CCTL) in conjunction with the boiling-detection program. A second use involved the vibration monitoring of the top, center, and bottom of the two steam superheaters at EBR-II. In this application, the bottom accelerometer became unusable when heated above 800°F, but regained its sensitivity upon cooling.

The main advantage of the high-temperature piezoelectric vibration sensor is its broad frequency response. The acceleration signal is

derived from the force-to-charge conversion by the piezoelectric crystal, with an inertial mass loading one crystal face and the acceleration loading the other crystal face. The low-frequency cutoff is determined by the combination of shunt capacitance of crystal and cable, and conductance of amplifier and cable. Two approaches are to use high input-impedance voltage amplifiers or low input-impedance charge amplifiers. For high-temperature transducers, special charge amplifiers have been designed to offset low cable impedance (by Kistler and Gulton). The upper frequency limit of accelerometers is determined by the mechanical resonance between the inertial mass and transducer compliances. This frequency varies in value between 20 and 150 kHz for most piezoelectric accelerometers. The customary practice in measuring acceleration is to cut off frequencies electrically at one-fifth to one-third of mechanical resonance, depending on the desired accuracy of acceleration measurement.

The design of high-temperature piezoelectric devices is quite difficult because of the wide thermal range involved. Several manufacturers are trying to develop sensors to operate at 1200°F and above for hot monitoring of jet engines (current fast-reactor applications require negligible numbers of units). Obtaining crystals to operate in this range is now feasible, with the recent availability of lithium niobate. Conventional accelerometers which use lead zirconate-titanate, quartz, or lead metaniobate are not operable above 700 to 800°F. Gulton's accelerometers use a custom ceramic which irreversibly degrades between 1150 and 1200°F. Other high-temperature piezoelectric materials are gem-grade tourmaline, which has low output, and lithium gallate, which is extremely brittle and still a laboratory curiosity. Piezoelectric materials can take high compressive loadings, but will fail at comparatively small shear or tensile loads. Thus, mechanical design for a wide temperature range must include sufficient compressive preload at room temperature to prevent crystal fracture upon heating and cooling.

C. Measurement Systems

1. Boiling Detection

The possibility of boiling liquid metals in proposed fast breeder reactors (LMFBR) which have a positive void coefficient has led to a search for various methods of detection of either incipient boiling or of nucleate boiling. The various methods and general approaches are indicated under Task 4-3.4, Systems for the Detection of Incipient Boiling in Sodium, of the LMFBR Program Plan.[37] Of prime importance for any detection system is that it be able to detect boiling and cause corrective steps to be taken before significant damage can occur to the core.

The primary methods of detection of incipient or nucleate boiling being considered at this time are:

a) acoustic;
b) neutronic noise;
c) ultrasonic.

Of these, only the ultrasonic method has the ability to detect incipient boiling; a boiling detector based on ultrasonics gives information about local conditions and must be placed in the core at positions where boiling is most likely to occur. The other two methods can possibly be used to detect small amounts of nucleate boiling.

The method receiving perhaps the most effort at this time is the acoustic method. This method can detect boiling only after it has occurred and thus does not qualify as a detection system for incipient boiling. The method to date shows great promise as a boiling-detection system, but the boiling may be masked in a background of cavitation noise from pumps, etc., plus vibrational noise from other parts of the reactor system. This background noise may be so strong as to obliterate completely noise due to small amounts of boiling in the core. What is needed is an alternative method insensitive to noise not related to void formation in the core.

An alternative to acoustic boiling detection is neutronic-noise boiling detection. This method is based on reactivity effects due to the variation of core physical characteristics such as sodium-bubble formation and collapse, giving rise to fluctuations in the neutron flux. The fluctuation in physical characteristics may be composed of three components:

a) density fluctuation due to sodium void formation by bubbles;
b) temperature fluctuation due to local thermal effects;
c) mechanical fluctuations due to vibrations of nearby fuel pins due to bubble growth and collapse.

The effect of the bubble void on reactivity is position-dependent.[101] Since the sodium-void coefficient is positive near the center of fast reactor cores and negative near the boundaries, there is obviously a position where it is zero. Boiling at such a position would be impossible to detect through analysis. However, it may be possible still to detect boiling from variations of temperature, vibrations, neutron energy spectrum, or spatial shape. Secondly, since a detector receives neutrons from a significant portion of the core, the effect of a small amount of boiling would be "smeared out" thus only large amounts of boiling would be detectable. Still another objection is concerned with the filtering effect of the reactor in transmitting high frequencies. This objection is removed somewhat in a fast reactor since the bandwidth is increased by about three orders of magnitude over water reactors, thus including effects on the power spectrum to about 10 kHz, an order of magnitude higher than that expected from the growth and collapse of sodium vapor bubbles in a subcooled liquid.

Acoustic Boiling Detection. Sounds generated by flowing coolant and pumps tend to obscure boiling signals.[102,103,106] In the NaK-cooled Dounreay Fast Reactor (DFR), the British have successfully detected boiling at full-flow operation. Boiling was produced in the NaK coolant by electrical heaters.[104] Acoustic emissions caused by the boiling were detected by microphones attached to rods which were inserted through the reactor vessel cover into the reactor coolant. The lower end of each rod was in the coolant just above the core. This successful detection of liquid-metal boiling might be explained partly by the fact that DFR

has electromagnetic pumps which produce only moderate turbulence despite in-core flow rates of 30 fps (9 m/s). However, fast breeder reactors for electric-power production most likely would use the more efficient mechanical pumps to produce high flows. How these pumps would affect acoustic boiling detection is still an unresolved question.

Acoustic Monitoring of EBR-II. To determine how background noise might affect boiling detection in a liquid-metal-cooled system employing mechanical pumps, Anderson monitored two sodium systems,[105] EBR-II at the National Reactor Test Station (NRTS) in Idaho, and the Core Components Test Loop (CCTL) at Argonne's sodium facilities. It was found that appreciable flow and pump noise existed in these systems, which may make boiling detection more difficult than for the case of the DFR.

It was found from monitoring EBR-II that the acoustic sound level at full-flow conditions was independent of reactor power for 0, 25, and 50 MWt, and remained relatively constant during full-flow operation during the 10-day monitoring period. The most significant results during these tests were obtained during reduced-flow operation for a reactor physics test. As motor speed was reduced to lower the flow velocities, the frequency spectrum of the accelerometer at the motor housing clearly showed harmonics generated by the bearings. Frequencies and amplitudes of these harmonics were directly proportional to motor speed between 54% flow and full flow (810 rpm). In contrast, sonic and ultrasonic spectra from the throttle valve and the holddowns maintained spectrum shape, but dropped rapidly in amplitude with decreasing flow rate. For the three holddowns, ultrasonic spectra below 20 kHz were comparable, but above 20 kHz they differed markedly. These spectral differences could be caused by different coupling to mechanical structures, and to placement and bonding of individual accelerometers. However, removing and refastening one accelerometer had no effect on signal output. The fact that the spectra were essentially unchanged at 54% flow, suggests that spectral peaks above 20 kHz may be caused more by geometry than by the acoustic source. It may be coincidental that holddown No. I, showing the noisiest signal, was closest to one of the two centrifugal pumps.

Acoustic Monitoring of the Core Components Test Loop. As an independent check on the flow-dependent background noise in EBR-II, Anderson monitored acoustically a similar sodium-flow system, the Core Components Test Loop. Both EBR-II and CCTL have variable-speed control of centrifugal pumps to control flow, secondary-flow throttle valves, argon atmosphere over the sodium, and equivalent system pressures. Test conditions at the CCTL were 1050°F (520°C), with sodium flowing at 400 gpm through 4-in. pipe, at 125-ft head, and for a pump speed of 1000 rpm. For these tests, two accelerometers rated to 1150°F (620°C) were mounted on sodium-filled components. One accelerometer was fastened to a base support of the test vessel, and the other to a rod welded onto the pump discharge line. Conventional accelerometers were attached to the upper pump housing, which incidentally proved quite useful when a slight binding developed in the face-seal bearings. Acoustic noise level at the bearing location was monitored and recorded on 24-hr circular charts, allowing the test program to be completed on schedule without a shutdown due to the pump.

When compared to the primary-sodium-flow noises at EBR-II, signals from the sodium flow system at CCTL had similar amplitudes and flow-related characteristics. Ultrasonic frequencies were attenuated by the relatively massive accelerometers (30-kHz resonance), but signals could be observed up to 20 kHz. As for EBR-II, a noise threshold occurred near 50% flow. At the noise threshold individual "pops" appeared to be ~10-kHz sine waves, decaying with a time constant of 10 to 20 msec. To check the decay behavior of reverberant sound, a hydrophone was pulsed to create sounds inside a water-filled tank of similar construction to the CCTL test vessel. From these tests, the decay of ultrasonic energy (20-100 kHz) corresponded to an equivalent sound-energy absorption coefficient at the tank wall of only 2 to 4%. In addition, amplitude of reverberant sound pressure at the wall of the water-filled tank was greater by an order of magnitude than the pressure of the original sound pulse.

From these results, it was concluded that in sodium-cooled fast breeder reactors, the presence of flow-induced background noise will complicate acoustic detection of boiling sodium. Extrapolation from subcooled boiling tests in water indicates that flow noise and expected boiling noise may be comparable. Therefore, even if boiling experiments show boiling sodium to produce more sound than in comparable water geometries, sensitivity of an acoustic boiling-detection system in a fast breeder reactor still may be limited by flow noise.

High-temperature Sensor Development. In order to resolve the sensitivity problem, high-temperature sensors to be directly immersed in sodium systems are being developed. Sensors for this type of application are as yet unavailable from commercial sources. For reactor use, the irradiation behavior of the piezoelectric material lithium niobate is being examined. Lithium niobate remains piezoelectric to its Curie temperature of 1210°C, but oxygen loss from the crystal may limit its use to below 800°C.

Neutronic-noise Boiling Detection. The state-of-the-art of neutronic-noise boiling detection was reported as part of an overall effort to determine the feasibility of developing a system for detecting the onset of boiling in proposed sodium-cooled LMFBR cores.[107]

The bulk of the literature on neutronic-noise boiling detection is based on experimental applications to water-cooled thermal reactors. Several researchers have detected anomalous noise which they attributed to boiling, although the evidence in some cases was inconclusive. Discrepancies have also appeared in the various reported results. Extrapolation of these results to LMFBRs is further complicated by the differences between the two types of reactor systems. For example, the frequency-filtering effect of an LMFBR is less than that of a thermal water reactor. Also, the boiling bubbles in low-pressure liquid metals are likely to be much larger than in high-pressure water. Further research is required to determine the nature and importance of these differences.

In view of the inadequacy of the available information, it was recommended that an evaluation of the maximum sensitivity of neutronic methods of boiling detection in LMFBRs be initiated using a more basic approach. This approach should rely heavily on theoretical studies to identify and evaluate all aspects of boiling-induced neutron fluctuations, including fluctuations in energy spectrum and spatial shape.

With regard to data acquisition and processing, more recently developed methods of statistical data analysis, such as fast Fourier transform algorithms, cross-correlation, and polarity correlation, should be explored because of their potential in decreasing computational times.

Theoretical identification of the nature of boiling-induced neutronic noise plus the data requirements of the computation procedure will determine the criteria for the data-gathering instrumentation. Evaluation of the feasibility of developing the required instrumentation will be a prime consideration in evaluating the feasibility of neutron-noise boiling detection.

The state-of-the-art report concluded that feasibility of a sodium-boiling detector is within the realm of existing technology, but that further theoretical and experimental research is required to demonstrate the feasibility of neutronic-noise techniques for detection of boiling in LMFBRs, and that many problems related to boiling-induced neutron fluctuations, data gathering, and computer processing of such data must be resolved before an effective system can be developed.

2. Fuel-Failure-Detection System

"Cladding failure" or "fuel failure" are somewhat unspecific designations of complex phenomena ranging from unobtrusive cracks or pinholes in the cladding to a violent disintegration of cladding and fuel. Safety considerations are involved in even milder types of failures to the extent to which there are reasons to believe that such failures can eventually lead to more serious consequences. Specifications for equipment instrumentation for cladding-failure detection thus embrace a wide choice of

requirements with respect to speed, quantitative indication, reliability, and location of the faulty pin in the core.

Most possible requirements - except perhaps quantitative resolution and speed - can be met by adapting instrument schemes originally developed for use in water- and gas-cooled reactors. Some of these have already been tested on existing liquid-metal-cooled reactors, while others would still require considerable engineering development. In addition, advantage may be taken of recent improvements in nuclear detection and computer technology which should allow some different approaches. In adapting existing systems, it is important to heed the lessons learned by experience with similar installations. One of these lessons, which will be stressed in this survey, is the requirement for adequate signal processing or filtering; another is the need for early planning of any hardware which must go into the plant.

Considering, first, minimal failures of the pinhole type, means are readily available to disclose such failures without location. The most convenient and sensitive scheme of discovering loss of hermeticity of any fuel pin is to look for relatively long-lived volatile fission products in the gas blanket. The signal is somewhat obscured by the presence of tramp uranium in the coolant, as well as by previous leaks. New leaks can be readily observed, however, insofar as accumulated fission gases, under considerable pressure inside the cladding, are expelled rapidly enough to cause a significant increase of fission products in a monitor loop through which the blanket gas is circulated. Detection schemes must discriminate against residual sodium vapor as well as activities induced in the blanket gas and its normal impurities. This discrimination is readily feasible by the "charged wire" method;[108-112] the same method has also been developed with charged plates or rods.[113-115] For increased sensitivity, the activity may be stripped from the wire and retained in a small detection volume[116] viewed by a detector which is set for a specific activity. In lieu of the "charged wire" scheme, gas chromatography has been successfully used on some plants.[117-118] The sensitivity of an integrating scheme can be simply estimated if one may assume that the overall transport time of the system is comparable to, or less than, the half-life

of the activity. The equilibrium concentration of that activity contained in the gas volume enclosed by the cladding is then volumetrically sampled by the counting system. To estimate the equilibrium concentration, the porosity of the fuel pin at operating temperature must be known; this information is difficult to establish for specific fuel. However, both theoretical estimates and experience[116] suggest that pinhole failures are indeed detectable.

It may be added that discrimination against tramp uranium and other background can be readily enhanced by tagging fuel pins with a suitable gas, i.e., a gas which activates to a convenient half-life and does not readily dissolve in the coolant, such as any noble gas (except, of course, the blanket gas). Tagging is also useful in connection with location, as discussed below. On the other hand, the appearance of activity in the gas blanket does not indicate the degree of failure, and thus could be connected with a relatively benign pinhole or, equally well, with the structural failure of one or several pins. In the latter case, other monitors, discussed further on, should also yield a signal; hence, the degree of failure can be inferred in principle from several failure detectors even when one of these has relatively poor inherent discrimination capability.

Gas-blanket monitoring clearly fails when fuel pins are vented, as has been proposed in some LMFBR designs. For any other type of fuel, the relative simplicity and reliability of a gas-blanket monitoring installation commends its use for general surveillance, and for confirmation and discrimination in connection with other systems.

With regard to the question of locating pinhole (or more extensive) failures, gas-blanket monitoring can effect a more or less precise location if subassemblies are tagged by including specific volatile isotopes in the internal gas plenum of the fuel pin or by bonding non-volatile tags into the fuel. The judicious use of both methods can evidently further discriminate between pinhole-type and more extensive failures. Both schemes are at present well-established by tests; details are briefly described in Appendix C.

Other available techniques of failure location involve sampling of each subassembly or group of subassemblies with a view of discovering the presence (or enhanced presence) of fission products. Technical possibilities of sampling are further discussed below. If it is assumed for the present that sampling streams of coolant are somehow available outside the reactor enclosure, it should be readily feasible to separate entrained volatile fission products from such a stream by sparging with helium; the sparging stream would probably require further removal of remaining sodium vapor and could thereupon be scanned by a charged-wire system. The system, to be sure, cannot afford to integrate, if it is reasonably assumed that such a system cannot be provided for each subassembly; hence, coolant streams from subassemblies must be cycled through the sparging system for a given time. Charged-plate systems have been specifically designed for such cycling; an advanced version of this system automatically performs background subtraction.[114-115] The sensitivity of the whole unit would depend considerably on the design of the sparger, which would have to be developed. Most sparging systems perform rather poorly; a somewhat better device, used on a water-cooled reactor,[119] might be found adaptable to sodium. Even without considering the sparging efficiency and efficiency of sodium cleanup, the detection efficiency of a sampling detection system is necessarily poorer than that of an integrating system; however, a system designed on the basis of the supposition that time is not very important could execute a logically designed search strategy on command by the more sensitive blanket-gas monitor. Normally, the system would cycle in a regular search so as to detect a more serious leak most expeditiously.

A location scheme based on sampling each subassembly, but cycling sampling streams through fewer detectors, presupposes a steady release of the detected activity from the leak. This implies considerable difficulties with intermittent leaks as well as with very small leaks, for which detection sensitivity may not be sufficient. In that respect, the tagging scheme would be expected to perform better. The possible delay through cycling can be minimized by a search routine, as considered above, in conjunction with a gas-blanket monitor; tagging detection may require more time. It should be stressed again that any system based on

fission gas release or tagging gas release is necessarily inapplicable for vented fuel.

Aside from these possible problems, it appears that location schemes based on the detection of gases released by a fuel failure can be developed for a LMFBR plant. Just as the blanket gas monitors based on similar principles, such location systems can be made sensitive to pinhole failures, but inherently do not discriminate well between such failures and more serious types. At present, there are two different possibilities, tagging or coolant-stream sampling, sparging and cycling. The first scheme requires relatively little on-site hardware, but implies a certain additional cost for fuel; the second implies rather serious hardware development costs, but then can accommodate any hermetic fuel. At the present time, it is not clear which approach is preferable, either for technical or economic reasons, or whether such installations are clearly demanded by the potential danger to the plant posed by a pinhole type of failure, assuming that more serious failures can be detected by other means discussed below. As for the question as to what course of action is indicated by the disclosure of a pinhole leak, this would largely depend on the probability that more troublesome failures gradually develop from small leaks, as well as on the probable time scale of such phenomena.

Considering now failures of "intermediate" type in which a significant area of bare fuel becomes exposed to the flowing coolant, some recent investigations disclose that prolonged exposure to sodium may cause oxide fuel pins to swell.[120] The readily envisioned sequelae to such swelling, promoted by mechanical stress as well as local temperature rise due to flow obstruction, suggest the potential need for a policy of removal of subassemblies containing affected pins from the core, on a controlled time scale. The game of failure location thus admits yet another variant: say that an intermediate failure has been clearly established by a whole-plant monitor; then some rapid and reliable scanning system may be employed during shutdown, when conditions in the core are

amenable to scanning with sensing equipment which for various reasons cannot be left in place permanently. As no detailed instrumentation system of this sort has been proposed, the potential of scanning during shutdown cannot be assessed at present.

Whatever policy of disposal of failed-element-containing subassemblies may be decided upon, the disclosure of intermediate failures, i.e., discrimination between such failures and pinhole failures, is clearly a desirable goal. As discussed above, discrimination is not reliable on the basis of detection of gas release alone; hence some other method is required. In principle, the local temperature rise due to coolant flow obstruction should be detectable, assuming that intermediate-type failures cause such an obstruction, either through swelling or through partial blockage of the flow channel with semidetached cladding, etc. Practically, however, the temperature is sensed only for a whole subassembly, whence the temperature rise would be masked by both fluctuations and sensor instability; similarly, blockage of the flow past one pin would be virtually undetectable with a flowmeter at the present state of the art (see section III.B.3.). This leaves only the option of detecting intermediate failures through the presence of some nonvolatile fission product or nonvolatile tag in the coolant. For failures which may be classified as critical, involving the violent disassembly of fuel pins and emission of debris, one can further attempt to detect the presence of such solid matter.

In comparison with gas-blanket monitoring, the detection of any activity in the coolant is strongly handicapped by the activity of the coolant itself. On the other hand, a certain advantage relative to gas-blanket monitoring stems from the possibility of working with short half-lives; an important consequence is that the occurrence of an intermediate or critical failure can be thus detected with a relatively short announcement delay; further, such a detection scheme can in principle work even with vented fuel. To keep the announcement delay short, however, it is necessary to process the count rate from whatever

detector is chosen in such a way as to avoid low-pass filtering, which is customarily used in count-rate-meter channels. A strong signal, due to the sudden appearance of a relatively large bare fuel surface, will thus result in a rapid rise of the output signal and consequent rapid detection, subject only to the coolant passage delay between core and detector and additional electronic delay (which is sometimes neglected in discussions of detection schemes for transient phenomena). With this "fast" signal-processing mode, the passage of fission product-contaminated debris through the detection volume after a critical failure can be expected to result in a rather characteristic "spike" signal shape, from which one can therefore infer that this type of failure has occurred. Slow (low-pass filter) processing will tend to make this signature difficult to recognize; at the same time, it can retrieve the count-rate increase from a modest bare fuel surface which would tend to be masked by fluctuations in a fast processing channel. This brief discussion may serve to point to the desirability of providing more detail on signal-processing systems in general descriptions of safety-instrumentation schemes; such detail is, in fact, material to the effectiveness of the whole channel. In the foregoing case, it is clear that the combination of a "fast" and a "slow" channel, fed by the same sensing element, can provide fast reaction and signature-recognition capability for strong signals as well as enhanced sensitivity for weak signals. The functional element in this dual channel can be implemented either by analog or digital circuitry; in the latter case, hardware solutions or software programs can be designed to extract information from the signal.[39,121]

Methods available for coolant monitoring include gamma-ray spectroscopy and delayed-neutron detection. Gamma-ray spectroscopy, which must contend with the strong background due to the coolant activity, presents many problems. Although detection of a strong specific activity may be marginally feasible in connection with coded fuel pins, discussed above, the prospects of distinguishing fission product activity from background are poor unless some means can be devised to retain fission products by immersing some device in the coolant stream. This possibility has been

investigated for water-cooled plants;[122] whether it would work for sodium is not known. Evidently, any such retention device results in considerable delay as the activity builds up, and thus could be considered useful only when background discrimination is important enough to sacrifice speed. Moreover, holdup of activity clearly militates against a locating scheme in which coolant streams from different subassemblies are cycled through the same detector. However, if speed of detection is considered unimportant, as in a confirming system intended for location of mild and intermediate failures, concentration of fission products by some means would be useful if phsyical samples of the coolant could be taken from different subassembly streams, through a suitably design sampling valve. The further processing of such samples includes a wide range of different methods, including chemistry and mass spectroscopy as well as gamma ray spectroscopy. For vented fuel, this search would necessarily have to concentrate on the least volatile fission products; samples may even have to be sparged to get rid of gaseous fission activity.

The detection of delayed-neutron precursors in the coolant uniquely circumvents the serious problem of coolant background inherent in the search for other short-lived fission products through gamma-ray detection. At the same time, most of the delayed-neutron precursors have half-lives which are so short that relatively slight delays, due to the passage of fission products through the break in the cladding, will seriously attenuate the available activity, while the signal available at a downstream detector site is also strongly affected by the detailed flow patterns which happen to exist, either in a stable or variable mode, between the failed-element location in the core and the detector. Identical failures in different core locations can thus yield very different signals.

The flow pattern also has a decisive influence on the effectiveness of a given sampling loop intake, whether each subassembly is sampled or a single loop serves to monitor the whole plant, as in the FERD system installed at EBR-II.[123] To secure an acceptable margin of reliability

for this scheme of failure detection, it is thus just as important to design an efficient sampling intake as it is to design the detection station and associated signal-processing equipment. An alternative which may become practically feasible in some plants is to site a detection station on each of the main coolant-circulation ducts, just ahead of the heat exchanger. This is not only highly advantageous from the point of view of speed of indication and S^2/N ratio, but offers substantial freedom from sampling uncertainty and thus is uniquely capable of detecting the passage of a small number of cladding flakes or other pieces of debris, which may readily bypass even efficient sampling loops. A fuller discussion of these siting possibilities may be found in Ref. 39.

Delayed-neutron detection stations tend to be bulky, as considerable graphite moderator is required to make neutron detection effective. This makes any scheme of individual subassembly sampling impractical unless streams from subassemblies are cycled through a small number of detection stations. Some gas- and water-cooled reactor plants have such systems, permanently installed, with as many as several thousand ducts leading to a battery of cycling valves, which feed into a number of detection stations. For a LMFBR plant, this number of penetrations of the primary enclosure is probably counter productive if overall plant safety is considered. However, if one or several cycling valves could be installed within the primary enclosure, valve design could be greatly simplified and only a few penetrations would be required. The same remark applies to sparging which, if carried out within the enclosure, would avoid any need for heating or shielding ducts which lead out of the reactor. A possible alternative to a fixed sampling tube is sampling each subassembly. One might further consider articulated sampling intakes, which may be put into operation only during a refueling shutdown, if mechanical design problems for on-line use should be prohibitive. It need scarcely be added that a shutdown-operated scan system must necessarily be based on a fairly long-lived fission product (which specifically eliminates delayed-neutron detection).

A general remark pertaining to various systems which detect the presence of certain elements in either the coolant or the gas blanket may be added, concerning the solubility of different chemical and physical species in sodium. Recent measurements[124-128] of the solubility of different noble gases furnish some information on the saturation uptake as a function of temperature; however, the exploitation of this information to estimate the signal strength in a certain specific detection scheme is difficult in view of the unknown effect of the mode of emission. For instance, emission of individual atoms from a bare fuel surface would be expected to lead to a considerably greater uptake than the delivery of a gas bubble; considerable variation in uptake is further to be expected with bubble diameter, and thus with local pressure and agitation of the coolant. A similar uncertainty exists relative to the solubility of solids; experience with EBR-I indicates that uranium tends to plate out on stainless surfaces. Following a number of fuel failures, this effect could thus lead to the formation of uranium deposits and their subsequent detachment as flakes, whose passage through the core would produce false failure signals in several of the described detection schemes.

In summary, the detection of various types of cladding failure, as well as the location of the subassembly containing a failed pin, appears technically feasible by a number of different means. A complete system may employ several schemes in some kind of detection and location strategy which depends largely on the type of fuel, the degree of reliability wanted, and other policy matters, not the least, cost. Most of the schemes outlined here exist, if at all, only in prototype form, and considerable development effort would have to be invested particularly in engineering sparging devices, sampling manifolds and valves, cycling valves, and sampling loop intakes. Tests of the alternative location method of xenon tagging are now under way, and fabrication of a number of tagged subassemblies has been undertaken with a view of providing this method of failure location for FFTF. Whether fabrication would be economical on the larger scale implied by a LMFBR core remains

to be determined. More work is evidently desirable concerning the various effects of solubility in sodium of different species on the signals from different detection schemes, particularly detection schemes working with the coolant. Finally, development is needed in the art of signal processing to extract the maximum of information.

The above survey of fuel-failure-detection schemes does not claim to be exhaustive, but is believed to have covered those technical possibilities which currently offer the best prospects. Other techniques, such as ultrasonic scrutiny of structures submersed in sodium, may become feasible in the future. A brief description of certain technical details, amplifying the above discussion, appears in Appendix C.

D. Failure: Modes, Mechanisms, and Detection

1. Introduction

The previous sections have described the principles of operation and availability of types of reactor sensors that may be necessary for monitoring LMFBR core integrity. However, no consideration has yet been given to the realistic use of these sensors. Sensors integrated into monitoring and protection systems have failed in the past, and failures will continue to occur regardless of reliability improvements. If these sensor failures occur in important monitoring or protection systems, the resulting system failure may have serious consequences; therefore, knowledge of sensor failures and how to detect them is important. This section describes the failure modes, failure mechanisms, and methods of failure detection of LMFBR core-monitoring sensors. The descriptions given will only treat the sensor and sensor-related failures, and will not consider the modes, mechanisms, and detection of failure in the electronic information-processing and readout equipment used to display or interpret the primary sensor signals representing the measured parameter.

The organization of this section consists of a few necessary but generalized definitions followed by a detailed discussion of sensor-failure modes, mechanisms, and detection. In the classification of sensors under the discussion of failure mechanisms, an attempt has been made to designate a sensor either by the parameter to be measured or by the method of operation or construction, so that a minimum of redundancy occurs.

Definitions. In any discussion of sensor failures it is best to first define "sensor" and then describe the characteristics which may allow the interpretation of what constitutes a sensor failure.

Sensor. A sensor is any device which is capable of responding to a physical parameter and then transmitting this response information to other devices which may then process or interpret the information. All sensors are characterized by their intended purpose, construction, method of excitation, method of response, as well as by the signal-response characteristics they exhibit; therefore, sensor failures should be characterized by the same attributes.

Sensor Failure. A sensor has failed when it is unable to monitor the intended parameter at the location of the intended measurement within prescribed accuracy limits. The types of sensor failures which will be considered relate to changes in sensor characteristics as a result of changes in the sensor itself or of changes in its relative operation with the devices to which it transmits the parameter information being measured.

A type of sensor failure which will not be considered in this section relates to changes in sensor characteristics as a result of changes in the system in which the sensor is intended to make measurements. An example of such a failure would be a time-response failure due to "crud buildup" on a thermocouple.

2. Failure Modes

The failure mode of a sensor is the direction of change of the signal-parameter relationship as a result of a failure of that sensor. A knowledge of the failure modes or potential failure modes of a particular sensor in a system environment provides insight for design and operation of monitoring and protection systems. A failure-mode analysis is necessary to predict the protection-system response to the sensor failure, thereby determining whether unsafe failures can occur. A failure-mode analysis may also provide insight to methods of examination of sensor signals to detect the possible presence of sensor failures.

There are only three failure modes which characterize sensor failure:

a) The information coming from a sensor will indicate an increase in the measured parameter.

b) The information coming from the sensor will indicate a decrease in the measured parameter.

c) The signal will fail to respond.

These failure modes do not just refer to steady-state informational content from the sensor, but are also concerned with the response of the sensor in time. For example, the increase of the time of response of a sensor to a changing plant parameter may be classified as having a decreased output compared to what it should be indicating. A sensor fails in one of these three ways where the particular signal is not only a function of the sensor characteristics, but also of the system or environment in which this sensor is placed. For example, if the two dissimilar wires making up a thermocouple short and form a junction which is not in the area of the original junction, any one of the three failure modes may exist. If the new junction is in an environment of a higher temperature than the original junction, the thermocouple generated will indicate a higher temperature than anticipated. If the temperatures of the original and shorted junctions are the same, there will be no change in signal output; however, the temperature being monitored is no longer the one originally intended. If the new shorted junction is at a lower temperature than the original junction, the signal output will indicate a decrease in indicated temperature. For another example, using a different mechanism of failure of a thermocouple, the open circuit, the modes of failure which can exist are either decreasing or failure-to-respond. If the circuit resistance with the open circuit existing is sufficiently low and the capacitance of the instrument readout system is sufficiently low, the value indicated by the thermocouple signal will decrease due to the removal of the source. However, if the thermocouple

circuit resistance is sufficiently high and there is sufficient capacitance in the circuit, the only indication of a thermocouple failure may be the failure of the thermocouple to respond to changes in the variable being monitored.

In the following section most of the types of sensors considered for LMFBR application will be discussed and the possible failure modes indicated.

3. Failure Mechanisms

Mechanisms of failure are the descriptions given to the physical, chemical, or electrical changes which result in alteration of the characteristic of a sensor so as to place its usefulness outside the acceptable range. The mechanisms of failure may be physical in nature: for example, leaks, broken parts, changes in system-component behavior such as magnet field or spring tension or compression or other physical parameter changes, or they may be chemical or electrical, or any combination of the three. Examples of chemical changes are corrosion, absorption of water by MgO insulators, chemical decomposition of material, or chemical changes as a result of transmutation of elements. Examples of electrical changes are changes in EMF output, ionization, resistance, capacitance, or inductance.

Failures usually, but not always, result in changes in magnitude of the sensor signals, indicating changes in sensitivity, accuracy, repeatability, range, speed of response, or stability. Failures can also be classified as slow or sudden, depending upon the relative time scale involved. Drift is also a characteristic of all sensor signals, and care should be exercised to exclude normal drift characteristics from consideration as long as the drift is within acceptable limits. There are mechanisms of failure, however, which cause an apparent signal drift; these will be discussed under the particular transducer involved. "Normal drift" as used here is applied to those changes in the information output from the sensor that are a result of either changes in the

sensor environment other than the parameter being measured or small variations in the sensor characteristics. Drift is considered further in Sect. III. E.

The mechanisms of failure to be discussed are divided into two types:

a) mechanical failures dealing with the structural integrity of the sensor itself;

b) operation or response failure dealing with the sensing and transmission characteristics of the sensor.

Seven important mechanisms of mechanical failure are:

a) leaks of sodium, gas or water vapor or other material into or out of a sensor as a result of

i. broken hermetic seals
ii. broken sheath
iii. broken diaphragms;

b) thermal and mechanical stresses resulting in broken or changed internal configuration as a result of

i. differential coefficients of thermal expansion
ii. thermal or mechanical shock
iii. vibration
iv. thermal or mechanical cycling or fatigue
v. overheating - overstressing;

c) wear or erosion;

d) crud buildup within liquid-metal-filled sensor components, resulting in increased time response or failure to respond;

e) sensor positional changes resulting in misinterpretation of the sensor output;

f) degradation of material strength properties due to radiation effects, resulting in signal error;

g) degradation of material strength properties due to chemical corrosion effects, resulting in signal error.

The above mechanical failures can also result in sensor or signal-transmission failure.

The important operational or response failure mechanisms dealing with sensing and signal transmission which are electrical or chemical depend upon the basic mechanism of information gathering and transmission. Some of the types of electrical failures dealing with sensors for use of LMFBR systems are:

a) an open circuit in the signal-transmission path;

b) a short circuit in the signal-transmission path;

c) shorting of the one leg of a signal path to ground;

d) degradation of components by temperature; for example

i. decrease of magnetic flux in a permanent magnet due to annealing

ii. change in sensitivity of piezoelectric materials;

e) changes in resistance, capacitance, inductance, permeability, or magnetic flux due to radiation damage or transmutation;

f) induced electrical noise from vibration;

g) electrical arcing due to electrical ionization;

h) degradation of component sensitivities by ionizing radiation;

i) degradation of sensor stability or sensitivity due to changes in excitation frequency;

j) changes in emf output of thermocouple due to material re-crystalization or transmutation.

Some important mechanical operational or response failure mechanisms include:

a) changes in spring constants of bellows and spring assemblies due to temperature or radiation effects;

b) changes in friction coefficients, causing mechanical positional errors;

c) changes in time response or response characteristics due to foreign material buildup within sensors or sensor transmission lines, such as

i. sodium oxide plugging of sodium-filled capillary tubes
ii. presence of gas in capillary tubes.

In the remainder of this section an attempt will be made to discuss the principle of mechanisms of failure of particular types of sensors as well as of general types of sensors. In this discussion the

classification method for sensors will present the important mechanisms of failure in a nonrepetitious manner. The classification is based partly on the parameter to be measured, such as temperature or neutron flux, and partly on construction types, such as piezoelectric, inductance, and resistance. In some instances the description of failure mechanisms will apply to a particular type and construction of sensor, such as an acoustic temperature monitor; in other cases it will apply to a general type of transducer material which can be used in many types of sensors, such as a piezoelectric crystal.

Radiation Effects. Radiation can affect both electrical and mechanical properties and components of sensors. Therefore, all sensors to be located near or adjacent to a nuclear reactor must be constructed to compensate for these effects or be replaceable within a time duration such that the effects will not cause significant errors to occur within the sensors. Some of the electrical and mechanical effects of radiation on sensors and sensor materials are as follows.

Ionizing radiation. Ionizing radiation can cause changes in the electrical conductances of the basic sensor materials, causing shifts of the sensor signals. The ionizing radiation can also cause charge buildup and discharge, which increase the noise level within the sensor materials. Radiation absorption also causes an increase of temperature within the sensor materials; this may cause materials to exceed their temperature limits or cause mechanical-thermal stresses within the materials. Radiation effects caused by either ionizing radiation or neutron radiation may change the basic properties of the materials present due to transmutation of the elements or breakdown of the structure of the basic sensor material. Dielectric or insulator breakdown due to structural breakdown in the sensors can cause changes in resistance, capacitance, or inductance, thereby causing errors. Mechanical changes which can occur due to irradiation are the embrittlement of the transducer metals and structural materials such that they can no longer withstand the environment.

Examples of the effect of reactor radiation on sensor materials are as follows:

a) Neutron radiation of thermocouples is reported to cause a shift of up to 4-5% in the emf output for even some of the most radiation-resistant materials such as chromel-alumel.

b) Piezoelectric devices are sensitive to gamma and beta radiations.

Temperature Measurement. Three methods of measurement of temperature that may be useful for LMFBR application rely on the use of the thermocouple, resistance thermometers, and acoustic methods. Sheathed thermocouples are the most highly developed. The mechanisms of failure of thermocouples are a short circuit between lead materials, a short circuit between lead materials and an electrical ground, an open circuit, decalibration of emf output due to neutron irradiation, and changes in emf output due to changes in insulation resistance. Other mechanisms of failure can occur when foreign material is present in a high-temperature zone to serve as an electrolyte. For example, voltage generated by galvanic action between dissimilar wires can cause a change in emf. Voltages generated in parallel with the thermocouple wires can cause either an increasing or decreasing failure mode depending upon materials and construction. The "parallel voltage" mechanism is not usually found with common LMFBR thermocouple materials and construction, and the effect of the parallel voltage generated may be removed by the use of proper amplification and display equipment. The short circuit between lead materials has already been covered as an example under the discussion of failure modes. The open circuit was also covered as an example. The change in emf output due to neutron irradiation is a gradual effect and results in either a decreasing or increasing mode of failure depending on the thermocouple materials present. The presence of water vapor within the insulation of the thermocouple results in a decreasing mode of failure. The effect of a

failure of an ungrounded thermocouple becoming a grounded thermocouple depends upon the readout instrumentation and the presence of electrical noise within the system; no generalizations can be made.

Resistance thermometers depend upon the change in resistance of an element to determine temperature and will be included in the general discussion of resistance devices.

The acoustic method of temperature monitoring depends upon the thermally induced change of sound velocity. The change in sound velocity is related to Young's modulus and the material density for longitudinal sound waves, and to shear modulus and density for shear waves. The method of operation is as follows:

A wire contained in a sheath is pulsed with a high-frequency acoustic energy, and the time to the receipt of the reflected energy from points of change in acoustic impedance is monitored. Reflections from acoustic discontinuities, such as change of cross section or sharp bends in the wire, are used to provide the basis for timing. The acoustic device is an averaging device in that it registers the change in the reciprocal of velocity of sound over a length of the wire between discontinuities. The length of wire used as a sensor element has a minimum requirement (of possibly a few inches) which is dependent on the frequency of the acoustic signal. This device is basically simple and depends only upon the very accurate external measurement of time for an acoustic pulse to travel the length of the sensor section of the wire. Two types of failure can occur that affect the acoustic energy as it travels in the wire. If mechanical failures allow good contact with the surrounding environment, then either the acoustic energy may be dissipated in the surrounding material and insufficient signal will be returned to read accurately the time difference, or the resulting acoustic-impedance reflections will obscure the desired signal. Another failure mechanism that could happen would be a break in the sensor section of the wire, which would give a decreasing mode of failure. A

poor coupling between the wire and the acoustic transponder could cause the signal to become lost in the base noise of the instrument.

Flow Measurement: The principal method for the measurement of sodium flow in LMFBRs is the permanent-magnet (PM) flow-through type of flowmeter. This device is self-excited, and has an output which is proportional to the magnetic flux and the velocity of sodium through the magnetic flux. The mechanisms of failure may be by open circuit or short circuit of the lead wires, or changes in the magnetic flux strength within the gap between the magnets due to mechanical considerations or changes of field strength of the permanent magnet. Any physical, chemical, or electrical effect which decreases magnetic field strength within the sodium-flow tube decreases electrical resistance of the insulator or affects the continuity of the electrical leads; this produces a decreasing mode of failure. A possible zero offset due to an emf generated by a thermocouple junction formed between the lead wires and some other material within the flowmeter could produce an increasing or decreasing mode of failure. In the construction of the flowmeter the leads are normally attached to the metal of the flowmeter assembly on opposite sides of the flow tube, thus giving a very low resistance value between sensor leads. A decrease in resistance of any insulator material, such as might be caused by water vapor, or an electrical short to ground in the lead or within the flowmeter, would be very difficult to detect by any testing technique. A probe-type PM flow monitor is under development in which the sodium flow is on the exterior of the probe. This device will have the same mechanisms of failure as the flow-through type.

The eddy-current probe flowsensor is an externally excited device which depends upon the displacement of a magnetic flux in the direction of travel of the sodium to unbalance the voltage induced in one or more coils to produce a signal proportional to flow. One basic construction involves the use of three coils; one coil is excited, and the other two coils, located on either side of the excited coil, are connected in series with opposing voltages. This arrangement produces a signal due to an unbalance in the induced voltage of the coils when the magnetic

flux generated by the center coil is displaced downstream. The possible mechanisms of failure are open and short circuits. The modes of failure for a short circuit can either be in the increasing direction or decreasing direction, depending upon where the short circuit exists. The open circuit would cause a decreasing mode of failure.

The eddy-current flowmeter could possibly have a fail-to-respond type of mode failure; however, this would require several simultaneous failures which have a very low probability of occuring at one time. The mechanism most likely to cause failure would be shorting of one coil to ground or the shorting of two turns within a coil. The mode of failure is either increasing or decreasing, depending upon which coil fails.

The flow-through type of eddy-current flowmeter may have the exciting coils around a pipe with the receiving coils in the center of the pipe; however, the method of operation and modes of failure are the same.

An acoustic flow monitor exists which depends upon the transmission of an acoustic signal both upstream and downstream within the flowing media. Sensors located a known distance from the transmission source receive the acoustic signal, and the phase shift of the two received signals is compared. Under steady-state flow conditions, if the transmitter and receivers are working, the signals being received are of the same frequency as transmitted. Therefore, the modes of failure of this device depend upon whether the transmitter or the receivers fail. If the transmitter fails, the known frequency is no longer present, and the differential phase between the two receiver signals reduces to zero, indicating a decreasing mode of failure. If, however, either receiver fails, the phase difference between the two receivers becomes oscillatory or of constantly increasing phase, depending upon the circuit used to make the comparison. However, for this type of flowmeter it may not matter which mechanism of failure occurs, since the use of another technique is possible to monitor the system operation: the presence of the transmitted acoustic frequency at each receiver can be monitored by the electronic readout equipment; failure to receive a signal of

that frequency is an indication of a transmitter or receiver failure.

A similar technique for acoustic flow monitoring which is being developed is to determine the time or time difference between receipt of a transmitted acoustic pulse by an upstream and/or downstream receiver. The change in the time or time difference between zero flow and full flow should be a linear function of flow rate. The baic failure modes of this technique are also dependent on whether the receivers or transmitters fail and, as with the continuous acoustic transmission, other electric mechanisms are available to detect failures.

The basic mechanism used in pressure-drop flow-monitoring depends upon the relationship of pressure and velocity and is usually sensed by a differential pressure device. The Venturi and orifice flowmeters are of this type. This type of flowmetering may have an increasing, decreasing or failure-to-respond mode of failure corresponding to the types of failure of the pressure sensors used.

Pressure Sensors. The types of pressure sensors used may be Bourdon tube, diaphragm, bellows, or a manometer type of device. They may also be null-balance or displacement devices. Bourdon tube, diaphragm, and bellows types of transducers when used as displacement devices are entirely mechanical in operation up to the point where the displacement is to be monitored and as a result is only subjected to the mechanical types of failure. The measurement of the displacement generated by these devices may be performed by mechanical, optical, or electrical (inductance, capacitance, resistance, piezoelectric) devices which in turn have their basic mechanism of failure. If the sensor is a null-balance device, the basic displacement is not allowed to take place by applying a counterbalancing force which must be controlled to maintain zero displacement. In this case the actual measurement that is made is the magnitude of the counterbalancing force. The addition of null-balance capability to the basic sensor complicates the failure-mode analysis and contributes to the types of failure mechanism which can occur. Because of the complications involved, no general restrictions can be placed on the possible failure modes.

Bellows and diaphragm types of sensors are used to separate one medium on one side of a barrier from the medium on the other side. The barrier used in high-temperature transducers is of metallic construction for which the expansion and contraction are limited in magnitude and direction. There are two important types of sensor construction which utilize bellows or diaphragms. One is the null-balance sensor, in which the barrier always remains in the same position due to a balanced force on both sides of the diaphragm or bellows. This allows the chamber of the bellows on the measurement side to be maintained at a constant and known volume regardless of the magnitude of the force exerted on the barrier. The other type of bellows arrangement allows a change in volume of the bellows on one side in order to increase the pressure or displacement on the other side of the bellows. Each arrangement has its advantages and disadvantages for performing measurements.

The mechanism of construction of the bellows incorporates an effective spring constant which may or may not vary as a function of the displacement of the diaphragm of the bellows. Bellows are usually used for the measurement of pressure or force. The modes of failure of bellows-type sensors are structural in nature, and, for the displacement bellows, may result in a decreasing, increasing, or stationary mode of failure. Temperature effects may relax the spring constants of the bellows assembly and allow overexpansion for a given pressure or force. Embrittlement or hardening of the bellows material may allow an increase in the spring constant, thereby indicating a decreased sensitivity, or the bellows or diaphragm of the bellows may rupture, allowing the materials in the separated chambers to mix. With the displacement bellows, the actual measurement is usually performed a distance away from the bellows or sensor assembly by another device which is sensitive to the presure or volume displacement of the original bellows.

Bellows devices are being developed for the measurement of sodium flow, pressure, and level.

Monitoring Neutron Flux. The principal devices that may be used to monitor neutron-flux information in an LMFBR are uncompensated and compensated ion chambers, fission chambers, self-powered detectors, and thermopiles.

Compensated ion chamber (CIC). This type of ionization chamber requires external voltage sources for excitation of the chamber. The chamber consists of two chambers of effectively identical configuration with an inner connecting gas space; one chamber measures both gamma flux and neutron flux, and the other chamber measures only gamma flux. The two chambers are connected such that the output of one subtracts from the other, thereby resulting in only the neutron signals being contained in the output. CICs, if initially hooked up and adjusted correctly, and assured of voltage sources of the proper values, can fail in either the increasing or decreasing mode. The failure-to-respond mode is unlikely to occur if the neutron signal is easily distinguished from the gamma background. The various mechanisms of failure which can occur are the following:

a) loss of voltage to the gamma chamber;

b) loss of voltage to the neutron-plus-gamma chamber;

c) loss of all voltage;

d) open circuit (failure modes equivalent to loss-of-voltage mechanism);

e) degradation of sensitivity due to the loss of sensitive material from gamma-plus-neutron chamber or both chambers (filler gas);

f) changes of sensitivity due to the gain or exchange of gas within the chamber;

g) cable breakdown (electrical).

This type of chamber is usually filled with gas at one atmosphere and at room temperature. Reactor operation will be at higher temperature, so that the chamber will probably have a higher internal pressure than its environment. The most probable result of a chamber leak would therefore be the loss of filler gas, which reduces the sensitivity of the chamber to both neutrons and gammas, giving a decreasing-mode failure. The exchange of gas within the chamber as a result of having an initial vacuum or creating a vacuum in the chamber by cooling can cause unbalanced chamber operation, and at the same time increased gamma and neutron sensitivity; the resulting mode of failure cannot be determined without knowledge of the gases and chamber construction and the location of the leak. The loss of neutron-sensitive material also can result in only a decreasing mode of failure. The loss of voltage to the gamma chamber will cause an increasing mode of failure, and the loss of voltage to the gamma-plus-neutron chamber will cause a decreasing mode of failure due to a change in polarity. The loss of all voltage will cause a decreasing mode of failure. An open circuit will cause an increasing or decreasing mode of failure, depending upon which circuit is interrupted; this malfunction of the chamber is equivalent to the loss-of-voltage failure already described, with the loss of signal lead equivalent to the loss of all voltage.

Fission Chamber and Uncompensated Ion Chamber. The fission chamber and uncompensated ion chamber, like the compensated ion chamber, depend upon an external source of emf or excitation. Operation of the fission counter depends upon the absorption of neutrons by a fissionable material and the production of heavy ionized particles. When operated as a counting chamber, the use of a discriminator allows selection of pulse height, making the fission counter much more sensitive to neutrons than the uncompensated ion chamber. When operated as a current chamber, the uncompensated ion chamber and fission chamber are very similar, both being sensitive to neutrons and gammas. The potential neutron sensitivity of the fission chamber is slightly greater than that of the uncompensated ion chamber due to the larger number of ion pairs produced by uranium and plutonium fission products compared to boron. When used as a current

chamber, the mechanisms of failure are the same as for the CIC except there is only one chamber and hence only one voltage applied.

There is an additional mechanism of failure when one of these chambers is used as a counting chamber. Changes in capacitance due to changes in configuration or mechanical breakage can cause increased response time and hence a lower saturation level in counting. Thus the increase in capacitance would cause a decreasing mode of failure.

All mechanisms of failure originating within the sensor itself, except the short circuit, will produce a decreasing mode of failure; however, electrical breakdown of cable or seal or chamber short circuit can cause an increasing mode of failure.

In the different types of ion chambers, failures can occur which may not be apparent while operating in the usual operating range of a chamber; however, these failures can cause the operating characteristics of the chamber to shift such that the neutron sensitivity changes in a nonlinear manner as a function of power level. This may occur if the voltage characteristics of the chamber change such that saturation of the chamber occurs. This effect would result in a decreasing mode of failure, since the chamber reading would be less than the actual value. Testing for such a failure would require recalibration of the chamber at the higher power levels or off-line measurement of chamber characteristic to determine if changes are occurring.

Self-powered Detectors. The self-powered detector requires no external excitation voltage and depends upon the emission of beta particles during decay of neutron-activated materials. The construction of this detector is such that there is an insulator material surrounding the central beta-emitting material. A collector material surrounds the insulator material. The electrons emitted by the beta-active material are of sufficient energy to pass through the insulator material and be collected on the collection surface. The current thus produced is monitored external to the detector. Since gamma radiation also induces high-speed electrons, the chamber will be sensitive to both

gamma and neutron radiation, dependent upon the relative cross sections of the materials and electrons present and the energy of the incident gamma radiation. The principal mechanisms of failure will be short circuits or open circuits, both being a decreasing mode of failure.

Thermopile. A thermopile consists of a series of thermocouples whose hot junctions are encased in fissionable material such that the difference in temperature of the junctions is proportional to the fission rate. The principle mechanisms of failure would be opens and shorts, and the modes of failure would be identical to those of thermocouples.

Other Sensors. Outside of the four principal measurement methods already discussed, the distinction of sensors by measurement function, such as sodium level, pressure, strain, and vibration, becomes difficult since the basic elements of the sensors can perform different measurement functions depending upon the method of sensor construction. For example, a piezoelectric device basically indicates a displacement or crystal distortion, and it can be incorporated into devices for measuring displacement, vibration, pressure, acceleration, sodium level, and acoustic energy. Because of this overlap of basic techniques for measurement, the basic measurement devices and their mechanisms and modes of failure will be discussed separately.

The basic electrical techniques usually used in LMFBR instrumentation involve magnetic-flux and piezoelectric effects, or the creation of changes in inductance, resistance, and capacitance. Each of these techniques has its unique problems and mechanisms of failure.

Piezoelectric devices. Piezoelectric devices depend upon the transmission of forces to the crystal to form distortions within the crystal; these distortions then generate a charge displacement in the crystal. The net flow of electric charge is transmitted to the readout instrumentation through the lead wires of the sensor. The mechanisms of failure that can occur in this type of sensor may occur anywhere along the chain just described. For instance, a decrease or

lack of the transmission of the force necessary to distort the crystal may change the sensitivity of the instrument, or the crystal efficiency for electromechanical conversion may decrease the transmission of acoustic energy to the crystal. The change in electrical resistance or piezoelectric activity of the crystal may change the characteristic sensitivity with regard to the amount of electrical charge generated. The changes in the impedance in the connecting cable may also change the sensitivity of the device. Each of these mechanisms of failure will result in a decreasing mode of failure for piezoelectric transducers.

An electrical short circuit or a mechanical open circuit may reduce the output of the transducer to zero. An open circuit in the electrical portion of the transducer may result in the failure-to-respond mode if the capacitance of the transducer is sufficient to maintain the charge on the electronic readout equipment, that is, providing the desired signal is the dc level or charge level rather than the ac signal or fluctuation level output from the transducer. If the ac fluctuation output from the transducer is the desired signal, then an electrical open circuit will result in a decreasing mode of failure. There is one "increasing" mode of failure which might occur in piezoelectric transducers of a very unique design. This mechanism of failure depends upon the construction and method of mounting of the piezoelectric crystal within the sensor. Normally, piezoelectric crystals are mounted with the distortion force being applied to either the X, Y, or Z axis. If such a mounting is used and the mechanical failure which occurs causes a bending moment on the crystal, a slight increase in transducer output may occur with certain piezoelectric materials. Of course, internal stresses may also cause the crystal to break or to lose sensitivity due to changes of elasticity. Also, gas buildup by radioactive decay of crystal materials could lead to fracture of the brittle crystal material.

Inductance. Inductance devices are based on the premise that an ac current of fixed frequency will vary in a coil or a series of coils as the magnetic permeability of the space around the coil varies. The variation of the magnetic permeability may be caused by

the displacement of the material within a coil or the replacement of one material by another. For example, the permeability of a coil will change if magnetic material is removed from a coil or if a liquid such as sodium replaces a gas such as argon within the area of the coil.

Some inductance devices depend upon the transmission of signals from one coil to another coil through a transformer effect. Under operating conditions the amount of signal being transmitted depends upon the distance and the properties of the material between the two coils.

The mechanisms of failure of inductance devices are those principally associated with coils and coil configurations. This includes the shorting of adjacent turns within the coil to decrease the impedance of a particular coil or the mechanical displacement of one coil relative to another, thus changing the inductance path of the magnetic field. The modes of failure can be increasing or decreasing in nature, depending upon the initial construction of the sensor. If the current in a single coil is the prime variable being monitored, then the shorting of turns of that coil will decrease the inductance and resistance, and thereby increase the current flow within the circuit. This may be either an increasing mode or a decreasing mode of failure depending upon the initial purpose and the direction of change of inductance that was to be monitored. If two coils are to be associated in a transformer-type arrangement, the shorting of turns in either the primary or secondary part of the transformer will usually result in a decrease of sensitivity of the device and thus in a decreasing mode of failure. A mechanical displacement of one coil with respect to the other coil may cause a decreasing or increasing mode of failure depending upon the direction of displacement and original construction.

Resistance Devices. Resistance devices, like inductance devices, are based on the premise that a dc or fixed-frequency-ac current will vary as a result of variations in the resistance of the sensor. The variation in resistance of the sensor unit can be the result of temperature, pressure, strain, or other effects on the active resistance element in the sensor. Resistance thermometers and strain

gauges are two such devices. Devices of this nature which rely upon small variations in resistance for the determination of the value of the measured parameter may require lead-compensation devices which balance or compensate for any changes in the resistance of the lead materials going to the principal transducer material, so as to separate out the effects of resistance changes in the leads and in the transducer. Devices of this type can have numerous mechanical configurations depending upon the desired sensitivity and environmental conditions being measured. Resistance thermometers may contain a large length of coiled wire and as a result will have all the deficiencies of other types of coil devices with regard to possible shorting.

The principal modes of failure of such devices are increasing or decreasing since resistance can increase due to either irradiation or an open circuit, or can decrease due to shorting of coils together.

Direct resistance measurements of the reactor materials rather than sensor materials is believed to be possible. For example, the resistivity of sodium is a direct function of the temperature. Such a device has been proposed for use in LMFBRs, but critical mechanical spacing and the presence of other factors which can change the resistance of a molten liquid metal may preclude the use of such a device in LMFBRs.

Capacitance devices. In general, capacitance devices do not readily lend themselves to incorporation in sensors, principally because the changes in capacitance which may result as functions of the parameter being measured are usually small in relation to the total capacitance of a sensor and lead system, and as a result are difficult to detect accurately.

Failure modes of capacitance devices are caused by breakdowns of the dielectric and shorting of capacitor plates or the open circuit. Thus, the capacitance devices can either have a decreasing or an increasing failure mode.

Magnetic Flux Device. This section treats devices in which the voltage generated for the sensor signal is a direct result of the cutting of flux by the sensor wires themselves rather than being a device such as a permanent-magnet flowmeter where the basic variable plays a direct part in the generation of the electric signal. Included in this type of category are devices based upon a dynamic microphone principle such as is used in some accelerometers and acoustic listening devices.

The failure modes of such devices are decreasing. Decreasing modes can be the result of decreases in magnetic flux of the magnetic material due to temperature or other causes, or to mechanical or electrical failures resulting in decreased signal output. These devices are usually self-exciting.

4. Testing and Detection of Sensor Failures

The items to be discussed here refer only to techniques which may be used to detect failures of sensors (including cable) but are not intended to provide a discussion of detection of failures in processing or readout instrumentation. Also, it is not intended to discuss the frequency of testing. However, the duration of the testing is an important parameter for sensors to be used on-line and, therefore, comments on the duration of performance of a calibration or test will be included. Consideration will also be given to the degree of automation which might be employed in the use of some of the testing techniques discussed. The guide line for the following discussion will be assumed to be that the duration of the testing should be as short as possible for sensors to be used continuously on line.

Ideal Method. The ideal method for the testing of sensors would be the periodic calibration of the sensor throughout its intended range of operation by subjecting it to the range of parameter measurements that it was intended to measure. This could be implemented by two techniques; either the actual system variable being monitored could be changed throughout its range and the measurements taken compared with

measurements of known accuracy, or the sensor could be removed from its operating environment, calibrated, and then returned to operation.

Consider the first technique for reactor applications. a) The periodic changing of the system variable to include the limits for calibration would require plant operation to exceed the normal or desirable range and result in reduced safety factors of operation or potential damage. b) The operation of the system variable below the desired value in order to calibrate may degrade plant performance and efficiency.

Consider the second technique. The removal of the sensor for recalibration throughout its range may require that the reactor be shut down or that a larger number of sensors be used. The resulting cost of plant shutdowns, maloperations, or periodic removal and complete recalibration of sensors precludes the use of these techniques for the LMFBR.

Compromise Methods. Realistic methods are safe, possible, and economical. The ideal method of complete calibration is not practical during continuous operation, so methods have been devised to perturb system variables to indicate that the sensor is working correctly. For example, it is possible to change the temperature of part of the coolant stream passing thermocouples so as to produce a change in the thermocouple reading without effectively changing the temperature of the total coolant flowing in the system. The raising of the thermocouple temperature gives an indication as to the operability of the thermocouple at the particular location being tested. Another technique is the incorporation of a heating element around a thermocouple such that its temperature can be raised independently of the flowing medium.

Still another technique which can be used to test the calibration or operability of sensors is to vary the parameter being monitored within known limits and to cross check with other types of sensors within the system. For example, to monitor flow, change the primary flow by 5% or 10% and see if the temperature rise across the core also

changes by 5% or 10%. Other variables such as reactor power have to remain constant if calibration is being performed. Correlation techniques can be used to augment this type of sensor testing.

If it is not possible to incorporate such testing systems within the design of the plant, there are other techniques which can be used to test the continuity, mechanical integrity, and operation of different types of sensors. These techniques are applicable mostly to the type of transducers based on electrical phenomena.

Electrical-impedance Monitoring. Time-domain reflectometry is used to determine and monitor the impedance of electrical cables and circuits throughout their length. The method used is to pulse a circuit with an emf and monitor the reflections received due to changes in electrical impedance within the circuit. Open circuits, short circuits, and the distance to these faults can be monitored with good accuracy. The disadvantage of this technique is that it requires the mechanical attachment of an electronic device and the utilization of personnel to monitor each device to be checked individually. This method of monitoring requires that the sensor not be functional for a very short testing time. Automatic application in the use of this technique has not been reported for reactor applications.

Piezoelectric-admittance Monitoring. Piezoelectric devices can be tested by applying to the lead wires a variable-frequency sinusoidal signal and then monitoring the electrical admittance of the sensor. This technique measures integrity of the piezoelectric device and assembly, since the mechanical compliance reflects back to the measurement instrument as a change in electrical admittance. The spectrum of electrical signals from the sensor indicates the useful frequency range; therefore, changes in mechanical compliance or measured spectrum would be an indication of sensor degradation. This method of monitoring requires that the sensor not be functional for a very short testing time. Automatic application in the use of this technique has not been reported for reactor applications.

Circuit-continuity Monitoring. Open-circuit testing devices which apply an ac signal of a frequency higher than the signal frequency usually found in that particular type of transducer are incorporated in some commercial instrument readout equipment. The ac current generated by the application of this signal is monitored; for an open circuit, the high-frequency signal will drop and an alarm will be given. Another device utilizes a dc voltage of magnitude greater than any to be expected on the measurement instrument. This voltage is applied through a resistor such that if an open circuit occurs within the sensor assembly, the sensor resistance then becomes very large and the high voltages applied to the inlet of the electronic circuitry give a high-scale trip signal. Circuit-continuity monitoring using both ac and dc methods allows continuous circuit monitoring without interfering with the basic sensor operations.

Performance Monitoring of Acoustic Sensors. Testing of acoustic sensors can be performed by the use of one device to excite others. By using a known signal and correlating the signals received by the other sensors the operability can be determined. This type of system has not been used in the nuclear industry, but would be amenable to either continuous, automatic on-line application or the use of very short testing times.

E. Limitations of Measuring Accuracy

1. Inherent Noise in Process Variables

Values of variables are established in the Design Basis to select a protective margin for critical plant variables and to determine the set points of trip monitors. These set points are initially selected on the basis of ideal noise-free signals, for example, 105% high-flux trip. In general, all process variables have some noise which is represented by a random deviation around a mean value. If a particular variable should have, for example, 10% peak-to-peak noise superimposed on the mean value, then instantaneous values of the variable will randomly exceed 105% and will result in spurious trips if the set point

is set at 105%. In order to avoid spurious trips, a compromise is reached and the set point is increased. The inherent noise in a process variable thus establishes a lower limit for a trip setting which will not result in spurious trips. This lower limit in turn sets the margin between the trip setting and the mean value of the variable. For exceptionally noisy processes this may require the acceptance of an undesirably wide margin.

Alternatively, the noise content of a signal may be reduced by applying filtering techniques, but an analysis is required to determine whether the filtered system has an acceptable transient response and does not introduce excessive delay in producing a trip signal. In general, if the spectral density of the noise is concentrated in the low end of the frequency spectrum, filtering techniques will not be effective.

2. Errors Due to Sensors and Circuitry

The accuracy of a measurement is the relation between the true value of a physical quantity and the value of the quantity obtained by measurement. The error of a measurement is the difference between these two values. The "true value" is simply the quantity obtained by a more accurate instrument, i.e., a standard. Strictly, the accuracy of the determination of a measured quantity depends on the precision with which the appropriate standard quantities can be maintained or reproduced. It is common practice to distinguish between "precision" and "accuracy." The word "precision" is related to the random error distribution associated with a particular measurement, and the word "accuracy" is related to the existence of systematic errors. Systematic errors arise from faults (such as incorrect or inaccurate calibration) or changes in condition (such as temperature and pressure) which could, if detected, be corrected or allowed for. Random errors are caused by various unpredictable fluctuations.

Static Characteristics. The static error of an instrument is the difference between the true value of a quantity not changing with time and the value indicated by the instrument. By calibrating an instrument against a suitable standard, the static errors can be determined at a number of points in the measurement range. These data form an error curve which is then used to correct instrument readings.

The reproducibility of an instrument is the degree of closeness with which a given value may be repeatedly measured. Perfect reproducibility means that the instrument has no drift, i.e., the instrument calibration does not gradually shift over a long period of time. For example, drift may occur in thermocouples and resistance-thermometer elements because of changes in atomic structure caused by transmutation.

Dead-zone error is associated with the largest range of values of a measured variable to which the instrument does not respond and may be found in certain kinds of mechanisms that can only indicate small and discrete changes in value of a measured variable, for example, make-break switching in a null-balance pressure transducer.

Errors caused by the presence of hysteresis result in a characteristic loop when an instrument is calibrated first in one direction and then in the other.

Dynamic Characteristics. Instruments do not respond instantaneously to changes in the measured variable. They exhibit a characteristic slowness or sluggishness due to such things as mass, thermal capacitance, fluid capacitance, or electric capacitance. In some cases, pure time delay is encountered in which the instrument waits for a reaction to take place. For example, a thermocouple measuring the core outlet temperature encounters a pure delay which is determined by the ratio of thermocouple distance from the core and fluid velocity.

Dynamic error is the difference between the true value of a quantity changing with time and the value indicated by the instrument with an assumed zero static error. The dynamic behavior of an instrument is

determined by subjecting the sensor to a known and predetermined variation in the measured quantity. The common variations are: step change, linear (ramp) change, and sinusoidal change. For an instrument which can be dynamically described by a first-order differential equation, the dynamic response is specified by its time constant, i.e., 63.2% of final value is reached in one time constant in response to a step change in the measured quantity.

F. Reliability

Reliability is defined as "the probability that a system will perform satisfactorily for at least a given period of time when used under stated conditions," and availability is defined as "the probability that a system is operating satisfactorily at any point in time when used under stated conditions." Reliability theory can be used to analyze the performance of a plant protective system.

In order to simplify reliability analysis, the following assumptions are generally employed: a) components are operating in their useful life phase for which the failure rate is constant, and the distributions of time between failures can be expressed by exponential distributions; b) component failure rates are estimated using published data for similar equipment; c) component failures are independent; d) testing and repairs neither alter the original design, nor add new faults.

As an example, consider a core protective system consisting of one thermocouple on the outlet of each of 265 subassemblies. The reliability of a single temperature channel is given by

$$R(t) = e^{-\lambda t},$$

where $R(t)$ is the reliability, λ the failure rate, and t the time.

For an assumed failure rate $\lambda = 0.1$ failure/yr and $t = 1.0$ year (refueling schedule), the probability that the temperature channel is still operating at the end of a one year is

$$R(1.0) = e^{-0.1} = 0.9048.$$

If the thermocouples are arranged in a reactor shutdown system of 1 out of N, where N = 265, the 1/265 system reliability is given by

$$R_s(t) = [R(t)]^N = e^{-N\lambda t};$$

then

$$R_s(1.0) = e^{-26.5} = 3.1 \times 10^{-12},$$

where $R_s(t)$ is the system reliability. Even if the failure rate were improved to 0.01 failure/yr (which corresponds to a mean-time-between failures of 100 yr), the system reliability would be $R_s = 0.071$.

The probability that the temperature channel has failed is given by

$$F(t) = 1 - R(t) = 1 - e^{-\lambda t},$$

for $\lambda = 0.1$, $F(1.0) = 0.09516$.

Furthermore, the failures can be safe (detected) or unsafe (undetected). The probabilities of safe and unsafe failures, without repair of safe failures, are given by

$$P(S,t) = \frac{\alpha}{\alpha + \beta} F(t);$$

$$P(U,t) = \frac{\beta}{\alpha + \beta} F(t),$$

where

$P(S,t) \equiv$ probability of safe failure
$P(U,t) \equiv$ probability of an unsafe failure
$\alpha \equiv$ safe failure rate
$\beta \equiv$ unsafe failure rate
$\lambda = \alpha + \beta.$

If it is assumed that safe and unsafe failures are equally likely, then for $\lambda = 0.1$, $\alpha = \beta = 0.05$ failure/yr, $P(S,t) = P(U,t) = 0.5\ F(t)$, and $P(S,1.0) = P(U,1.0) = 0.0476$. For the 0.1-failure/yr rate, the probability that the 1/265 system will fail is

$$F_s(t) = 1 - R_s(t),$$

and

$$F_s(0.1) \approx 1.0.$$

The corresponding safe and unsafe system failure probabilities are

$$P_s(S,t) = \frac{\alpha}{\alpha + \beta} F_s(t);$$

$$P_s(S,1.0) = 0.5;$$

$$P_s(U,t) = \frac{\beta}{\alpha + \beta} F_s(t);$$

$$P_s(U,1.0) = 0.5,$$

where $P_s(S,t)$ is the probability of system safe failure and $P_s(U,t)$ the probability of system unsafe failure.

The system reliability can be improved by using redundancy and M-out-of-N logic for each measurement. If it is assumed that each channel can have three states: working, failed-safe, and failed-unsafe, then there are 27 combinations which describe the state of the 2-out-of-3 logic system. Thirteen combinations result in a system which is working (will produce a shutdown signal when called upon), 7 combinations of safe failures result in shutdown, and 7 combinations result in an unsafe failure of the logic system (a logic-system shutdown signal cannot be generated because the system has at least two unsafe failures). The relationship between the channel probabilities and 2-out-of-3 logic system probabilities are:

$$P_L(W,t) = 3[P(W,t)]^2 - 2[P(W,t)^3 + 6\,P(W,t)P(S,t)P(U,t);$$

$$P_L(S,t) = 3[P(S,t)]^2 - 2(P(S,t)]^3;$$

$$P_L(U,t) = 3[P(U,t)]^2 - 2[P(U,t)]^3,$$

where

$P(W,t) \equiv$ probability that channel is operating;

$P_L(W,t) \equiv$ probability that 2/3 system is operating;

$P_L(S,t) \equiv$ probability of 2/3 system safe failure;

$P_L(U,t) \equiv$ probability of 2/3 system unsafe failure.

The relationships for a 2/4 logic system are.

$$P_L(S,t) = 6[P(S,t)]^2 - 8[P(S,t)]^3 + 3[P(S,t)^4;$$

$$P_L(U,t) = 4[P(U,t)]^3 - 3[P(U,t)]^4;$$

$$P_L(W,t) = 1 - P_L(S,t) - P_L(U,t).$$

If repair of safe failures is performed and it is assumed that the mean time to repair a component is much shorter than mean times between safe or unsafe failures, then the following expressions are obtained:[136]

$$P(W,t) = \left(1 - \frac{\alpha}{\rho}\right) e^{-\beta t} + \frac{\alpha}{\rho}\, e^{-\rho t},$$

$$P(S,t) = \frac{\alpha}{\rho}\left(e^{-\beta t} - e^{-\rho t}\right);$$

$$P(U,t) = 1 - e^{-\beta t};$$

$$\rho = 1/T_r,$$

where T_r is the mean time to repair and ρ the repair rate. If it is assumed that

$$T_r = 8.76 \text{ hr/repair} = 10^{-3} \text{ yr/repair},$$

then $\rho = 10^3$ repair/yr.

If high and low temperature limits are used to detect failures around nominal values, then it can be assumed that all failures are detected. Furthermore, if they are repaired, then

$$P(W,t) = \frac{1}{\rho + \lambda}\left[\rho + \lambda e^{-(\rho + \lambda)t}\right]$$

and

$$P(S,t) = \frac{\lambda}{\rho + \lambda}\left[1 - e^{-(\rho + \lambda)t}\right].$$

Table 10 presents a comparison of reliabilities for 2/3 and 2/4 systems with and without repairs. Without repairs, the system reliability is 0.03 at the end of one year and 0.962 at the end of 0.1 yr, assuming that all failures are repaired at the end of each operational cycle. The use of a 2/4 logic system increases the probability of safe failures and decreases the probability of unsafe failures. If safe failures are repaired as soon as they are detected, the one-year system reliability is 0.159 and 0.888 for 2/3 and 2/4 logic, respectively, and the 0.1-yr system reliability is 0.980 and 0.9998 for 2/3 and 2/4 logic, respectively. If all failures are detected and repaired, i.e., by using high and low limits, then the system reliability is 0.999992 and 0.99998 for 2/3 and 2/4 logic, respectively, and is independent of the operational span, i.e., the same for 0.1 and 1.0 yr.

The above comparisons are intended only to serve as a guide for design and are not absolute. The failure rate was assumed for a channel consisting of one thermocouple and associated signal-conditioning equipment, and assumed perfect logic components. The results are informative, in that it is clearly indicated that provisions must be made for on-line repairs or alternatively the plant must be shutdown at approximately 0.1-yr intervals for repairs.

TABLE 10

COMPARISON OF SYSTEM RELIABILITY

λ = 0.1 FAILURE/YR $T_r = 10^{-3}$ YR/REPAIR

t(yr)	LOGIC	P(W,t)	P(S,t)	P(U,t)	P_L(W,t)	P_L(S,t)	P_L(U,t)	R_s(t)	COMMENTS
1.0		0.9048	4.8×10^{-2}	4.8×10^{-2}					No repairs
	2/3				0.987	6.6×10^{-3}	6.6×10^{-3}	0.03	
	2/4				0.987	1.3×10^{-2}	4.2×10^{-4}	0.03	
1.0		0.9512	4.8×10^{-5}	4.9×10^{-2}					Safe failures detected and repaired
	2/3				0.993	6.8×10^{-9}	6.9×10^{-3}	0.159	
	2/4				0.9996	1.4×10^{-8}	4.5×10^{-4}	0.888	
0.1		0.9900	5.0×10^{-3}	5.0×10^{-3}					No repairs
	2/3				0.9998	7.4×10^{-5}	7.4×10^{-5}	0.962	
	2/4				0.9998	1.5×10^{-4}	4.9×10^{-7}	0.962	
0.1		0.9950	5.0×10^{-5}	5.0×10^{-3}					Safe failures detected and repaired
	2/3				0.99992	7.4×10^{-9}	7.4×10^{-8}	0.980	
	2/4				0.9999995	1.5×10^{-8}	4.9×10^{-7}	0.9998	
		0.9999	1.0×10^{-4}	0					All failures detected and repaired
	2/3				0.99999997	3.0×10^{-8}	0	0.999992	
	2/4				0.99999994	6.0×10^{-8}	0	0.999998	

IV. DIGITAL COMPUTER APPLICATIONS

(by C. E. Cohn, K. Porges, and R. H. Vonderohe)

A. State-of-the-Art of Computer Applications in Present-day Nuclear Power Plants

In recent years there has been increasing interest in the utilization of digital computers for operations of nuclear power plants. This interest has covered the areas of data logging, reactor-model calculations, and reactor control and safety systems. As with many departures from generally accepted methods, acceptance of digital computers for direct reactor applications has been slow, particularly in the areas of reactor control and reactor safety. (As used here "direct reactor applications" refers to on-site utilization rather than remote data processing or simulation.)

One of the prime contributing factors to the slow adoption of digital techniques in reactor operation is the complexity and the relatively lengthy lead times required for implementation. Much of the existing digital implementation was installed after the fact rather than being incorporated in the initial design. This fact virtually precludes utilization of digital equipment for reactor control or protection in other than a superficial manner. Existing systems substantiate the open-loop utilization of digital computers.

The most common utilization of digital computers for reactor applications is in monitoring and data acquisition. Initially these tasks were limited to monitoring the status of alarm contacts, data logging, recording trends in certain plant parameters, and performing various operator-assistance functions. In no case, however, was the computer ever delegated control or protection responsibility other than in presenting the operator with printed or displayed information to utilize at his discretion. More recently, digital computers are being used to perform more significant calculations such as plant performance, heat balances, reactivity inventory, limiting heat-transfer

parameters, and instrument-calibration factors, in addition to the previous functions. Still, with one exception, the loop has never been closed.

The single closed-loop utilization of a digital computer at a reactor site is in the operation of turbines, generators, and associated equipment during startup. At this point in time significant advances in the utilization of computers have been incorporated only in tentative proposals and in the open literature in the form of prophecies or predictions. However, both the tentative proposals and the predictions indicate a radical departure from previous philosophy. Not only have both protection and control systems been termed practical and realizable with digital computers, but proposals are being presented for digitally implemented protection systems. As yet integrally incorporated protection and control systems, while being the next logical step, have been beyond the current range of prediction.

B. Application of Digital Computers to Protection Systems

1. General Considerations

Digital computers, while they may be designated "General Purpose," operate according to rigidly specific rules of logic. Except for a small class of machines, digital computers function by the rapid execution of a serial stream of instructions which may have many different loops and/or branches. These instructions are extracted from the memory and executed serially. Although there are frequently several paths into and out of memory, the fact remains that only one instruction may be executed at any given instant. Because of this fact a computer being utilized to monitor numerous points must do so on a cyclic basis as designated by the running program. As a result, the cyclic servicing of multiple points is inherently slower than individual analog monitoring systems for each point.

Once the capability has been provided for the computer to monitor a particular parameter, it is a simple task to extend the number of

parameters being monitored. The price that is paid for monitoring numerous points is that the total monitoring time must now be divided among the number of points being monitored. As the number of points increases, the time between successive scans of each point increases The limiting factor then becomes the minimum scan repetition rate. Frequently certain parameters require monitoring at a higher repetition rate than others. This is very easily accommodated by the instructions. The significant merit of digital monitoring is the relatively small economic expense of greatly increasing the number of sensors.

For the problem at hand, namely, a digital protection system, one very important factor must be considered: the presentation of the information to be monitored. If the information is presented in a compatible digital format, the point-to-point scan time is extremely fast, of the order of several microseconds. However, the rapid digitalization of many sensors is a formidable task. Analog-to-digital converters are relatively fast for the actual conversion of a single analog voltage. The problem is one of feeding multiple voltages into the converter. If an analog-to-digital converter were supplied for each sensor to be monitored, the cost, even with a relatively small number of sensors, would become prohibitive.

On the other hand, the sensor signals may be presented to the computer as analog voltages. In this case the signals must be multiplexed to one or several analog-to-digital converters at the computer by means of relays or solid-state switches. The introduction of relays into the monitoring circuitry produces two undesirable effects. First, the reliability suffers because of the introduction of higher failure rate electromechanical devices. Secondly, the sensor scan cycle will now become significantly longer because of the multimillisecond time for relay closure. For solid-state switches operating at a 10-kc switching rate, the switching time is comparable to the calculation time required for each point.

Solid-state multiplexers are currently available that utilize Field Effect Transistor (FET) switching of analog signals into an

analog-to-digital converter. The input impedence of these FET switches is extremely high, permitting a single analog signal to be connected to multiple inputs without loading problems. This is an important consideration if, for example, the same signal information is required at two or more distinct locations.

The sampling speed of these multiplexing devices is approximately 10-kHz, and each device will accommodate approximately 1000 inputs. However, these devices may be paralleled into a computer, increasing linearly both the possible number of signal inputs and the possible sampling rate.

In a hypothetical situation, assume that 4000 analog signals must be multiplexed into a computer for analysis. By utilizing four FET multiplexers, each capable of sampling at a 10-kHz rate, several options are available. First the signals may be sampled serially, resulting in a 100 usec time between samples. With this approach all of the signals could be sampled every 0.4 sec, with 100 usec available for calculations and storage for each signal. This 100 usec corresponds to up to 100 possible computer instructions. Additionally, it would be possible to control the sampling sequence by the computer program in the event that certain signals were deemed more critical than others, or in the event that one or more signals had exceeded prescribed limits.

Second, data from the four multiplexers could be accepted by the computer at the maximum sampling rate for each. With this approach, all 4000 signals could be sampled every 0.1 sec. However, in this case the calculation and storage time for each sample would be reduced to 25 μsec or up to 25 computer instructions, with the provision still available to control the sampling sequence if it were desired. Obviously, sophisticated calculations cannot be performed on each sample in 25 μsec. Therefore, calculations would probably be limited to absolute boundary determinations and change per unit time. Periodically, these less sophisticated calculations could be foregone in favor of such things as plant performance and reactivity calcuations. Another possible alternative is to provide small unsophisticated computers to determine signal limits and rate changes while a more sophisticated computer is

dedicated exclusively to the more sophisticated calculations.

2. Reliability

From the standpoint of the computer, the prior treatment of the information is immaterial. That decision is one of economics and speed requirement. However, of great concern in any protection system is the question of reliability. Certain reliability requirements must be met by any system, whether it be analog or digital.

Prior to developing specific reliability functions, certain definitions must be assigned and certain assumptions must be made. These definitions and assumptions are as follows:

a) Any digital computer which has exhibited a malfunction is unreliable until such time as the cause of the malfunction has been determined and corrected.

b) Sufficient hardware and software checks are available to determine the presence of a computer-system malfunction within the time "t."

c) The mean time to repair (MTTR) a computer system in hours is "R."

d) The mean time between failures (MTBF) for a computer system, in hours, is "F" and is assumed to exhibit negative exponential distribution.

e) A single-computer system by itself fails to meet minimal protection requirements because of expected maintenance and repair periods.

In a two-computer system, if machine "A" fails i times during a year and the failure times are uniformly distributed over the year, each failure requiring R hours for repair, then the probability of machine "B,"

with k failures uniformly distributed over the year, failing within a period ($\pm$R) of a machine "A" failure is

$$(2\ i\ R/8760)\ k, \tag{11}$$

where 8760 is the number of hours in a year. Therefore, the total probability that machine "A" and "B" are in a failed condition simultaneously during the year is

$$\sum_{i=0}^{\infty} \sum_{k=0}^{\infty} P_i P_k \frac{2ikR}{8760} = \frac{2R}{8769} (\Sigma_i P_i)^2 = \frac{17520R}{F^2}, \tag{12}$$

where P_i is the probability of i failures during the year, and the machines are considered identical (i = k).

As a result of condition e above, the smallest configuration that can be considered for protection is an N = 2 system, where N is the number of computers. For N = 2 the number of simultaneous failures is given by $17520R/F^2$. The number of times that less than two machines are working during the year is essentially i + k.

Expanding to an N - 3 system, there are three combinations of two. Therefore, the probability that two machines are down during the year

$$(3)\quad (17520R)/F^2 = 52560\ R/F^2 = P\ \{2,3\}\ . \tag{13}$$

Additionally, it is interesting to denote the probability, for an N = 3 system, that two machines will fail within a "t" minute interval. This probability is given by replacing R above with t/60, resulting in the expression

$$876\ t/F^2 = P\left\{\frac{2}{t}, 3\right\} \tag{14}$$

By a similar exapnsion it may be determined for an N = 4 system that the probability of having three machines in a failed condition at some time during the year is given by

$$\left(\frac{6R}{R}\right)\left(52{,}560\ \frac{R}{F^2}\right) = \frac{315{,}360R^2}{F^3} = P\{3,4\}\ . \tag{15}$$

Then the probability of going from three working machines to one working machine within a "t" minute interval is the probability of one machine being down times the probability that two of the remaining three will fail within a "t" minute interval. This expression is

$$\left(\frac{4R}{F}\right)\left(\frac{876\ t}{F^2}\right) = \frac{3504Rt}{F^3} = P\{\frac{3}{t},4\}. \qquad (16)$$

Similarly, the probability of an N = 5 system to go from three working machines to one working machine in a "t" minute interval is

$$\frac{(10\ R^2)\ (876\ t)}{F^4} = P\{\frac{3}{t},5\}. \qquad (17)$$

Inherent in expression 17 is the fact that two of the five machines are already known to have failed.

C. Requirements for Core Protection

As pointed out previously, digital computers can very easily and economically accept data from a large number of sensors. However, the incorporation of a large number of sensors into the reactor is a problem which is virtually independent of the computers themselves until such time as the sensor-to-sensor scan time exceeds the minimum requirement.

The actual decision as to how many and what types of sensors are necessary for core protection must be made independently of the implementation in either analog or digital hardware. Once the number and type of sensors necessary are determined, the implementation becomes a problem of economic considerations. Below "k" sensors, implementation would be most economical with separate analog scram channels. Above "k" sensors, implementation would be most economically handled with digital computers if and only if given reliability requirements can be met. The number "k" must be determined.

Once the decision has been made that the required number of sensors is sufficiently large to warrant digital implementation, considerations

of digital reliability must be explored further.

1. Requirements for Plant Availability

By utilizing information supplied by manufacturers of digital equipment and the previously derived probability expressions, the minimum redundant requirements will be explored to preclude experiencing more than one false reactor trip per year as the result of a digital-system failure. For an N = 2 system to be reliable it must be operated on the basis that both computers are fully operational and neither machine indicates a reactor trip. If either machine fails or indicates a reactor trip condition, the system must be tripped. It can easily be seen that to preclude exceeding the requirement of one false trip per year the mean time to fail for each computer must exceed one year. At the present time such reliability cannot be achieved, although some experimental, self-repairing computers are approaching the necessary requirements.

The next possible configuration is N = 3. With a three-computer configuration, one computer may fail and/or indicate reactor trip while the other two are operational and do not indicate reactor trip. In this case a two-out-of-three decision would still be valid and ensure safety. However, if two of the three computers should fail during the same period of time, the system would have to be tripped. Expression 13 above specifically covers this case:

$$52560\ R/F^2 = P\{2,3\}.$$

Manufacturers' figures indicate a valid mean time to repair of R = 2.5 hrs. However, the interpretation of F (MTBF) from manufacturers' figures is considerably more difficult. Not only would different companies arrive at a different value of F for a given machine, but different sections within the same company would probably not agree either. Therefore, F will be treated as an estimated unknown.

Assuming the probability for one false reactor trip in a year of 0.5 (P{2,3}), the above expression can be evaluated for F:

$$F = \sqrt{\frac{52560 \times 2.5}{0.5}} = \sqrt{26,25 \times 10^7} \simeq 513 \text{ hr.}$$

This figure of approximately three weeks of continuous operation is not beyond the realm of current realizability if only the computer, bulk storage (disk), and the data-collection channels are considered. For an N = 4 system using expression number 15, and making the same assumptions, evaluation gives

$$F = \sqrt[3]{\frac{315,360\ (2.5)^2}{3 \times 0.5}} \simeq 110 \text{ hr,}$$

which is definitely realizable. An additional consideration which may be given here is the utilization of an extra computer to be used off-line for program development, etc., this may be used to replace a failed machine, thereby reducing R to 0.5 hr or less.

2. Reliability Requirements to Preclude Catastrophic Failure

The next consideration is the redundancy requirement to preclude catastrophic failure of the reactor: not more than one failure causing trip per 10^8 yr. At this point the assumption must be reiterated that sufficient safeguards are present to determine within a "t" minute period that a failure has occurred. Implementation of these safeguards must take several forms. First, it must be possible to separate failure of data-collection hardware from legitimate out-of-tolerance readings. This includes sensor checking and checking of analog-to-digital conversion by means of known, standard reference voltages. Second, it must be possible to perform internal diagnostics sufficiently often to determine the presence of arithmetic or memory failures. Third, it must be possible to detect the presence of failures which cause the computer to enter a "halt" state by periodic cross-referencing with the other computers. Fourth, the assumption must be made that all programs being run by the computers are totally debugged.

With an N = 3 system, the probability of a failure to shutdown is given by expression 14. In evaluating the expression, it will be assumed that it is possible to determine a computer failure within a one-minute period ("t" = 1). Evaluating expression 14 with t = 1 and using F = 513 hr,

$$\frac{876}{(513)^2} \simeq 3.9 \times 10^{-3} = P\{\frac{2}{t},3\}.$$

The probability 3.9×10^{-3} is the probability that two of three computers will fail undetected in a one-minute period during a year. This probability is considerably greater than the desired 10^{-8}.

For an N = 4 computer system the probability of a failure to shutdown is given by expression 16:

$$\frac{3504\ Rt}{F^3} \simeq 6.5 \times 10^{-5} = P\{\frac{3}{t},4\}.$$

Similarly, for an N = 5 computer system the probability is given by expression 17:

$$\frac{10R^2 \times 876\ t}{F^4} \simeq 79 \times 10^{-8} = P\{\frac{3}{t},5\}.$$

The probabilities $P\{\frac{3}{t},N\}$, as just determined, do <u>not</u>, in actuality, indicate the probability of a catastrophic failure, but are instead the probabilities of computer failures which would preclude the detection of an unsafe reactor condition.

D. Economic Comparison

In this section an attempt will be made to compare, on an economic basis, digital versus analog safety systems. No attempt will be made here to define the number or types of sensors required to provide adequate safety protection. That decision must be made on other considerations, and is the entering argument for this discussion.

Having defined the sensor configuration, safety-system implementation becomes mainly a matter of economics. If the assumed number of sensors is "n," then for $n < k$ the safety system would most economically be implemented with analog scram channels. For $n > k$, implementation would be most economical with a digital system. On the basis of a probable configuration for digital implementation, and assuming that analog scram channels cost approximately $1000 each, an attempt will be made to determine the value of k (the break-even cost point for reactor trip channels).

Earlier an analysis was given for the minimum redundancy requirements for digital computers to meet protection goals. For this discussion, an economic comparison will be made for an $N = 3$ system (i.e., three digital computers are sufficiently redundant to ensure adequate safety protection and system availability). The fundamental principle involved with a digital safety system is converting the analog signal from a sensor to a digital number, transferring that number to a digital computer, and determining in the digital computer the significance of the sensor signal. Although there has been some interest in sensors which output digital signals directly, this discussion will be limited to conventional sensors which output analog voltages.

When discussing the hardware required to input and digitize sensors, it must be remembered that the incremental cost per sensor is not a constant. The reason for this is that some of the hardware is modularized, i.e., one analog-to-digital converter is required for a single sensor, but the same converter may be used for several hundred sensors. Similarly, other hardware components are required for a few inputs, but may also accommodate many inputs.

Several analog multiplexing systems are being marketed that will accommodate a large number of inputs. However, these systems were not specifically designed to handle large numbers of input. Because

of this fact, it is quite possible that the future may find significant cost reductions for such systems. For this analysis, however, existing price levels will be utilized.

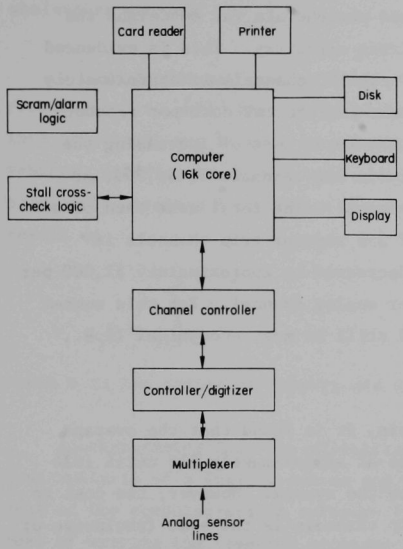

Fig. 26. Block Diagram for Digital Data-acquisition System.

Figure 26 is a block diagram of the required hardware for analog signal multiplexing and digitizing, and a probable computer configuration. According to redundancy requirements, this system must be triplicated in its entirety so that common mode failures will be minimized. By incorporating redundant analog-signal processors as well as computers, the safety system would have two areas common to each computer subsystem: the sensors and the scram-alarm logic.

In calculating the cost for the digital-system implementation, mention should be made of the fact that certain computer peripherals, such as the display, may be shared on an availability basis, that is, the display may be utilized on any of the computers until a computer malfunction occurs, at which time the display would be connected to a working machine. The approximate market cost of the hardware in Fig. 26, which would permit the multiplexing and digitizing of $1 \rightarrow 128$ sensors, is $194,000. Adding in the cost of the redundant computer systems, the total digital safety system hardware cost for up to 128 sensors would be $512,000.

For analog implementation of the safety system, in order to obtain a cost comparison, the figure of $1,000 per scram channel will be used. This includes the sensor, amplifier, trip circuitry, and display.

Clearly, for a system with 128 or fewer sensors, implementation would most economically be achieved with analog scram channels (i.e., \$128,000 < \$512,000). As pointed out previously, the incremental cost for adding digital scram channels is not linear. For the initial digital system, the cost of the computers and peripherals far outweighs the cost of the multiplexing and digitizing circuitry. This is evidenced by the fact that the cost for the first 128 channels is approximately \$4,000 per channel. Now, however, the incremental cost per reactor-trip channel drops significantly. The total cost of increasing the reactor trip channel system capacity to 256 channels is \$6,300, or approximately \$16 per incremental channel. The total cost then of a digital safety system consisting of 256 reactor trip channels is \$518,300. Note that the cost has decreased to approximately \$2,000 per channel, or about twice the cost per analog channel. For this number of channels, an analog system would still be most economical (i.e., \$256,000 <518,300).

Continuing with the analysis, it is found that the average incremental cost per channel remains at approximately \$16 until 1024 channels have been incorporated into the system. However, the cost to digitally implement 640 reactor-trip channels is the same (exclusive of the sensor cost) as the cost to implement 513 reactor-trip channels digitally, namely, \$537,200. It may, therefore, be concluded that k, the equal cost number, is approximately 537. For 537 or fewer channels, implementation would be most economical with analog systems. For 538 or more reactor-trip channels, implementation would be most economical with digital systems. The cost findings may be summarized as follows:

$$n < 538 \Rightarrow \text{analog},$$

$$n \geq 538 \Rightarrow \text{digital},$$

where n is the number of sensor channels.

Several factors concerning digital implementation of a safety system should be mentioned. The first pertains to the cost analysis. For the analysis performed here, the cost of the sensors has been

omitted throughout. The reason is that the sensor cost is directly related to the type of sensor and its physical location relative to the reactor. Obviously, all flowmeter sensors would be more costly than all thermocouples, and in-core sensors would require more expense than whole-core sensors.

If $1,000 per analog scram channel is realistic, the break-even figure, k, would have to be adjusted by the cost of the sensors. This adjustment may be made by summing the cost of the individual sensors, dividing by $1,000, and adding the resultant figure to the previously obtained k to obtain the new break-even quantity k'. The result is

$$k' = k + \frac{\sum_{1}^{n} \$}{\$1000},$$

where n is the number of sensors and $ is the individual sensor cost.

Another factor that has historically been omitted from the initial cost analysis of a digital system and has been omitted here also is the cost of the computer-system software (programs). Very frequently, the cost of writing the computer programs and ensuring that they are functional is quite substantial. A software system for the digital safety system described here could well require several man-years of effort, although most of the required computer diagnostics to detect system malfunctions would undoubtedly be vendor-supplied.

Having once achieved a running software system for data acquisition and analysis, several advantages would become evident over analog reactor-trip channels. The first advantage is the capability of rapidly changing sensor-reading scales, such as would be required during reactor startup. Another advantage would be the capability of ripple-smoothing sensor readings caused by reactor transients. This capability would be readily and widely variable by keyboard input. Still another advantage would be variable capability of alarming and/or scramming based on the progression of conditions. For instance, detected malfunctions in one subassembly might be a condition for alarm

until such time as one or more adjacent subassemblies malfunctioned, which would be cause for reactor trip. In this regard the inherent capability of a digital system in determining the event of catastrophic sensor failure would be very helpful.

One consideration of importance in any system comprised of a large number of sensors is electrical connections through the containment. Since each penetration requires additional monetary expenditure, the number of passages through the containment should be minimized from the economic standpoint. Several possibilities exist for minimizing these penetrations in a digital system. Refer to Fig. 26; it is possible physically to place the analog signal path up to and including the channel controller inside the containment. Unfortunately, doing so seriously restricts the repair capability on these units for obvious reasons. On the other hand, the number of lines passing through the containment could be reduced from one per sensor to perhaps a total of 20. A possible solution might be to provide redundant multiplexers inside the containment, thereby requiring approximately 40 lines through the containment per computer system while providing at least backup capability for each system in the event of multiplexer malfunction.

One fact to be kept in mind for an analysis of this nature is that the price figures used for the comparison are off-the-shelf prices of items not designed specifically for this purpose. In particular, they were designed for small numbers of inputs. It is quite realistic to envision significant future cost reductions for hardware more aptly designed for a configuration of this magnitude as well as similar cost reduction due to advances of semiconductor technology.

E. Special Applications of Digital Computers

1. Detection of Anomalous Reactivity

One diagnostic use of a digital computer is the comparison of actual and expected reactivity. The actual reactivity is derived from the observed flux by an inverse-kinetics algorithm, while the expected

reactivity is calculated from control-rod positions and known power-feedback effects. Any anomaly, or discrepancy between the actual and expected reactivity, may be taken as an indication of trouble and may be used to alarm or trip.

A digital computer is being installed on the Enrico Fermi Fast Breeder Reactor (EFFBR) for this use.[137] This is a routine and straighforward computer application. However, the limits of performance of the EFFBR system are open to considerable improvement. The significant limits are:

(a) precision of 2¢ in anomalous reactivity, and

(b) calculation time of 1.2 sec.

The value for anomalous-reactivity precision was derived by the authors from a trial run using data from previous reactor operation, presumably read from a chart record. Better precision is attainable by averaging of the neutron-flux signal over the entire time between samplings. However, the flux data used by the authors were presumably averaged only over the response time of the recorder, so their scatter would be greater and the precision of the results would naturally suffer. By the same token, the use of point sampling for the flux signal is a serious error in the system design. Since an inverse-kinetics algorithm is a sort of imperfect differentiator, results are quite sensitive to scatter in the flux readings.

The attainable precision, therefore, should be much better than what the authors found. Reactivity measurements by inverse-kinetics calculations on flux readings can yield quite precise results. In a typical run with the Argonne ZPR-9 fast critical assembly, flux readings were taken over one-second intervals from a boron-loaded chamber running at a current of about 4 μA. The standard deviation of the derived reactivity points was estimated as 0.04 Ih.

This error would be expected to vary inversely as the square root of the current in a boron chamber and to increase as the measuring interval is reduced by at least the square root of the time.

As mentioned above, the flux was integrated over the sampling interval by putting the chamber current into a current amplifier and putting the amplifier output into a voltage-to-frequency converter. The pulses from the latter were counted by a scaler that was read into the computer and then reset at the end of each interval.

It is not practical to use a pulse counter as a flux detector at high flux levels. Since one neutron absorption in a boron chamber releases about 10^4, a chamber current of 1 μA corresponds to 10^8 neutron detections per second, which is a rate far too high to count.

The calculational speed is strongly dependent on the capabilities of the computer. The IBM-1800 computer with which the EFFBR system was implemented is the slowest in its class. Its memory cycle time of 4 μsec is slower by a factor of 2 to 5 than that of similar computers from other manufacturers. Furthermore, computers like the IBM-1800 with just 16-bit word length are inherently handicapped in speed for any given calculation. A 24-bit computer of the same general structure could be two or four times as fast, and a 32-bit or longer word should be even better. In addition, hardwired floating-point arithmetic can give a speed gain of a factor of 10 or 20. All in all, an improvement in calculation time of one or two orders of magnitude should be readily attainable.

EBR-II is being equipped with a Sigma-5 computer having a 32-bit word length with speed capability far superior to the IBM-1800. Use of this speed capability in conjunction with the correct method of data collection will yield a unique opportunity to explore the limits of the diagnostic capability of this scheme.

2. Subcriticality Measurements

The matter of subcriticality measurements in LMFBRs has been examined in depth by N. J. Ackermann of Oak Ridge National Laboratory. His conclusions,[138] may be summarized as follows:

The most promising method for measurement of subcriticality down to $30 appears to be a multiplaction measurement. Another method studied, namely, measurement of the prompt-neutron decay constant through noise analysis, is not suitable that far subcritical because of detector-efficiency limitations. However, it is suitable for measuring a moderate subcriticality of $3 to $5, which can in turn serve as a reference point for the multiplication method. Presumably such a reference point could also be established through the removal of reactivity by means of one or more well-calibrated control rods, although Ackermann believes that noise analysis is more desirable for that purpose.

The pulsed-neutron technique is, in principle, also capable of measurements down to $30. However, use of the pulsed-neutron technique requires observation of a fundamental-mode decay. In a large, heterogeneous LMFBR-type core, this may not be achievable at $30 subcritical. It is not known how far subcritical one can go and still observe a fundamental-mode decay in such a core. Furthermore, ancillary problems make the technique impractical. To achieve this performance, a self-contained pulsed neutron generator would have to be placed very close to the core, say in a reflector-element position. A self-contained generator of this type is not sufficiently reliable or resistant to the environment for long-term operation, as in continuous shutdown monitoring, and would therefore require a drift tube long enough to remove it to an acceptable environment. However, commercially available self-contained neutron generators deliver neutrons essentially isotropically, hence the intensity at the end of a long drift tube would be insufficient. A substantially better performance would be available from a deutron, proton or electron accelerator as charged particles can be readily focussed over a distance of 30 ft., and thus made to impinge onto a distant target. An electron beam, in particular, could be made to strike a Bremsstrahlung target well outside the core whence strongly forward-directed bursts of x-rays of mean energy in the vicinity of the photofission peak of the fuel would excite enough of the fundamental mode to produce an analyzable response in a set of appropriately located fission detectors. Such an installation, however, still requires a straight primary enclosure penetration or reentrant cavity

implying a number of obvious safety hazards. Moreover, the overall cost of such equipment, requirement of a trained operating and maintenance crew, and cost of additional shielding makes it essentially impractical at present.

The Reactor Controls Group at ORNL has been working with a neutron counter which can be insensitive to gamma rays even in radiation fields as high as 10^7 R. They are working on the problem of correcting the multiplication measurements for changes in detector efficiency due to loading changes and for the contribution of higher modes at very large subcriticalities. Such corrections should be less for a spontaneous-fission source distributed throughout the fuel than for a localized point source.

3. Excursion Monitoring

The application described here is different from the other material in this report in that its primary function is not to prevent accidents. Rather, it serves a function analogous to that of the flight recorder in an airplane. It would be of considerable value to have a record of neutron flux versus time during a reactor excursion. Current advances in digital electronics enable great improvements to be made in the art of recording such data.

The major problem in recording arises from the conflict between two mutually contradictory requirements. First, the risetimes that are characteristic of fast-reactor excursions are in the microsecond range. Thus, the recording medium must have wide bandwidth if a true picture of an excursion is to be obtained. On the other hand, the recorder must be in standby status for an indefinite period of time (hopefully its entire life), but must be ready to start recording at maximum rate at any instant. With recording media involving mechanical motion, these two requirements are extraordinarily difficult to reconcile while retaining any reasonable degree of reliability. Chart recorders of any type do not have the required speed, while magnetic tape recorders, which have been greatly improved in recent years, still require a certain headstart to run up to speed. An endless tape loop or disc memory

can circumvent this requirement, but involves largely unknown wear problems over a period of several years of continuous running. An endless loop system originally installed in the EBR-II fuel failure monitor[147] was eventually abandoned because of maintenance difficulties.

To avoid such problems, a buffer memory system could be provided entirely by electronic means. The simplest of these would comprise two counter registers, in addition to a core memory. One would count pulses from a neutron detector, while the other would count pulses from a constant-frequency clock oscillator. If the clock register became full before the data register, this would indicate that the neutron flux was below the threshold. The two registers would be reset and the cycle would repeat.

If the data register became full before the clock register, the contents of the clock register would be written into the first word of the core memory. The registers would be reset, and counting would again begin. From then on, each time the data register became full, the contents of the clock register would be written into the memory. This would continue until the memory became full. Writing the clock register instead of the data register provides for better utilization of the available memory space, where the neutron flux during the excursion varies over a wide range. After the excursion, the data in the memory could be read out by auxiliary equipment, which would not necessarily have to be permanently attached to the device.

This simple and highly reliable digital system can meet all requirements for excursions of relatively long periods, but does not have the capability of responding to a doubling time in the microsecond range. Making reasonable assumptions concerning the normal data rate, and data register capacity, it can be shown that a 50 μsec exponential increase in the input, which happens to occur just before a reset, would grow by more than two orders of magnitude before a proper record is started, such that the onset of the transient is lost. On the other hand, a high normal count rate, providing faster reaction, will lead to

counter saturation after only a few groups are actually recorded. The data register capacity, which plays here the role of an alarm level, must exceed the normal mean data register content at reset by a sufficient margin to keep the rate of false alarms due to count statistics at an acceptable level; at the same time, such a large data register capacity delays the start of the record.

Since this problem is in part connected with the random phase relationship between the regular reset and the onset of the excursion, it can be ameliorated by additional data registers, reset in time-staggered fashion. With a large number of such channels, distributed evenly over the reset interval, the performance with respect to transient detection begins to approach that of a digital count rate meter.[53] Instead of this approach, it is clearly more practical to provide a straightforward delay, exactly as in a tape loop or other mechanical buffer storage device, by entering detector pulses in a shift register in addition to the data counter-register. If one assumes that the alarm condition (data register full before clock register could be fortuitiously delayed by as much as five periods, say 250 microseconds, and accepts a channel dead-time of 250 nsec, a single shift register of 1024 bit capacity (currently selling for $10 to $20) will provide enough buffering to obtain a record of the transient from onset to counter saturation (or destruction). High-speed shift registers, operating up to 20 Mhz, are available so the intrinsic capability of fission chambers (of proper design) to deliver pulses of 10-20 nsec length can be exploited, in connection with digital derandomizers.[53] The modest cost of shift registers of large capacity, made possible by the development of MSI (medium scale integration) single-chip technology, encourages more extensive applications of these devices. For example, a set of 20 SR's of 1024 bit capacity would store 5 milliseconds of transient record at 0.25 microsecond resolution, enough to allow permanent storage of a short transient through recirculation in the shift registers. For longer transients, this delay would allow conformation of a transient by some means which would effectively prevent unnecessary interruption of other tasks in which a permanent core memory could normally be usefully employed.

The described systems are entirely composed of elements which have a very high resistance to mechanical stress and radiation, although adversely affected by heat. Periodic check-out would be straightforward and nondestructive. Even if the device was rendered inoperative or was physically damaged during an excursion, the information already stored in the memory could be retrieved if the core stack remained reasonably intact.

For best reliability, such a system should be completely independent of operating instrumentation and computers. However, for economy, if a digital computer is present, this function could be included in its repertoire of jobs. Alternatively, circuits could be provided to take over the computer's memory for this purpose in the event of an excursion.

Acquisition of Fast Count Rate Transients. In a wide variety of surveillance or monitoring systems, nuclear event counters are used to indicate the intensity of some process. Certain untoward circumstances may result in a sudden rapid and large excursion of this process, with a concomitant variation in the detector count rate or event rate (the word event is used here to distinghish these counts from other counts, e.g., clock-pulse counts). The art of producing a faithful record of such unpredictable transients has been considered in a number of recent articles. In these discussions the basic assumption is implied that the recording medium normally is on standby, or normally operates with a slow response, and must thus be shifted to a fast-response mode, or otherwise activated, when a transient worth recording occurs.

The possible use of a computer for data acquisition has been considered, among other methods.[121] For a transient which one would expect to be extremely rare, the count-channel output ordinarily need not be recorded at all, which frees the computer for other tasks. A priority interrupt program would then be actuated by a transient detector and storage of the transient can thereupon begin immediately. Inevitably, however, the transient must already have started to rise when the alarm is given by the transient detector.

In more specific detail, the alarm discriminator may be assumed to be a digital count-rate meter normally registering an average of N events, given a normal event rate n_0 and a processing time T_0. The digital count-rate meter (or EPUT meter) is controlled by a clock, feeding oscillator pulses into another register; when the clock-pulse store reaches a certain preset number, the event-register contents are dumped, possibly into a display, and accumulation restarts immediately. A preset number A in the event register thus constitutes a digital alarm level. Any time this alarm level is reached, the priority interrupt program goes into effect and channel counts are henceforth inscribed in the computer memory. The recording mode is chosen to secure constant statistical resolution, i.e., the number of clock pulses in a time span controlled by the event store is recorded. The recording function ceases whenever the set on the clock-pulse register is reached before the set on the event register, i.e., when T_0 elapses before A events have occurred.

The question then arises how early, i.e., how close to the normal rate level, this system can "catch" a certain type of excursion. For a practical example, we consider a monitor for a reactor plant, for which such excursions tend to have exponential shape; more specifically, we consider fast reactors of LMFBR type, with a period of the order of $\tau \sim 50$ μsec. The choice of the various parameters which will influence the detection of such a transient is connected with some rather general statistical considerations. For example, the selection of the event-register set or alarm level A is directly related to the statistical uncertainty attached to each measurement or percent fluctuation p:

$$A = (p)^{-\frac{1}{2}}$$

The choice of n_0, on the other hand, depends on the expected range of transient intensities which must be recorded. For present purposes, we consider four decades as an adequate range and further assume that the channel can operate at rates up to 10^7 events per second with reasonable accuracy (which supposes, to be sure, that the detector is designed to deliver very short pulses and all electronics including amplifier,

discriminator, and event scaler have adequate bandwidth). The resultant and normal event rate thus comes to

$$n_0 = 1000 \text{ events per second.}$$

The choice of T_0 then determines the normal event count $N = n_0 T_0$, given a minimum event count A = 10 or 25 which actuates acquisition at 30% or 20% statistics, respectively. Evidently, too small a choice of T_0 will make the system quite insensitive to all but very large excursions, and the latter will be recorded only very poorly; on the other hand, a large choice of T_0 will result in a correspondingly large false-start rate due to statistical excursions in the normal event count N. Since such a false start need not necessarily affect the operation of the reactor, a fairly high false-start rate is by itself not objectionable. However, it does result in frequent interruption of those other tasks for which the computer is supposed to be available. Moreover, some criterion is needed after each such occurrence which determines whether to erase the record or keep it; this involves a type of decision that computers are not easily programmed to render. For purposes of this discussion, we may assume[121] that the false-start rate is tolerable for

$$A = N + 4\sqrt{N} \tag{18}$$

Solving Eq. 18 for N with the choices A = 10 and 25, one finds the following values for T_0 at $n_0 = 10^3$, as well as other quantities whose specific meaning will become clear presently:

Statistics, %	A	N	T_0 msec	T_0/τ	$\frac{A}{N}\frac{T_0}{\tau}$	$\left(\frac{A}{N} - 1\right)\left(\frac{T_0}{\tau}\right) + 1$
30	10	3.034	3.034	60.68	500	333
20	25	8.404	8.404	168.08	200	140.3

Now let a transient occur at some unknown time t after the last regular dump of the event and clock register; then the time T at which the event register is full (hence, acquisition begins) is given by

$$1 + \left(\frac{A}{N}\right)\left(\frac{T_0}{\tau}\right) = \frac{T}{\tau} - u + e^u, \tag{19}$$

where we have put

$$u = (T - t)/\tau,$$

which amounts to the acquisition delay after the onset, measured in transient periods. Now the minimum delay results when the onset occurs at a time t' which just allows filling the event register at the next regular dump: $T' = T_0$ and

$$\left(\frac{A}{N} - 1\right)\left(\frac{T_0}{\tau}\right) + 1 = e^{u'} - u'. \tag{20}$$

On the other hand, a slightly later onset results in missing the deadline, and another clock interval is thus required for accumulating; the additional delay is given by

$$u'' = \ln\left[1 + \left(\frac{A}{N}\right)\left(\frac{T_0}{\tau}\right) e^{-u'}\right]. \tag{21}$$

This additional delay must be added to u' to obtain the maximum delay; on the other hand, u'' is in fact the first acquisition (the first datum) for the case of minimum delay. We can further find the growth factor of the transient at the end of the kth acquisition (for minimum initial delay) or $(k + 1)$ τth acquisition (for maximum delay initially):

$$G_k = \exp(u' + u'' + u''' + \ldots u^{(k)}) = (kAT_0/N\tau) + e^{u'}. \tag{22}$$

For any other phase of the transient onset with respect to the normal count and dump cycle, the initial delay (hence, growth factor and actual numerical value of the data) will lie somewhere in between the values which can be computed from the above equations. Specifically, we find for $n_0 = 10^3$ and parameter values indicated in the above table, that acquisition only begins when the transient has already grown by a factor of between 340 and 840 for 20% statistics, or between 150 and 350 for 30% statistics. After this rather uncertain start, every count adds 500 to the growth factor for the 20% statistics example, or 200 for the 30% statistics example.

These numbers tend to indicate that even for a channel of unusually wide count range, as was assumed here, the saturation limit is reached after only a few data points, from which one can infer neither the period nor, of course, the intensity of the transient. For smaller transients, the response is even worse, if indeed there is any recording at all. The problem is twofold: on the one hand, the uncertainty of the phase relationship between onset of the transient and the count cycle introduces an intolerable spread in the data; on the other hand, the recording of an exponentially rising count-rate is necessarily difficult to read when the mean interval between recorded events is much larger than the period, i.e., when T_0/τ is large.

The first difficulty is circumvented by using a count-rate metering device which has no phase or cycle, e.g., an instrument based on a shift register. Even more effectively, a shift register by itself can be used for temporary storage, as further considered below.

The second difficulty has an even simpler solution: since the intensity-range requirement and a normal mean-event interval comparable to the transient period are obviously irreconcilable when the period is only 3-1/2 decades longer than the minimum time resolution available from the very best counting system, one is forced to use two channels, one for starting and one for peak-intensity recording, which feature normal event rates of an appropriate difference.

The implementation of temporary storage has been dealt with in recording transients on a very different time scale, i.e., fission product radiation-detector rate excursions due to a "slug" of fission product contamination passing a detection station located on a coolant duct. As this event can be estimated to result in a count-rate "spike" of at least 0.1-sec mean duration, a satisfactory solution was found by using a magnetic-tape loop. For the present case, even a magnetic-disc storage system would probably be too slow and also might be considered rather costly. Various digital electronic storage schemes involving standard memory configurations may be considered, but most turn out to be too cumbersome or too slow. Fortunately, the recent development of

medium-scale integration and large-scale integration shift registers offers a very satisfactory solution, both from the point of view of reliability and cost. With the addition of a "derandomizer" and other circuitry, such a storage unit can be constructed to offer a ratio of 10^5 between storage time and resolution, or 0.01-μsec resolution at 1-msec storage, for less than $1000, of which $400 represents the cost of the shift register.

The whole system would then use a high-rate detection channel, operating at 10^4 to 10^5 events per second normally, which would pass its output through a shift register; another channel could be set for a normal rate of 100 to 10^3 events per second. An "alarm" actuated by a digital system of whatever logic is suitable, can then perform the following functions: (a) open an electronic gate to recirculate the shift-register contents after a suitable further delay,* such that the onset of the transient is permanently stored in the shift register; (b) switch the input from the high-rate channel into an encoder, such as the unit considered above (a clock register controlled by an event register). The encoder output is written into the memory until a certain limit is reached, set to correspond to input-channel saturation; and (c) likewise, feed the output of the low-rate channel to another encoder, hence to another part of the computer memory. This combined unit may be used to record the onset of a large, fast transient, or all of a relatively short and small transient, entirely in the shift register, whence it can be replayed for detailed processing. The system will record medium-strength transients with good statistics partly in the shift register and partly in encoded form in the memory. Finally, large transients are portrayed over their initial rise in the shift register, and subsequently through the low-rate channel-memory input. It may be added that the low rate detector may well be located in such a way as to protect it against possible damage in the kind of event it is designed to cope with.

*The exact delay is, of course, rather unimportant; hence, the alarm system can be set for a low false-start rate -- which may turn out to be an important consideration in practice.

4. Correlation Studies

This section covers a number of areas. First, a computer could be used to correlate readings of different instruments in order to improve the reliability of scram action and reduce the likelihood of false scrams. Not much can be said about this, as it would just be an extension of methods currently studied by fault-tree analysis and implemented in wired logic. All the computer could contribute here is to allow use of logic schemes more elaborate than can be economically implemented in wired form, or permit dealing with gradations of quantities rather than restricting actions to fixed threshold levels. (For example, one could trip on a quantity derived from some combination of sums or products of directly measured quantities, with linear or nonlinear weighting.)

Consider the problem of measuring the transfer function of an LMFBR. Three potentially useful methods are:

a) sinusoidal or nearly sinusoidal excitation, e.g., an in-core oscillator;

b) noise analysis, either of a single quantity or a cross-correlation between two quantities;

c) pseudo-random binary excitation.

In-core mechanical reactivity oscillators have been extensively used in LMFBR studies. They yield precise and easily interpreted information. However, operation has been extremely difficult and expensive in liquid-sodium environments.

Noise analysis deals with the inherent fluctuations in various reactor parameters (e.g., neutron flux) resulting from various driving functions, such as neutronic fluctuations, mechanical vibrations, and flow turbulence. Derivation of the autocorrelation function or auto spectrum of the fluctuations in a single parameter shows the time-domain

or frequency domain characteristics of those fluctuations. Derivation of the cross-correlation function or cross-spectrum of the fluctuations in two different parameters gives some information about the relationship between those parameters.

The weakness of noise analysis is that there is no easy way to tell whether a given feature of a spectrum arises from the plant transfer function or from the driving function, particularly if the latter has significant contributions from mechanical effects. Some indication as to the nature of the driving function might be obtainable from the amplitude distribution. If the driving function is primarily composed of neutronic fluctuations or a large number of independent mechanical vibrations, the amplitude distribution will be closely Gaussian. However, if one vibrational mode predominates, the amplitude distribution will depart significantly from Gaussian.

In spite of the above limitations, noise analysis is an attractive technique. It can derive data from the normal plant instrumentation with no interference with plant operation. Recent advances in analysis techniques (the Fast Fourier Transform) bring on-line real-time analysis within the range of feasibility. Noise analysis could thus be used for anomaly detection. The noise spectrum of selected plant parameters could be monitored, and a significant deviation from the expected spectrum could produce an alarm.

The diagnostic power of this technique for LMFBRs has not been explored to even a fraction of its full potential. (Does anybody really know, for example, what the neutron noise spectrum of an at-power LMFBR looks like?) Considerably more effort in this direction is certainly warranted.

Pseudorandom binary excitation is a way of driving a system for transfer-function measurement that has many advantages over simple sinusoidal excitation. Here the driving function is two-valued and has a particular form designed to insure spectral content over the full frequency range and to simplify data analysis. The details of the

transition between the two values are unimportant, and the transition speed need not be much faster than the highest frequency to be analyzed. This insensitivity to the details of the transition simplifies the design of excitation mechanisms. In particular, it is very easy to apply to electrical signals.

This scheme has been used for tests, for example, on the KIWI, NERVA, and EBWR reactors. For example, the excitation has been applied to the propellant-pump demand signal. The scheme has not been used on LMFBRs.

Finally, one could conceive of measuring flow in a sodium channel by sensing sodium temperature at two points along the channel and cross-correlating the readings from the two sensors to estimate the transit time of the flowing sodium. Ashton and Bentley[139] discuss an abbreviated cross-correlation scheme that would take up about 2% of the time of a computer of 2-μsec memory cycle and could obtain the transit time to 5% accuracy in one hour of real time.

As of the date of their paper, the authors had not tried their scheme in an actual sodium system. A factor that they did not consider is the determination of the optimum spacing of the temperature sensors relative to the thermal time constant of the sodium stream.

This type of flow measurement has also been considered by Boonstoppel et al.[140] They mention the possibility of impressing additional fluctuations on the system to facilitate the measurement. For sodium, one could conceive of placing a small electrical heater at one point and impressing power on it in a pseudorandom binary sequence, while cross-correlating this with a temperature measurement downstream. Here, if the binary sequence did not have too long a period, it might be practical to do the autocorrelation in a hard-wired device independent of the computer, so that the computer would only have to select the channel to be tested and then record the results. The limitation on this technique, of course, would be the heater power required to produce a detectable signal in the presence of the normally occurring temperature fluctuations.

Work in this area has also been reported by Randall,[141] who has made successful tests in a water system preparatory to sodium experiments. In addition, E. S. Kenney at Pennsylvania State University is working on a gamma-ray noise-flowmeter concept.

5. Digital Sensors

Customarily, sensors for temperature, flow, and other physical quantities present their readings in analog form to an analog instrumentation system. When making the change to a digital system, one might consider using sensors that are inherently digital or, alternatively, digitizing as early as possible.[142] By this means, some of the problems of drift and calibration of analog sensors might be ameliorated, and degrdation of signals transmitted over long distances might be reduced.

Some of the suggestions to be made here would, at present, be more expensive than contemporary analog practice. However, the suggestions could become economically more attractive in the future as advances in the integrated-circuit art reduce the cost of digital electronics.

An obvious application is where averaging of a signal is necessary or desirable to minimize noise. This is true for neutron flux measurements, as was discussed in Sect. 1. Here a voltage-to-frequency converter can feed a binary scaler that can be read into the computer and then reset periodically.

For other signals, such as thermocouples, one could consider placing an analog-digital converter as close to the signal source as possible, and transmitting the data to the control center in high-level digital rather than analog form, the former being much less susceptible to noise pickup. Thus, the one analog-digital converter in the conventional system would be replaced by a multiplicity of converters, one for each signal, and the analog multiplexer would be replaced by a system of digital logic gates. As mentioned above, such a system would probably be economically prohibitive at present, but might become attractive in the future.

Beyond this, one could consider going to transducers that produce outputs directly in digital form. For example, one might measure temperature with a tuned circuit whose resonant frequency is temperature-sensitive. This would be connected to an oscillator which would put out a pulse train at that frequency. Pressure could be measured similarly with a capacitance transducer connected into a tuned circuit. A scaler would count the pulses and so establish the frequency. The electronics for such a transducer should be simpler than an analog-digital converter, but similarly amenable to the benefits of integration.

Work already being done in digital measurement of flow was mentioned in Sect. 4.

6. Computer-speed Tests

In planning data acquisition and control applications in nuclear power plants by means of a computer, it helps to know the time required for certain computational tasks on various computers. This information assists in computer selection and indicates how much real-time computational load may be carried by a given machine.

Such information has been obtained from speed tests on a limited but representative selection of small computers. (These tests were performed during December 1969 and January 1970 and so do not reflect any subsequent improvements in software.) A special program was written in FORTRAN to test the speed of various single-precision floating-point operations and functions. Each operation was tested in a DO loop which repeated it a large number of times (500 to 200,000, depending on the particular operation) with different operands.

On the PDP-9, CDC-1700, and IBM-1130, loops were timed by stopwatch. On all others except the SEL-840MP, a 3-in./sec recorder was connected to the halt light. On the SEL-840-MP timing was done with an interfaced binary scaler and clock generator.

For each loop, gross time per operation was total time over number of cycles. To obtain net times shown, the DO cycle time was subtracted.

Sine, square root, and natural-logarithm operations required subtraction of the time for an add operation used in forming the argument.

Table 11 shows parameters of the computers tested and measured operation times. All machines have hard-wired fixed-point multiplication and division, and all but the SEL-840MP with EAU use subroutines to perform floating point-arithmetic. Also shown is the amount of memory occupied by the timing program and its library subroutines. Practically all is occupied by instructions; only about two or three dozen words are for data. The program occupies about the same number of memory bits regardless of word length, implying that a shorter word produces no savings in memory cost for a given job.

Various factors produce the observed disparities in speed. On some machines the sine, square root, and logarithm subroutines are themselves programmed in FORTRAN, so the approximation algorithms are executed in floating-point arithmetic. Also, the SEL-840MP carries 11 significant figures in its single-precision floating-point arithmetic, while the others carry just 6 or 7. Evidently, the third-generation short-word (i.e., 18 bits or less) machines do not yield the computational speed that their fast memory cycles would lead one to expect.

The objection might be raised that these results are representative solely of FORTRAN programs or floating-point arithmetic, and so do not apply to typical control applications programmed in machine language and performing various types of data manipulation. However, those objections are not really valid. To begin with, most of the elapsed time in these measurements, particularly in the arithmetic operations and functions, is spent executing hand-coded library subroutines, and only a small fraction is spent executing compiler generated code. Secondly, floating-point arithmetic might be considered simply as one type of data manipulation in which the bit pattern known as the "floating-point argument" is operated upon in a prescribed way to obtain another bit pattern known as the "floating-point result." The relative efficiency of this type of data manipulation can be taken as an index of the relative efficiency of other types of data manipulation. Actually, the use of FORTRAN is the only way that it is really practical to make such

measurements on a wide range of computers.

Note that these tests measure only computation speed and do not indicate the efficiency of the input/output or interrupt arrangements.

TABLE 11
Computer Parameters and Test Results

Computer	DDP-24[a]	SEL-840MP		DATA-620[c]	SEL-810A[d]	PDP-9	CDC-1700	IBM-1130[c]
Computer Parameters								
Bits per word:	24	24		16	16	18	16	16
Memory cycle time, μsec	5.0	1.75		1.8	1.75	1.0	1.1	3.2
Memory occupied by timing program and library subroutines:		Non-EAU	With EAU[b]					
Words:	953	1210	944	1907	1622	1615	1845	2078
Bits:	22872	29040	22656	30512	25952	29070	29520	33248
Operation Times, μsec								
ADD	440	313	19	518	553	500	540	850
DIVIDE	413	389	37	790	2622	580	720	1130
MULTIPLY	369	287	26	732	611	500	550	960
SINE	584	5893	846	3396	9862	5220	4520	3600
SQUARE ROOT	377	841	272	806	13459	4070	8420	5070
LOG	548	6004	623	4576	11262	4770	5920	5500
IF	28	11	11	24	85	90	190	200
FIX	130	79	86	260	162	160	330	370
FLOAT	105	50	53	356	615	160	760	540
STORE SUBSCRIPTED VARIABLE:								
1-DIMENSION	196	88	28	53	192	240	370	640
2-DIMENSION	221	98	39	242	213	300	380	750
DO (1 CYCLE)	43	18	18	266	18	15	16	52

[a] Results also apply to DDP-124 if operation times are multiplied by 0.35 and 40 μsec are added for ADD, DIVIDE, MULTIPLY, SINE, and LOG. Increase memory requirement by 20 words.
[b] EAU = Extended Arithmetic Unit (hardware floating-point).
[c] Results also apply to Varian Data Machines 620/i.
[d] Results also apply to SEL-810B if operation times are multiplied by 0.45.
[e] Results also apply to IBM-1800 if operation times are multiplied by 0.625 for the 2-μsec memory or 1.25 for the 4-μsec memory. Re-entrant software may run slower.

V. RESULTS AND CONCLUDING COMMENTS

(by D. Okrent and J. B. van Erp)

A. Results of Some Previous Studies

Many of the results of transients reported in Chapter II are similar to those reported by General Electric.[19-20] These safety studies included flow-reduction and loss-of-flow transient calculations involving both the entire core and single subassemblies. Some typical results obtained by General Electric for whole-core flow-reduction transients are illustrated in Figs. 27 and 28. In Fig. 27, safe and unsafe regions are indicated in a plot of percent of remaining flow against time for flow reduction in an oxide-fueled reactor design, assuming reactor trip to be initiated by a 10% flow reduction as sensed by core flowmeters. Figure 28 gives the maximum cladding surface temperature as a function of time for both hotspot and nominal peak rod conditions for a 75% flow reduction occurring at -60%/sec. Although calculated for whole-core transients, the results are generally relevant to single subassemblies, assuming the same flow reduction and reactor trip.

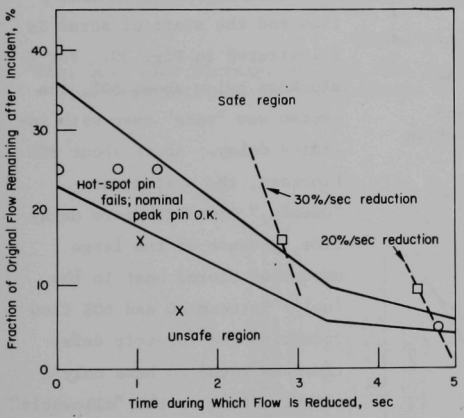

Fig. 27. Map of Whole-core-accident Flow Reduction.[20] No superheat assumed; squares indicate boiling not reached any place in core; Xs indicate cladding exceeds local sodium boiling.

Some results obtained by General Electric for flow blockage transients in single subassemblies are illustrated in Figs. 29 and 30.

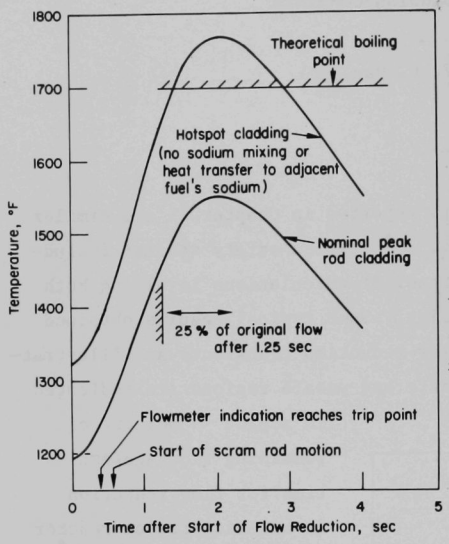

Fig. 28. Maximum Cladding-surface Temperature after 75% Flow Reduction at -60%/sec.[20]

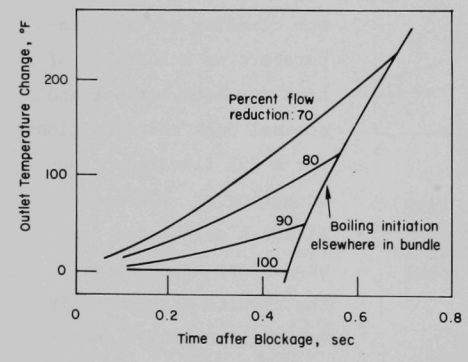

Fig. 29. Behavior of Coolant Outlet Temperature with Flow Blockages in Peak Fuel Assembly.[20]

Subassembly outlet temperature is plotted in Fig. 29 as a function of time after blockage for various % flow reductions. Because the cooler upper blanket regions act as a heat sink, it is found that sodium boiling initiates elsewhere in the bundle while the outlet temperature has changed only 100-200°F.

The effect of delay between the initiation of flow reduction and the start of scram is illustrated in Fig. 30. For % blockage below about 50%, the system was "safe" even with infinite delay. Above about 80% blockage, the system was "unsafe," even with zero delay time, because of the large amount of stored heat in the fuel. Between 50 and 80% flow reduction reactor-trip delay time was found to have only a slight effect on the "allowable" flow blockage. What is not clear from Fig. 30 is the "degree of unsafeness" which results above 80% flow blockage - that is, boiling or clad damage may result for all reactor-trip delay times, but the overall course of events and the consequences may vary

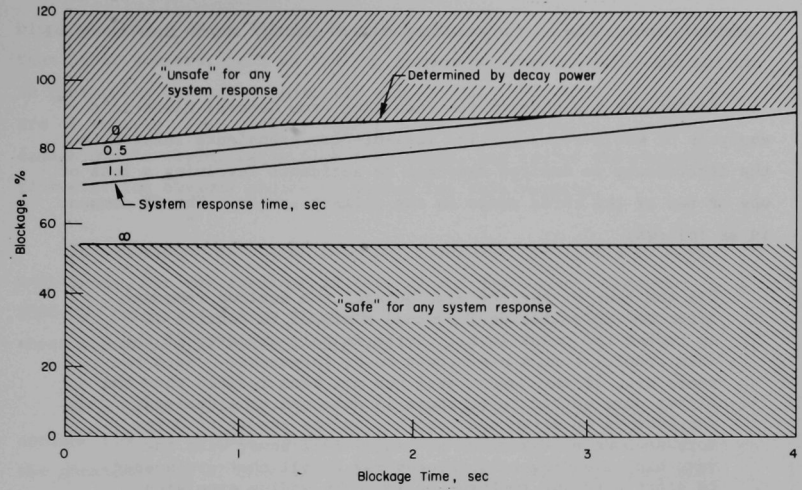

Fig. 30. Flow Blockage of Peak Fuel Assembly.[20] (System response time = time from initiation of flow change to start to scram.)

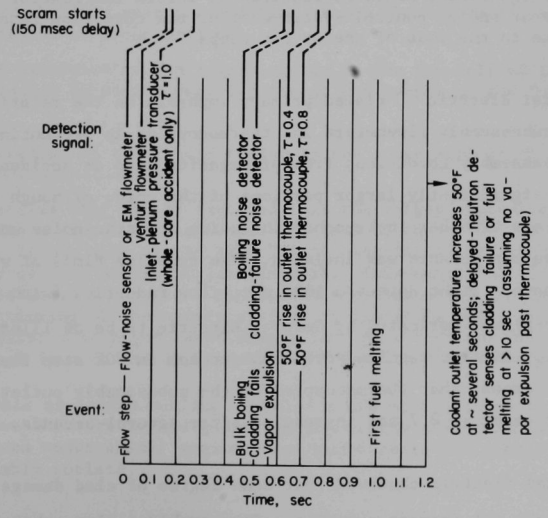

Fig. 31. Comparison of Instrumentation for 100% Flow Reduction (no scram).[20]

markedly depending on the continuation of energy input into the fuel during the delay of reactor trip.

An interesting observation resulting from General Electric's analysis of whole-core, partial loss-of-flow transients relates to the discrepancy in desired response to accidents involving a loss of one or two of the three pumps in the primary system. The GE comment is as follows:

> "In the case of the one pump outage, the desired response after any detection device sends a signal to control is to reduce the power level. Scram is only employed if the shim control system has proved to be inoperable. With two pumps out, if the power level has not been reduced when the higher core outlet temperature is detected, the desired response is to scram the reactor, as the result of a few more seconds of operation at nearly full power with the very high cladding temperatures may be all that are needed to start cladding rupture, followed by sodium expulsion and the start of a nuclear excursion.
>
> "Therefore, a series of parallel detectors, including pump tachometers, and flow metering devices on the primary pump discharge lines, would be required to inform the reactor operator and/or control system whether the core flow reduction is due to the loss of one or two pumps."

General Electric[20] placed primary emphasis on the relative roles of subassembly flowmeters and thermocouples in preventing off-design subassembly conditions from propagating into an accident involving significantly larger portions of the core, although the possible role of other instruments including acoustic noise and delayed-neutron sensors was included. The relative times at which various sensors might detect a 100% step flow reduction (with no reactor trip) was estimated by General Electric to be as illustrated in Fig. 31. Similar results were obtained for an 80% step flow reduction, except that thermocouples at the subassembly outlet sensed the event at 0.7 sec instead of after several seconds.

General Electric observed that some degree of clad damage and fuel failure might not present a public safety problem; also, that it was flow

blockages above about 70% which were potentially damaging. They observed that other sensors, such as boiling detectors, might be effective in protecting against large-scale propagation, that the thermocouples are of somewhat less utility than flowmeters in protecting against damage due to rapid, large flow reductions, and called the channel flowmeter the obvious choice of sensor for this purpose.

The questions of reliability and redundancy requirements were mentioned,* but not examined in Ref. 20 and the General Electric 1000-MWe reference design proposed the use of three flowmeters and three thermocouples in each core subassembly.[143]

In a later study of the effect of an instantaneous loss of coolant flow to an FFTF subassembly. General Electric[19] examined the phenomenology of this event in more detail, and arrived at the following principal features:

"Blocked subassembly fuel temperatures increasing at ∿ 1000°F/sec.

"Coolant boiling near the midpoint of the blocked subassembly fuel region at about 0.75 sec.

"Rapid expulsion of the liquid sodium in the top half of the fuel region by sodium vaporization at the center of the fuel region.†

"Evaporation of the liquid sodium in the lower half of the fuel

---

* It was stated that "it is expected that the safety system may be designed with a probability of unsafe failure of about 10^{-6} to 10^{-5} per year." It was also stated that "plant unavailability associated with safety systems should be less than 5%. This unavailability includes false scrams, repair or replacement requirements, and even proper functioning of the safety systems in instances where conditions appear to exist that might cause damage but later turn out not to have caused damage (due to the impreciseness of the instrumentation)."

† The analysis of sodium boiling, expulsion and condensation in cooler regions above the core raised questions concerning the probability that (or conditions under which) sodium vapor would reach the plenum above the subassembly outlets.

region, limited by the thermal transient - complete dryout at about 2.5 seconds.

"Clad melting beginning at about 1.3 seconds.

"Fuel melting beginning at about 3 seconds.

"Liquid sodium reentry possible near the channel wall after fuel region dryout at about 2.5 seconds.

"Rapid heating of the sodium on contact with the hot fuel pins may result in generation of an acoustic pressure wave capable of rupturing a low ductility, overheated duct.

"Several reentry cycles of sodium contacting the hot fuel region material may produce sufficient pressure pulses to damage and possibly rupture the adjacent fuel assemblies.

"Clad and fuel melting and slumping will contact sodium below the fuel region in the 4 to 6 seconds range.

"Expulsion of the molten clad and fuel may occur on contact with sodium.

"Melt-through to the adjacent duct begins in the 10 to 15 seconds range."

The following recommendations were made by General Electric with regard to system instrumentation requirements:

"The results of this hypothetical accident study show that it appears possible that some damage to adjacent fuel assemblies may occur as early as 2-3 seconds after a complete flow blockage. This implies that detection and remedial action (reactor scram) may be required to occur in less than three seconds. The instruments currently planned to monitor FFTF core behavior include:

Neutron monitors
Fuel assembly exit thermocouples
Fuel assembly exit flowmeters
Fuel assembly exit fission gas samplers.

"The reactivity effects of voiding will be between 10 cents (optimum configuration) and 5 cents (entire assembly). This reactivity addition may result in a reactor scram signal, depending on the trip point. The assembly melts and slumps between 4-8 seconds after blockage. A larger reactivity change can be hypothesized due to slumping that will result in a scram signal, but too late to prevent possible damage while at power.

"The thermocouple signal on total flow blockage will not be a sensitive indicator of total loss of flow because the thermocouples are far removed from the hot core region and axial conduction through the sodium is limited, and because of the heat capacity of the cooler reflector and plenum regions which absorbs much of the transient energies associated with the early phases of the accident. In the more realistic case of a partial flow blockage, significant temperature increase may be indicated at the outlet thermocouples. The temperature response would be determined by the degree of partial blockage.

"The fuel assembly exit flowmeters would give a rapid and clear signal of flow blockage or partial loss of flow. An electromagnetic flowmeter proposed for FFTF should have a very rapid response and should effect a reactor scram in less than 3 seconds.

"The FFTF fission gas detection system response time (~20 sec) is too slow to be of use in detecting a complete flow blockage early in the accident.

"Condensation of sodium vapor created by local boiling or superheat within a fuel assembly may generate an acoustic disturbance that can be detected. If this 'noise' can be detected reliably and early in the course of the flow blockage accident, action can be taken by the protection system to minimize the consequences. The boiling detector could provide an additional means of core surveillance, supplementing the present FFTF duct outlet thermocouples and flow meter. Space considerations and the prediction that the frequency range of interest for detecting boiling is approximately 20 to 60 kHz leads to a detector design with the transducer located at the outlet of the fuel duct. It is estimated that the signal-to-noise ratio is enhanced in this frequency range. The pressure transducer must endure a 1200°F and high radiation environment. The noise signal will be propagated along the vertical axis of the duct, with relatively little attenuation in the structure. The resonant frequency of the transducer should be about 50 kHz.

"The use of wave guides is an alternate design approach to monitor the boiling noise. The main advantage is that the pressure transducer requires no development, since it operates in a low temperature region. The main disadvantage is that the wave guides complicate the mechanical design of the region above the core. This complication is sufficient that the development of an in-core transducer seems preferable.

"There is a possibility that changes in flow patterns caused by a partial flow blockage may produce measureable changes in the background acoustic noise level. Although this possibility has not been evaluated for feasibility it offers the potential for detecting the blockage before boiling or significant superheat develops. Depending on the signal-to-noise characteristics associated with the changed flow patterns, there is a possibliity that a detector developed to monitor sodium vapor collapse might also serve this purpose. A limited evaluation of the feasibility of this approach seems to be warranted."

B. Some General Considerations

In judging the types of sensors and their mode of use in an integrated instrument system, various considerations enter, including the following:

1) the requirements for public safety protection (i.e., AEC licensing requirements);

2) the requirements for plant protection (i.e., protection against economic loss);

3) the cost requirements.

Considerable overlapping exists, of necessity, between the functions of the systems which are aimed at, respectively, protection of the plant and the protection of the public safety. In many cases, a particular system (instrumentation or other) will serve both functions. In such cases, however, the design and performance requirements posed by public safety requirements may be more stringent.

There may also be many gray areas, where an instrument system can serve an important function in protecting the public safety, but for which design and performance criteria less stringent than those for conventional safety systems are appropriate or acceptable.

The more important requirements for LMFBR core-protection systems might be summarized as follows:

1) The reactor-trip system should have very high reliability (e.g., high reliability for instrument channels having sufficient diversity of sensor types, high reliability for safety rod drive system(s), and sufficient mechanical strength for safety rod guide tubes).

2) The reactor-trip system should have time-response characteristics (e.g., sensor response time, safety-circuitry delay time, and reactivity-insertion rate) such as to be capable of shutting down the reactor for any accident (be it of the whole-core or of the localized type) prior to exceeding the limits of acceptability for public safety protection.

3) The reactor trip system should incorporate instrument channels capable of detecting localized core accidents within certain time limits so as to be capable of shutting down the reactor prior to escalation of such accidents to a level unacceptable from a public safety point of view.

On the other hand, an evaluation of instrument systems designed to protect the plant against major economic loss might include consideration of the following:

1) the probability for the occurrence of a particular accident or malfunction against which one wishes to protect the nuclear power station;

2) the extent of the damage that could (potentially) be caused by the particular accident or malfunction, and the economic implications thereof;

3) the cost of installation and maintenance of the proposed instrument system, aimed at protecting the plant against the accident or malfunction considered;

4) the cost of special design features of the plant (including fuel subassemblies)required to make installation of the proposed instrument system possible;

5) the cost of reactor downtime and possible damage, due to spurious action of the proposed plant-protection system, for the case that the system would be of the automatic-action type;

6) possible economic benefits that might result from improved plant performance due to the added instrumentation.

C. Protection Against Localized Core Accidents or Malfunctions

1. Introduction

As was pointed out previously, LMFBRs require sensing and reactor-trip capability for protection against localized core accidents or malfunctions. A crucial question is whether this requirement can be met by means of reactor-trip channels based on whole-core sensors, or whether reactor-trip channels based on sensors installed on each individual subassembly are necessary.

In order to obtain a feeling of what is involved the following may serve: If sensing and reactor-trip capability for each individual subassembly were to be required, then the total number of reactor-trip channels could be as high as ∿300 or ∿560 for a 1000-MWe plant, respectively, for 1 or 2 channels per subassembly. This is to be compared with a total of between 15 and 20 reactor-trip channels for an LWR of equal power. Such a large disparity between the number of reactor-trip channels for LMFBRs and LWRs could have an adverse effect on the competitive position of LMFBRs, as the economic implications are very much larger than just the cost of the additional instruments and associated equipment. Some of the many other aspects that have to be considered in this respect are the following: (a) cost of (preventive) maintenance, (b) cost implications of the presence of sensors and leads in fuel design, core design, refueling operation, etc., in view of, amongst others, accessibility requirements, and (c) possible decrease in plant availability due to increased rate of spurious scrams.

There are intermediate approaches to dealing with local anomalies which lie between the philosophy of "reactor trip only on whole-core

sensors" or "reactor trip based on sensors installed on each individual assembly." Sensors might be installed on each subassembly, with part or all of these sensors to be used only for plant surveillance, alarms, or partial power reductions. Alternatively, sensors from a number of subassemblies could be combined to form a single reactor trip channel.

The aim of the present section is not so much to determine which system is best (as this will depend not only on the type and size of the particular LMFBR in question, but also on a host of unknown factors connected with the still-evolving overall approach to nuclear safety in general and LMFBR safety in particular), but rather to compare the merits of the various possible systems and to indicate where significant gains can be made through research and development.

In the following, primary attention will be given to the two distinct types of reactor-trip channels, i.e., those actuated by whole-core sensors, and those actuated by sensors installed on individual subassemblies.

2. Protection Systems Having One or More Reactor-Trip Channels Per Individual Subassembly

General Aspects. The sensors that are usually considered for a system of this type are flow and temperature sensors. In principle, the former can be installed either at the inlet or at the outlet of the subassembly, whereas the latter is most commonly considered installed at the subassembly outlet.

An important consideration regarding the various possible protection systems is the mode of operation of the reactor at reduced power (e.g., during startup). Basically, three modes of operation could be considered at reduced power: (a) constant volumetric flow, (b) constant ΔT (constant outlet temperature), (c) both flow and ΔT(outlet temperature) variable.

Whereas the constant volumetric flow mode of operation would be economically attractive (as it would allow the use of standard induction motors, as is the practice for LWRs of the PWR type), the high temperature difference across the core (for nominal operating conditions) imposes considerable restraints on the magnitude of the allowable temperature transients. Moreover, the desirability of having near-constant steam conditions would require a relatively constant temperature distribution in the primary circuit over a certain range of power levels. In actual practice, one would probably choose a control system designed to follow some optimized temperature program. Such a temperature program would probably be fairly flat from 100% to, say, 30% of nominal power.

In view of the above, it is likely that future large scale LMFBRs will be designed for variable coolant flow, necessitating variable speed cooling pumps. This, in fact, means that a protection system employing flow signals obtained from individual subassembly sensors would require either variable trip setpoints for the flow, or, otherwise, power-to-flow ratio devices for each flow sensor. Low coolant flow by itself, therefore, would not be a good indication of approaching dangerous operating conditions (see Chapter II); high coolant temperature is. This is one aspect which favors temperature sensing over flow sensing.

Performance of Reactor-trip Channels Based on Flow or Temperature Sensors. Table 4 gives some insight into the difference of protection offered by reactor-trip channels actuated by flow or temperature sensors for the case of partial flow blockages affecting the total subassembly flow.

If we use a fairly arbitrary definition of clad damage and ignore possible effects resulting from the additional heat input associated with a time lag to scram, the flowmeter is favored over thermocouples by only a difference of 5% (at a level of 60%) in allowable sudden flow reductions, if clad damage is to be avoided.

It has been argued[20] that, in the case of a total sudden flow blockage, affecting an entire subassembly, outlet-temperature sensors would not give any signal for many seconds, so that flow sensors would still be needed for that type of localized core accident. Whether or not this long a time lag would be applicable to temperature sensors at the subassembly outlet appears to be controversial. According to the model employed in the calculations of Chapter II for a total blockage accident, boiling will initiate in the core midplane in $\sim$ 0.65 sec. The upper half of the cooling channel is then subsequently voided in from 0.1 to 0.2 sec. While the originally boiling sodium, which is thrown out of the core channel, may cool down partly in flowing through the upper blanket regions, and the vapor bubbles even condense, it is not clear that temperature sensors at the subassembly outlet would not be subject to an appreciable temperature increase. For no temperature increase to result, none of the overheated sodium in the core must reach the subassembly exit. If a signal is achieved at the subassembly exit from the first voiding surge, the difference in time for generating a reactor-trip command signal for flow and temperature sensors for this accident is $\sim$ 1 sec. As was shown in Chapter II, there might be little appreciable difference in the outcome of an accident of this type, whether the reactor is tripped on flow or on temperature. In either case, clad damage and boiling occurs. For a 1 sec time lag, little or no fuel melting would occur prior to reactor-trip; the heat stored in the fuel increases by about 50%.

A comparison remains to be made of the performance of flow and temperature sensors for the case of an accident or malfunction affecting a localized region inside a subassembly. In Chapter II it was shown that it is very difficult to detect flow starvations or flow blockages in localized regions of a subassembly prior to the occurrence of clad damage and sodium boiling. This is due, on the one hand, to the fact that the measured variables are total flow and mixed-mean outlet temperature (rather than flow and temperature in localized regions of the subassembly), and, on the other hand, to the fact that a blocked region that is large enough to be detected would probably already have resulted

in sodium boiling and clad damage. The time difference between obtaining a signal from the flow sensors and the temperature sensors does not seem significant enough to give perference to flow over temperature sensors. It would appear that, for this type of accident or malfunction, fission product detectors could be of great use, particularly if the rate of development of the accident is relatively small in the beginning stages.

Another type of accident affecting initially a localized region in a subassembly is fuel-pin rupture due to a fuel-enrichment error. Here the rate of development is probably considerably higher than for the previous accident due to the presence of molten fuel in the fuel pins. Again, there appears to be only a relatively small difference between the times required for obtaining signals from flow or temperature sensors (see Table 8).

It appears from Fig. 17 that complete blockages of a single cooling subchannel do not lead to clad damage or to sodium boiling. From Figs. 17 and 18 it seems reasonable to assume that sodium boiling may occur if a minimum of four adjacent subchannels are blocked in the core region in such a way that one flow-blocked subchannel is surrounded by three flow-blocked subchannels. In that case three adjacent fuel pins would be affected over half of their heat-transfer area and three fuel pins would be affected over 1/6 of their heat-transfer area. Though localized boiling and clad damage might occur under such circumstances, it is not certain that fuel melting would take place. Only if from 9 to 12 subchannels, arranged concentrically around a single fuel pin, were to be blocked would fuel melting probably take place in the centrally located fuel pin.*

It is not easy to foresee what would happen under those circumstances. Initially boiling and fission gas release would take place. Some

*The quantitative nature of these estimates is subject to strong influence by the degree of cross flow.

local flow instability may occur (local "chugging"). Eventually, if the flow-blocked area keeps growing, fuel-coolant interactions may take place. In any case, before the fuel failure has propagated throughout the entire subassembly, reactor-trip command signals might have been generated by either flow or temperature sensors, depending on their sensitivity and the course of events.

A fuel-pin rupture due to an inadequately monitored loading error may start off with the injection of molten fuel into the coolant. In this case a substantial part of the fuel in the fuel pins of the subassembly could be molten from the beginning of the accident. Reactor-trip command signals would be generated by flow and temperature sensors prior to melting of all fuel, but obviously the amount of molten fuel could be substantially larger than that for the case of a localized flow blockage inside a subassembly.

It appears that the following conclusions may be drawn: (1) Reactor-trip channels, actuated by either flow sensors or coolant-outlet temperature sensors installed on individual subassemblies, are capable of detecting local subassembly accidents either prior to or at the time that pressures damaging to neighboring subassemblies might be generated. Also, (2) everything considered there does not appear to be any large advantage of subassembly flow sensors over subassembly coolant-outlet temperature sensors for the purpose of protection against localized core accidents (assuming each type to have equal reliability and the capability to sense the desired parameters).

The possible advantage of diversity of signals remains a separate consideration.

3. Protection Systems Based on Whole-core Sensors

General Aspects. The incentive for applying whole-core sensors, where possible, in the protection system is related, as has been pointed out previously, to the considerable reduction in the number of reactor-trip channels that such an approach would enable to be made.

The whole-core sensors that are most often considered with respect to protection against localized core accidents are the following: (a) localized boiling detectors, capable of detecting subcooled boiling in localized regions inside a subassembly, (b) pressure pulse detectors, capable of detecting pressure pulses due to the collapse of sodium bubbles in the upper part of the subassembly or in the reactor upper plenum, (c) anomalous-reactivity detectors, capable of sensing reactivity effects due to voiding of a subassembly (high sensitivity) and fuel movement (low sensitivity).

The feasibility of localized (subcooled) boiling detectors has not been proven. The main problem is that the signal-to-noise ratio is rather low, because (1) the detector would have to be installed at a relatively large distance from the source of the acoustic signal, and (2) other acoustic signals of equal or greater strength are present, e.g., due to the pumps. If feasible, localized boiling detectors will probably have to be provided with rather extensive electronic equipment for the purpose of signal processing so as to enable recognition of subcooled boiling through characteristic frequency patterns. This type of detector might be developed into a useful diagnostic tool for certain classes of accidents (in particular, flow blockages and flow starvations, affecting localized regions inside a subassembly), but it appears unlikely that it will be sufficiently dependable to be used in the reactor-trip circuitry, as then it may become the source of an intolerably high rate of spurious reactor trips.

Pressure-pulse detectors offer much greater promise as sensors capable of being used in reactor-trip circuitry because (1) they can probably be installed close enough to the source of the signal (pressure pulses due to sodium-bubble collapse in the upper subassembly sections or plenum), and (2) the signal should be well above the acoustic background noise. An estimate of the collapse of a sodium vapor bubble with an initial radius of 3 cm, subjected to 100°C subcooling at a system pressure of 1 atm, indicates a pressure generation of $\sim$ 400 atm in the bubble at the point of rebound. Calculations of the pressure distribution in the liquid for the same conditions indicate a pressure pulse of

$\sim$ 4 atm at a distance of 30 cm from the center of the bubble.[144] The energy content of the pressure pulse is relatively small, but the signal is high. Hopefully, therefore, the signal-to-noise ratio may be high enough to allow the use of fairly simple detectors (including strain-gauge pressure transducers) without the need for highly complex signal-processing equipment. A number of pressure-pulse sensors, installed with a judiciously chosen spacing in the reactor upper plenum (possibly also lower plenum, if deemed necessary), and tied into the reactor-trip circuitry, might provide a very useful reactor-protection system. Approximately five complete reactor-trip channels based on pressure pulse sensors (each with sufficient redundancy, e.g., 2-out-of-3 or 2-out-of-4) might be sufficient for a large-size LMFBR. Furthermore, since these sensors can be installed in regions of low neutron flux, the problem of aging due to neutron irradiation could probably be held within tolerable limits.

The same sensors presumably would also respond to any damaging pressures generated within the core region of a subassembly as a result of potential fuel-coolant interactions.

The third type of whole-core sensor, the anomalous-reactivity detector, aims at detecting, over a relatively short time period, any unaccounted-for change in overall reactivity. The emphasis here is on fairly rapid changes (due to voiding and/or fuel movement) in reactivity, not on an absolute reactivity balance. (Anomalies in reactivity occurring over long periods of time are also of interest, but would require additional information and more complex procedures for analysis of the data.) The limitation to relatively rapid changes in reactivity may permit the development of fairly simple equipment (possibly of analog type) for this purpose, which could be backed up (mainly for purposes of calibration) by a plant digital computer. It is important that the equipment be fairly simple so as to be able to obtain the high reliability (e.g., through redundancy) required for use in the reactor-trip circuitry.

As to the sensitivity to be sought in anomalous-reactivity detectors, it is useful to mention that sodium voiding of a single fuel subassembly has, for large LMFBRs, an overall reactivity effect ranging from -10¢ to + 10¢, whereas meltdown of a single fuel subassembly in the worst geometry could add or subtract up to about 50¢. However, much smaller reactivity changes (of either sign) are more probable, and until actual experience exists, the presence of other small, fast reactivity shifts (say due to a shift in subassembly support) cannot be ruled out as a possible complication.

Performance of Reactor-trip Channels Based on Whole-core Sensors. A protection system based on whole-core sensors of the types discussed on p. 208 probably does not protect against clad damage caused by a flow reduction affecting the total flow of a subassembly. This is simply because the use of these sensors requires the accident to have proceeded beyond the point where local boiling starts before detection is possible (i.e., when the coolant temperatures have risen locally beyond the threshold value for clad damage, unless the existence of a film of sodium on the clad prevents damaging clad temperatures).

This disadvantage of whole-core sensors with respect to flow and temperature sensors installed on individual subassemblies may not be of overriding significance, however, because (1) the safety margins inherently available in the system against this type of flow reduction are relatively large ($\sim$ 50% of nominal flow), (2) it should be possible, through proper design, to make flow reductions >50% very improbable, and (3) even with a very fast reactor-trip system, actuated by either flow or temperature sensors, installed on individual subassemblies, it may not be possible to avoid clad damage for flow reductions > $\sim$ 65% (see Table 4).

In order to evaluate the protection offered by whole-core sensors of the type discussed against flow reductions resulting in sodium boiling (i.e., flow reductions >65%, according to Table 4), the limiting case of a total sudden flow blockage of a subassembly will be examined. Table 6 gives the times for the various sensors to generate a signal.

It is seen that the pressure pulse sensor is estimated to give a signal in $\sim$ 0.85 sec as compared to $\sim$ 0.05 and $\sim$ 0.95 sec, respectively, for flow and temperature sensors. The time difference of $\sim$ 0.8 sec between flow sensors and pressure pulse sensor for generating a signal is less significant than it may appear, since cooling of the fuel remains relatively good until 0.65 sec subsequent to the occurrence of the flow blockage, when boiling initiates in the core midplane. For the case of reactor-trip by means of pressure pulse sensors, the fuel in the core midplane remains thus thermally insulated for only $\sim$ 0.2 sec prior to generation of the reactor-trip command signal, and for $\sim$ 0.45 sec prior to complete shutdown of the reactor, assuming a total reactor-trip delay time of $\sim$ 0.25 sec. Thermal insulation of the fuel in the core midplane for 0.45 sec will not lead to any fuel melting, as can be seen from Fig. 14. It may be, therefore, that for all practical purposes the outcome of this accident is about the same whether the reactor is tripped by means of flow sensors or by means of pressure pulse sensors. In both cases there will be substantial clad damage, and in both cases there should not be any fuel melting prior to reactor shutdown, thus avoiding fuel-coolant interaction (and possibly core distortion) before the safety rods have been inserted. What happens after the reactor is shut down depends on whether the flow blockage persists and on whether natural circulation of the coolant is capable of avoiding excessive fuel melting due to decay heat. This is, however, not different for the two cases.

From Table 6 and Fig. 14 it can be concluded that also an anomalous-reactivity detector of sufficiently high sensitivity (i.e., one capable of sensing reactivity effects due to sodium voiding) might have been able to generate a reactor-trip command signal sufficiently early to avoid fuel melting prior to reactor shutdown. Anomalous-reactivity detectors of low sensitivity, requiring fuel movement to occur before detection is possible, would not be capable of avoiding fuel-coolant interaction prior to reactor shutdown. Reactor-trip channels of this latter type would, however, still have merit as a means for providing diversity and a backup.

A further conclusion that can be drawn from Table 6 is that there may be, for the case of a total flow blockage of a subassembly, only a small time difference ($\sim$ 0.15 sec) between the signal generated by localized-boiling detectors and that generated by pressure pulse sensors. Thus, on the basis of this particular accident analysis, there is little incentive for developing localized-boiling detectors to the level of performance dependability that application in reactor-trip circuitry could be considered. However, for flow blockages affecting localized regions inside a subassembly, it may be that only localized-boiling detectors can provide a signal before the accident has affected a substantial part of the subassembly.

As mentioned on p. 64, an error in fuel enrichment affecting most or all of a subassembly could be detected by thermocouples installed in each subassembly before occurrence of clad damage, boiling, etc.; in contrast, whole-core sensors do not have this capability. Furthermore, partial flow blockage during power ascension should similarly be detectable by either flowmeters or thermocouples installed in individual subassemblies. These may prove to be important arguments in favor of individual subassembly monitoring, independent of decisions as to whether the sensor is used for reactor-trip, for an alarm, or to initiate a reduction in power or other operational limitation.

The following conclusions may be drawn: (1) reactor-trip channels actuated by pressure pulse sensors and high-sensitivity anomalous-reactivity detectors may be capable of adequately limiting the spread and consequences of localized core accidents; (2) reactor-trip channels actuated by pressure pulse sensors and high-sensitivity anomalous-reactivity detectors offer a lesser level of protection than do reactor-trip channels actuated by flow and temperature sensors installed on each individual subassembly; however, the significance of the difference requires further knowledge and experience in order to be evaluated.

4. Protection Systems Based on Both Whole-core Sensors and Sensors Installed on Individual Subassemblies.

General Aspects. This section examines whether a protection system based on both whole-core sensors and sensors installed on individual subassemblies would offer some advantages over the systems treated on pp. 203-212.

As was pointed out previously, there is a strong economic incentive to get away from reactor-trip channels actuated by sensors installed on each individual subassembly in favor of reactor-trip channels actuated by whole-core sensors. It will therefore be assumed that the main protection against local core accidents is to be provided by reactor-trip channels based on whole-core sensors, in particular pressure pulse sensors and anomalous-reactivity detectors. However, since coolant-outlet temperature sensors for the subassemblies are desirable and if the decision is made to install them (perhaps in view of their relative low cost and easy repairability), then one might consider using these sensors for something more than just plant surveillance. Possible additional uses of these temperature sensors are to:

1) block automatic extraction of control rods;

2) start automatic power cutback by a limited percentage of nominal power, say $\sim$ 20% (possibly equal to that required for accommodating at full power the worst possible loading error);

3) reactor-trip.

The actions of items (1) and (2) must be implemented on an individual subassembly basis to be of any use. Presumably they do not constitute a very severe intervention in the plant operation, so that a higher rate of spurious actuation can be permitted than for reactor trip. Obviously, a high frequency of spurious power cutbacks would not be acceptable, but probably this could be avoided by fairly simple means, not necessarily requiring a large redundancy of sensors.

The action of item (3) could serve as a backup for the reactor-trip channels actuated by whole-core sensors. One might then decide not to require the same level of protection from the backup reactor-trip channels as from the primary reactor-trip channels, in order to be able to maintain a relatively low number of reactor-trip channels. One could, e.g., combine the coolant-outlet temperature sensors of n subassemblies in a m-out-of-n logic for the purpose of generating a reactor-trip command signal.* In this way less redundancy (or no redundancy) is required for the temperature sensors for each subassembly. Obviously, the level of protection offered by such a systems depends on the values of m and n.

Protection Systems Against Local Core Incidents Based on a Combination of Whole-core Sensors and Subassembly Sensors. The ultimate optimum choice of protection systems to be employed against local core incidents will depend on many factors, including the actual propagative nature of subassembly anomalies, the degree to which propagation can be tolerated safely (in the sense of being able to shut the reactor down and remove decay heat, and the technology of instrument systems. At this stage of development, a variety of approaches to instrument system usage is possible. van Erp[146] has suggested as one possible choice the following system for core protection:

1) Five reactor-trip channels actuated by pressure pulse sensors, each with two-out-of-three logic.

2) Two reactor-trip channels actuated by high-sensitivity anomalous-reactivity detectors (analog type), each with two-out-of-three logic.

3) Approximately 14 reactor-trip channels, based on subassembly temperature sensors arranged in 3/19, 4/19, or 5/19 logic, and covering core regions of 19 subassemblies per scram channel, or alternatively to item (3):

---

*Babcock and Wilcox[145] suggested an approach such as this, using adjacent subassemblies. van Erp[146] has suggested a broadening of the general concept.

3a) Approximately 38 reactor-trip channels, based on subassembly temperature sensors, arranged in 3/7, 4/7, or 5/7 logic, covering core regions of seven subassemblies per channel.

The following quasi-protection subsystems are also provided:

4) Block automatic extraction of control rods on high outlet temperature for each individual subassembly (setpoint value SP_1).

5) Start automatic power cutback by X% on high outlet temperature for each individual subassembly (setpoint value $SP_2 > SP_1$; $X \sim 20\%$ of nominal power).

Furthermore, the following surveillance subsystems, with alarm functions, are provided:

6) outlet temperature sensors for each subassembly;

7) flow sensors in a limited number (say $\sim$ 10) of subassembly-positions;

8) localized-boiling detectors;

9) fission product detectors;

10) core-vibration detectors.

The usual reactor trips on bulk coolant temperature, total core neutron flux, etc., would also be employed.

Each subassembly is to be provided with from one to three outlet temperature sensors, which are to be used for the functions specified under (3), (3a), (4), (5), and (6).

The reactor-trip channels described under (3) or (3a) do not offer protection against sodium voiding or rather extensive fuel damage to a

single subassembly, if it is assumed that the outlet temperature sensors of contiguous subassemblies will only give a higher signal after these subassemblies have been affected through, e.g., mechanical distortion, melt-through, etc. They may detect a cluster of overheated subassemblies, however, and for the protection of the public health and safety, this may prove to be significant.

van Erp[146] also suggested the possibility of deliberately mixing the outlet flow of subassemblies (if practical) in a manner that thermocouples from several subassemblies would receive significant signals from a major increase in the exit coolant temperature from one.

D. Protection Against Whole-core Accidents

The problem of protection against whole-core accidents appears not to be one of developing novel types of instrumentation, or even the generation of a dependable reactor-trip signal in a timely fashion, but rather to limit, through proper design and operation of the core and cooling system, the possible rates of reactivity insertion or loss of coolant flow. In addition, there exists the need to provide reliable safety systems, considering the entire chain from sensor signal to insertion of safety rods, and to avoid, if possible, the initiation of serious transients in flow and power by the malfunctioning of control and safety systems, particularly as they relate to provisions employed to prevent thermal shock in the event of sudden reactor shutdown.

For the purpose of illustration, van Erp[146] has suggested an instrument system for protection against whole-core accidents, consisting of the following subsystems:

1) two manual reactor-trip channels;

2) three high-neutron-flux reactor-trip channels, i.e., one each for the source-range, the intermediate-range, and the power-range neutron-flux instruments. (The source-range reactor-trip channel can be manually bypassed only after having obtained a permissive signal

from the intermediate-range instruments; the intermediate-range reactor-trip channel can be manually bypassed only after having obtained a permissive signal from the power-range instruments. Both source-range and intermediate-range reactor-trip channels are automatically reinstated upon lowering of the neutron flux);

3) one low-flow reactor-trip channel for each primary coolant loop (actuated by power-to-flow ratio devices; flow measured by means of flow sensors installed on each primary coolant loop);

4) reactor-trip channels for loss of power to, or malfunction of, each primary coolant pump (actuated by, e.g., voltage sensors, wattmeters, breaker position monitors, and rate-of-change tachometers).

5) high-outlet-temperature reactor-trip channels for each primary loop (actuated by sensors on primary coolant loops; possibly with lead/lag networks to compensate for coolant transit time and sensor time constants);

6) high-ΔT reactor-trip channels for each primary loop (actuated by sensors on primary coolant loops, measured across core plus blankets; possibly with lead/lag networks to compensate for coolant transit time and sensor time constants. Items (5) and (6) could possibly be combined;

7) Reactor-trip channels to protect against loss of secondary heat sink (actuated by sensors in intermediate sodium loop and steam-generating loop);

8) seismic reactor-trip channels.

From the accident analyses presented in Chapter II, it follows that, as long as the reactor-trip system functions correctly, it should be possible to meet a performance criterion such as "whole-core accidents should not result in clad damage or fuel melting, except for some low-

probability accidents, for which some clad damage may be permissible."* For a serious loss-of-flow transient, such as that caused by a locked rotor of a primary pump on a two-loop primary coolant system, the maximum coolant temperature reached is approximately 730°C, for the case in which the reactor-trip signal is generated by a 30°C increase of the outlet temperature, without the benefit of a lead/lag network (see Fig. 22). Flow sensors, electrical voltage or power sensors, or rate-of-change pump-speed sensors should have given earlier reactor-trip signals, in which case the maximum coolant temperature would have remained still lower.

Figure 23 shows that for a reactivity transient at nominal power with insertion rate as high as 3.0 $/sec the highest coolant temperature reached is only 648°C if the reactor-trip signal is generated by high flux (120% of nominal value). A reactivity accident at nominal inlet coolant temperature, starting from a power level of 1% of nominal with a reactivity insertion rate of 1.0 $/sec and with scram on high neutron flux (120% of nominal), results in a peak value of the neutron flux of 157% of nominal and in a maximum coolant outlet temperature below the value corresponding to nominal steady-state operation (Fig. 24).

Whole-core transients are considered in this report only with a properly functioning reactor-trip system. Without such a properly functioning system, any of the transients discussed in the foregoing could develop into a major accident. Reliability of the reactor-trip is therefore of the utmost importance.

E. Concluding Remarks

Any definitive determination regarding the proper choice of instrument systems to protect LMFBR cores against local anomalies must

*These analyses assumed a "3g" acceleration of the safety rods. Further study, as well as some determination of limits on clad-damage thresholds, reactivity-insertion rates, and sensor reactor-trip settings would be required to ascertain whether the difference between an acceleration of say, 3g and 1g is important.

await the development of more information concerning the relation between instrument capability, potential and probable effects from fuel-failure propagation, core resistance to deformation, and capability for safety-rod insertion in the presence of distortion. Actual experience with various instrument systems will probably be required to adjudicate the possible conflict between the objectives of fast, reliable reactor trip and good LMFBR economics.

Some of the important considerations and questions are the following:

1) How are the relatively intangible advantages of diversity of sensors for protection against the same event to be evaluated?

2) In view of the possible problems in achieving and maintaining a very low probability of spurious reactor shutdowns from a protection system employing trip signals based on each individual subassembly, should one accept the possibility of relaxing the normally rigid protection-system requirements asked of reactor-trip channels for these instrument systems? For example, if reactor trip on a 2/3 basis from each individual subassembly is to be normally employed, can the protection-system requirements be reduced to 2/2 if a thermocouple fails between times of convenient replacement? Or, is it possible to accept operation until the next fuel-handling period with a limited number of subassemblies unprotected by thermocouples if all the thermocouples in a few subassemblies fail?

3) If the employment of multiple flowmeters in each subassembly in order to achieve a low probability of spurious reactor-trip signals proves to be impractical or prohibitively expensive, will it be possible to employ a single flowmeter and, by proper testing and interpretation of signals, distinguish between a sensor fault and a true anomaly? As in (2) above, would operation with flowmeters known to be faulty, be permissible until the next shutdown, if only a limited number of subassemblies were unprotected in this fashion?

4) Are there potentially serious adverse effects such as an excessive number of penetrations or difficulties in refueling introduced by the hundreds of leads which would accompany thermocouples and flowmeters for each subassembly?

5) Since analysis indicates that, to some extent, delay for a fraction of a second in the sensing of a local anomaly and the initiating of a reactor trip may be acceptable, are there gains to be made in instrument reliability or cost by accepting some such delay, either within the framework of similar sensors or sensors employing different approaches?

6) How important will be the detection of gas bubbles in the primary system? If important, what sensitivity is required?

7) Will possible safety questions associated with an anticipated transient involving the rapid loss of most or all primary-system coolant flow provide added incentives for any of the instrumentation intended primarily to detect local core anomalies?

8) How will the uncertainties in core design and behavior introduced by stainless steel swelling influence the need, the accessibility, and the usefulness of the various instrument systems? For example, may short- or long-term shifts in thermocouple reading result from bowing or other forms of subassembly distortion?

9) How might flow irregularities from subassembly exits influence various instrument systems?

10) How great will be the need to locate precisely and efficiently which subassembly has been subject to clad rupture during normal operation?

11) How important will be the role of computers in LMFBR safety systems? What common-mode failures could their use introduce? On the other hand, would computers enable the more ready use of possible com-

binations of signals to provide some of the bases for reactor-trip or some other form of protective action, where a single signal would be deemed to lack sufficient reliability or meaning? Some such possible combinations of signals might be the following:

a) concurrent anomalous readings or indications of local flow blockages (within a subassembly) by a flowmeter and thermocouple might lead to fast run-in of rods.

b) essentially concurrent signals of two of several sensors (subassembly exit thermocouple, exit plenum pressure, bulk boiling, local boiling). Here, two signals above their alarm settings but below their scram settings might lead to reactor trip; two signals below their alarm setting but above their normal background might lead to a fast rod run-in;

c) an increase in delayed-neutron activity above normal might trigger:

(1) a review of the recent past, and near future data from the subassembly exit thermocouples and flowmeters for anomalous behavior, with actions to be taken accordingly.

(2) A review of recent past readings on pressure-sensing or boiling detectors, with actions to be taken accordingly;

(3) A reduction in the signal requirement for alarm, rod-run-in, or reactor trip for thermocouples, pressure sensors, or boiling detectors;

(4) a normalization of base reactivity at conditions one minute before the delayed-neutron indication and a sharp reduction in the reactivity anomaly required to cause rod run-in or reactor shutdown.

APPENDIX A

Mean-square Current Reading

A number of recent reports[40-43] give excellent descriptions of the rationale of mean-square or "Campbelling" output channels, as well as performance data from several practical versions of such systems. In the adaptation of such channels to a large LMFBR plant, stronger backgrounds, and more electronic and cable noise, would have to be accommodated, whereas a shorter response time may be desirable, if not mandatory.

To provide a framework for this discussion, a statement of Campbell's theorem is indicated. Briefly, we may describe the whole counting channel circuit, including the detector, as a composite filter with several time constants which responds to an input event by delivering a current pulse

$$i(t) = i_m F(t/T), \tag{2}$$

where i_m is the peak current and T the mean duration of the current pulse. We suppose that input events occur randomly at a mean rate $\bar{n}$. When $\bar{n}T > 1$, the resulting superposition of individual pulses produces a fluctuating output current I, characterized by a probability distribution; this distribution is in turn describable in terms of its cumulants λ_k. Campbell's theorem[58-62] now asserts that

$$\lambda_k = \lim_{\bar{n}T \to \infty} \left\{ \bar{n} T i_m^k \int_0^\infty [F(t/T)]^k \, d(t/T) \right\} . \tag{3}$$

Superposition of pulses with different amplitudes as well as different shape factors results in replacing amplitude and integral in Eq. 2 by suitably weighted averages.

In a fission-chamber channel, amplitude dispersion results not only from the distribution of ionization per event, but also from the geometrical distribution of ionization tracks in the chamber; the latter

also causes some fluctuation of the shape factor, if filter time constants are comparable to the chamber collection time (including the relatively long collection time for positive ions). These dispersions have a practical effect on the fluctuations attached to a readout system which is arranged to measure the second cumulant, equal to the mean-square channel current $\overline{I^2}$ when pole-zero uncompensated circuits are used (such filters cannot pass a dc current). The readout device usually further removes high-frequency components of the mean-square signal. Overall readout fluctuations, composed of contributions due to dispersion in nT, dispersion in i_m, and dispersion in F(t/T), may thus be smoothed by choice of a large mean pulse duration T or low-readout filter-cutoff frequency -- in either case, smoothing inevitably increases the response time to a sudden increase in input rate n.

We add now some remarks concerning the main object of mean-square readout, the improvement of gamma (and noise) background discrimination. To illustrate, one may write the mean-square current due to signal rate $n_s = N_s/T$ and background rate $n_b = N_b/T$ as

$$\overline{I^2} = \left\langle i_{ms}^2 \right\rangle \left\{ N_s + \left[\left\langle i_{mb}^2 \right\rangle \Big/ \left\langle i_{ms}^2 \right\rangle \right] N_b \right\} \int F^2(x)\, dx, \qquad (4)$$

which shows that the background correction is much smaller than the relative background contribution to the dc current (which one can observe with a pole-zero compensated or other dc-coupled filter). The factor $\left\langle i_{mb}^2 \right\rangle \Big/ \left\langle i_{ms}^2 \right\rangle$ is very roughly equal to the square of the ratio of mean charges delivered in the ion chamber by Compton recoils and fission fragments, respectively, and thus depends strongly on the design of the fission chamber as well as on the incident gamma spectrum. Improvements in chamber design can in principle reduce this ratio; at the same time, the hard gamma environment of an LMFBR may make it worse (in comparison with a water-cooled reactor channel). The number $N_b = \overline{n}_b T$ includes contributions from noise pulses, especially cable noise and pickup. One of the inherent problems of mean-square readout is the relative ease with which ac signals within the accepted frequency band can contribute to the readout; such signals abound in reactor installations and must be carefully screened out.

In using a mean-square readout channel for surveillance during startup, the fluctuation problem described above is usually dealt with through a fixed filter, which delivers level and period indications at a fixed response time, with fluctuations varying inversely with power level. From the user's point of view, one would prefer an instrument which responds always as fast as possible, subject to a maximum fluctuation limit. This performance can be achieved by filter switching or continuous filter tuning. Opto-electronic devices which allow continuous variation of a light-sensitive resistance with a light-emitting diode are available; such devices might be employed in an analog feedback system to secure automatic rapid response at high input rates. A more ambitious approach, aiming at greater overall reliability and reduced maintenance requirements, would be a digital channel in which input counts as well as currents are digitized at an early stage and processed from there on. A digital period meter with count input has been described.[54] Digital processing further offers certain possibilities of on-line performance testing which also remain to be developed.

APPENDIX B

Current-pulse Operation of Fission Chambers

Fission chambers have an intrinsic efficiency roughly proportional to the fissionable coating thickness and plate area. A fission fragment emitted by the coating forms a fission track in the gas in about 2 nsec; track length at STP, in suitable gases (argon or methane) amounts to 1.5 cm, but most of the ionization is deposited in the first 0.5 cm. Thus, a chamber with 1-mm plate spacing and a gas pressure of 2-3 atm. yields of the order of 10^6 ion pairs per fission. Neglecting the deposition time and making the simplifying assumption that all the ionization is deposited halfway between plates, one finds a current pulse

$$i(t) = (Qv/d)(1 - e^{-t/RC}), \qquad t \leq d/2v$$

and (5)

$$i(t) = (Qv/d)(e^{d/2vRC} - 1)\, e^{-t/RC}, \qquad t \geq d/2v,$$

where $Q = 1.6 \times 10^{-13}$ C and v, the electron transport velocity, amounts to 2×10^7 cm/sec in methane (slightly slower for argon-methane mixtures), d is the plate spacing, and RC is the time constant of the amplifier input circuit.

Note now that conventional voltage-pulse amplification collects the current on a capacity C = amplifier input capacity + cable capacity + chamber capacity. R is kept large, and thus a voltage pulse of peak height Q/C appears at the amplifier input; d and v are relatively unimportant. In contrast, for current-pulse amplification the pulse height rises to a peak $(Qv/d)(1 - e^{-d/2vRC})$, where now R is the cable impedance, say 25 ohm, while C is the device capacitance only. It is thus evident that d must be made small in order to secure large pulses: as the pulse charge Q is compressed into a narrower time interval, pulses rise well above noise; the faster the chamber, the better the

S^2/N ratio. For available amplifiers with common-base input stage configuration and 100-200-MHz bandwidth, input noise amounts to less than 1 μA.[63] In contrast, a chamber with d = 1 mm, v = 10^7 cm/sec, and Q = 1.6×10^{-19} C delivers a nominal peak current of about 16 μA per fission, at a pulse length somewhat more than 10 nsec.[64] A conventional chamber filled with "slow" gas cannot match this noise discrimination even when bandwidth is restricted, but still allows current-pulse amplification in the input amplifier, followed by integration in a subsequent stage -- a stratagem which results in better performance than obtainable with conventional preamplifiers whenever the cable connecting the fission chamber and preamplifier is unavoidably long. This, as has been frequently pointed out, makes special efforts to locate preamplifiers as close as possible to the detector, in a relatively hostile environment, unnecessary.

Conventional fission chambers, offered by several vendors, feature 100-200-pF capacity with typical plate spacings of 3-5 mm. Filling gas is pure argon or argon with added nitrogen; sensitivities from 0.1 to 0.8 cps/nv (thermal) are offered. To achieve such a sensitivity, enriched fissionable coatings of several hundred μg/cm^2 are required, resulting in rather broad fission pulse-height distributions and corresponding plateau slopes.

In optimizing design for fast current-pulse amplification, some tradeoff between plate spacing and area is required to avoid an undue increase of the capacity when spacing is diminished; this implies a reduction of sensitivity, since coating thickness cannot be further increased without resulting in unacceptable degradation of the pulse-height spectrum. This tradeoff can, however, be compensated by designing part of the chamber as a folded transmission line with the characteristic impedance of the cable, to which it must be matched by a conical coupler. The capacity of this transmission line part is then immaterial, and only the remainder of the chamber contributes to pulse risetime and length according to Eq. 5.

High-temperature cables of appropriate impedance and required temperature stability are not available. Transmission lines operating at room temperature can be readily designed to have inherent risetimes less than 1 nsec/100 ft,[65] but the increase in resistivity of conductors at high temperatures and required radiation-resistant construction would be expected to worsen this performance by a considerable margin. Another problem may be the accommodation of temperature-dependent changes in dielectric constant versus expansion of dimensions, through which the line impedance may become mismatched.

To sum up: current-pulse operation of fission chambers is feasible with chambers of conventional design but more efficacious if a chamber of special design, which secures fast collection and thus large current-pulse amplitude, is used in conjunction with a special cable of low impedance. Such a channel can operate in pulse-counting mode at mean rates over 10^7 pulses per second, using electronics which are available off the shelf; advantages of this counting mode are stressed elsewhere. At the same time, such a channel still is compatible with current or mean-square current readout, at somewhat improved performance in comparison to conventional chambers to the extent to which mean pulse height due to gamma background can be reduced by certain design options.

APPENDIX C

Brief Description of Detection Schemes

A. Fission Gas Monitors

1. Charged Wire, Plate, or Rod

A blanket gas or sparging stream is introduced into a sampling volume with conducting walls at positive voltage with respect to a wire, plate, or rod electrode located inside this volume. Ions formed by beta decay are attracted to, and lodged on, the electrode. The latter is continuously or intermittently translated to another volume, well-shielded from the sampling volume, where it is viewed by a gamma or beta detector. This exposes the detector only to chain decay characteristic of fission products, whence the system discriminates against all other induced beta activities.

Integrating detection is achieved by stripping the activity from the wire in a small water volume; the wire is continuously cycled through sampling and detection stations. Noble gas fission products which decay in the sampling volume are thus effectively transferred to the detector. If the transport loss of gas activity is negligible, the sampling volume samples the gas blanket volumetrically, and the number of counts delivered by the detector is equal to the product (volume fraction) × (detection efficiency) × (number of active atoms expelled by cladding perforation).

2. Charged Point Counter[129]

A small beta detector is suspended in the sampling volume, accumulating ions formed by beta decay when the walls are charged to positive voltage. Discrimination is effected through the range of beta particles. Aside from decays taking place on its surface, the counter only responds

to beta particles from a surrounding volume defined by the mean beta range, much smaller than the sampling volume. A second counter at wall potential can be used for background subtraction.

3. Chromatographic Selection

Samples of the blanket gas stream are introduced to a train of surface traps with well-defined retention time, thus allowing, for example, rapid evolution of argon and relatively long retention of xenon. Xenon activities can be separated by selective valving and introduction into a shielded counting trap.

4. Gas Detachment

Any system which aims at the quantitative detection of fission gases to indicate fuel failure must assume a certain credible mechanism for gas detachment from the fuel, which involves both direct emission from the fuel surface and diffusion from deeper layers. Detailed calculations and investigations of these phenomena have been carried out in the FFTF program, and preliminary reports on findings are contained in Refs. 130-133. A second problem involves the sparging and drying efficiencies of the gas separator, together with the mean delay resulting from that equipment, particularly if samples are taken from every subassembly through a cycling valve. Some of these problems have been considered in the text, and specific mention is made in the summary concerning the need for engineering development of these hardware items.

Gas-detachment studies tend to discount rapid failure detection by some means which may be devised to detect large bubbles in the subassembly flow. At high flow velocities, gas bubbles of more than minute size are unstable; hence, even a large gas bubble emerging from a crack or pinhole would be well dispersed by the time the stream arrives at the upper grid plate, where bubble-detection equipment could be located. While bubble detection, say by acoustic imaging,

is therefore virtually ruled out, gas evolution or boiling still may result in a detectable density effect in a very sensitive flowmeter of the eddy-current type; such a signal could conceivably be detected by correlation.

5. Gas Solubility

The problem of gas solubility is clearly related to the above-mentioned problem of gas detachment, since solubility depends on bubble size. Whereas gas detachment concerns chiefly schemes based on fission gas detection, solubility also affects tagging-gas uptake. Insofar as conditions of flow and temperature vary across the core, while the structure of a cladding failure is unpredictable, indications of fuel-failure sensors are inherently nonquantitative, and inference regarding the seriousness of a failure from the observed signal strength becomes correspondingly uncertain. Improvements in that respect may, however, become available through studies of gas solubility and detachment, as well as experience with on-line failure-detection systems.

6. Gas Tagging

This scheme[134] involves the following sequence of events: subassemblies are tagged by mixing a certain isotopic mixture of xenon into the internal plenum gas of the fuel pins, which are combined in each subassembly. Upon receiving an indication of fuel failure from the blanket-gas monitor (which is based on fission product gas activity), a sample of the gas blanket is taken. By this time, this sample will include tag xenon released through the cladding failure. The subassembly containing the failed element, or elements, is indentified by mass spectroscopically comparing relative intensities of single mass-peaks. The method is thus immune from solubility and gas-transport effects, so far as differentiation between subassemblies is concerned, but encounters difficulties described above regarding discrimination between degrees of failure.

As the number of subassemblies increases, it becomes more difficult to provide clean differentiation with the available four isotopes which are not produced in fission (except, to some extent, in fission with very fast neutrons). Admixture of krypton provides two more such isotopes, which may broaden the scope of available variations and permutations sufficiently for an LMFBR core. An upper limit to the differentiation is set by both fast-neutron fission production and neutron capture depletion. In conjunction with a single mass spectrometer, a complete scan requires considerable time, especially when both xenon and krypton are used; however, an automated system could probably be designed to reduce this time considerably, if scanning-time reduction should be considered important.

B. Detection Systems Based on the Coolant

1. Gamma Detection

A small volume of coolant is viewed by a Ge(Li) detector cooled at least to room temperature and well-shielded from any external background. Let X_s and X_b be the concentrations of signal and background activities contained in the source volume; consider a single background gamma ray (assuming nonvented fuel; the background is virtually due to sodium only) which registers a peak at spectrometer channel N_b; let V_d be the detection volume, R_s the resolution for a signal gamma peak registering in channel N_s, e the detection efficiency (assumed to be uniform over the gamma spectrum), a the photopeak fraction of the detector, and t the counting time. Then one readily finds for the signal^2/background ratio S^2/B within the signal photopeak

$$S^2/B = (X_s^2/X_b)\ [a^2/(1 - a)]\ (eV_dN_b/R_sN_s)\ t.$$

Assume the following parameter values:

$$X_b = 10^6;$$
$$eV_d = 10^{-2};$$
$$a = 0.1;$$
$$N_b/N_s = 3;$$
$$R_s = 0.005.$$

Then the required concentration of the signal activity to achieve unit S^2/B in a 1-min count amounts to 500 decays/sec/cm^3 coolant; the total background count rate under these conditions is 10^4/sec. Unit S^2/B, to be sure, affords no particular discrimination against false alarms; thus, with the assumed parameter values, a specific activity of 5000/sec would be required for substantial assurance. The prospect of fission product detection is thus rather uncertain, whereas the chance of detecting a tag activity (incorporated inside the cladding or coated onto pin surfaces) would be substantially better. Since the range of suitable elements is limited by various compatibility requirements, a viable scheme of failure location could be devised by coding all fuel with the same element and using cyclic sampling. A single, fairly sophisticated gamma-ray spectrometer could then be optimized for this detection and would not impose unacceptably severe maintenance requirements on operating personnel. On the other hand, a two-tag scheme[135] offers in principle the prospect of dispensing with the coolant-sampling manifold and would require only a single, on-line coolant-bypass loop. In comparison with gas tagging, fuel tagging with a solid delivers a much faster indication, but is considerably less sensitive, owing to the coolant background; this lack of sensitivity should, however, be considered an advantage, since solid tagging will thus discriminate between a pinhole leak and an intermediate or critical failure, and may even be designed to indicate fuel disassembly if it should be possible to tag only the core of a fuel pin. The cost of fabrication of tagged fuel is at present unknown. A particularly effective location system could be based on a combination of gas and fuel tagging, or tagging and sampling;

such a system could be designed to achieve location as well as degree of failure discrimination at minimum delay, and with high reliability, in comparison to the performance of any system relying on a single scheme.

2. Delayed-neutron (DN) Detection

All the delayed-neutron precursors are halogens; 16% have half-lives less than 1 sec, 40% with 2.3 sec, 20% with 6.2 sec and 22% with about 20 sec, while the remaining 3% only have a half-life of 60 sec. The total production of DN emitters amounts to 1.5% per fission. Delayed-neutron detection for gas-bonded (oxide) fuel is a matter of detecting a small but steady increase in the neutron count rate after a fuel pin has lost a fairly large fraction of its cladding, rather than the detection of a sudden release of activity. Although the signal is thus small, it also may be expected to be fairly steady, which favors DN location by cycling of flow channels through a single detection station. Neutron detection is an inherently inefficient process; S^2/B considerations therefore require a very careful design of the coolant-transport system as well as the detection-station geometry. If we let V_d be the detection volume viewed by a bank of neutron counters embedded in moderator, V_t the total volume occupied by coolant in transit at flow rate F, and λ the decay constant, we may estimate very approximately (for ideal flow) a signal attenuation of

$$\alpha(\lambda) = (\lambda V_d/F) \exp[-\lambda V_t/F]$$

for each delayed-neutron group. In order to save at least some of the activities which decay in less than 6 sec, V_d and F must be made as large as possible, and V_t as small as possible. In a sampling loop, this calls for a powerful pump which can drive coolant through a narrow duct at high flow rate, with a widening or coil in the detection station. Widening is unfortunately limited by considerations of optimum neutron-detection geometry.

Detection of debris from ruptured fuel cans is possible with the same detection system, but requires very different electronics.[121] If retention of halogen DN precursors in the detection volume on a specific surface should be possible, this would evidently render DN detection very much more efficient. Delayed-neutron detection is inherently non-quantitative in view of the sensitivity of the signal to the detailed flow pattern.

REFERENCES

1. H. Blanc, N. Lions, and J-P Millot, "The Cabri Sodium Loop," *Proc. Int. Conf. on the Safety of Fast Reactors*, Aix-en-Provence, France, Sept. 19-22, 1967, Commissariat a l'Energie Atomique (G. Denielou, Ed.), pp. I-2-1 through I-2-14.

2. A. M. Judd, "Loss-of-coolant Accidents in a Large Sodium-cooled Fast Reactor," *Proc. Conf. Safety, Fuels, and Core Design in Large Fast Power Reactors*, Oct. 11-14, 1965, ANL-7120, pp.67-81.

3. J. F. Schumar, E. W. Barts, J. C. Carter, R. J. Dunworth, R. O. Ivins, B. M. Hoglund, and R. E. Wilson, *Fuel Element Failure Propagation Program Plan*, ANL/MET-01 (1969).

4. WASH 1110, *Liquid Metal Fast Breeder Reactor Program Plan, Vol. 10-Safety* (Aug. 1968).

5. R. W. Miller, A. Sola, and R. K. McCardell, *Report of the SPERT I Destructive Test Program on an Aluminum Plate-type Water-moderated Reactor*, IDO-16883 (1964).

6. A. F. Firstenberg, G. H. Humberstone, L. G. Neal, L. B. Wentz, and S. M. Zivi, *Kinetic Studies of Heterogeneous Water Reactions Annual Summary Report for 1966*, Space Technology Laboratory Rep. STL 372-50 (1966).

7. R. O. Brittan, "Analysis of the EBR-I Meltdown," *Proc. Second United Nations Int. Conf. on the Peaceful Uses of Atomic Energy*, Vol. 12, p. 267, Geneva (1958).

8. W. J. McCarthy, Jr. and W. H. Jens, "A Review of the Fermi Reactor Fuel Damage Incident and a Preliminary Assessment of its Significance to the Design and Operation of Sodium Cooled Fast Reactors,"*Proc. Int. Conf. Safety of Fast Reactors*, Aix-en-Provence, France, Sept. 19-22, 1967, Commissariat a l'Energie Atomique, pp.Va-1-1 through Va-1-23.

9. C. E. Dickerman and L. E. Robinson, "Fuel Meltdown Experiments in TREAT," *Proc. Int. Conf. Safety of Fast Reactors*, Aix-en-Provence, France, Sept. 19-22, 1967, Commissariat a l'Energie Atomique, pp. I-1-1 through I-1-15.

10. J. J. Barghusen, D. R. Armstrong, J. F. Boland, R. W. Mouring, and J. C. Hesson, *Fuel Failure Behavior during Transient Meltdown in a Sodium-filled Piston Autoclave*, Trans. ANS *12*, 2, 863-864 (Nov. 1969).

11. *Reactor Development Program Progress Report for November 1968*, ANL-7518, pp. 123-125.

12. *Reactor Development Program Progress Report for February 1969*, ANL-7553, pp. 113-116.

13. *Reactor Development Program Progress Report for September 1969,* ANL-7618, pp.133-134.

14. *Reactor Development Program Progress Report for October 1969,* ANL-7632, pp.131-134 and 141-142.

15. P. B. F. Evans, E. J. Burton, E. Duncombe, D. Harrison, G. O. Jackson, and N. T. C. McAffer, "Control and Instrumentation of the Prototype Fast Reactor," *Proc. London Conf. Fast Breeder Reactors,* May 17-19, 1966, pp. 765-794.

16. *Proc. Conf. Safety of Fast Reactors,* Aix-en-Provence, France, Sept. 19-22, 1967, Commissariat a l'Energie Atomique (G. Denielou, Ed.).

17. *Proc. London Conf. on Fast Breeder Reactors,* London, May 17-19, 1966, Pergamon Press (P. V. Evans, Ed.).

18. ANL-7520, *Proc. Conf. Sodium Technology and Large Fast Reactor Design,* Nov. 7-9, 1968.

19. L. M. McWethy, *An Analytical Evaluation of the Consequences of a Hypothetical Instantaneous Loss of Coolant Flow to a Fast Flux Test Facility Driver Fuel Assembly,* GEAP-10059 (July 1969).

20. GEAP-5710, *Methods, System Optimization, and Safety Studies for a 1000 MWe Sodium-cooled Fast Reactor - Task III and V Report of 1000 MWe LMFBR Follow-on Work* (Feb. 1969).

21. D. Okrent, "Design and Safety in Large Fast Power Reactors," *Atomic Energy Review,* Vol. VII, No. 2, IAEA (1969).

22. J. C. Carter, G. J. Fischer, T. J. Heames, D. R. MacFarlane, N. A. McNeal, W. T. Sha, C. K. Sanathanan, and C. K. Youngdahl, *SAS1A, A Computer Code for the Analysis of Fast-reactor Power and Flow Transients,* ANL-7607 (Oct 1970).

23. *Comparison of Two Sodium-cooled 1000 MWe Fast Reactor Concepts. Task I Report of 1000 MWe LMFBR Follow-on Work,* GEAP-5618 (June 1968).

24. *Conceptual Plant Design, System Description, and Costs for a 1000 MWe Sodium-cooled Fast Reactor. Task II Report of 1000 MWe LMFBR Follow-on Work,* GEAP-5678 (Sept. 1968).

25. *Research and Development Requirements for a 1000 MWe Sodium-cooled Fast Reactor. Task IV Report of 1000 MWe LMFBR Follow-on Work,* GEAP-5769 (April 1969).

26. M. A. Grolmes (ANL), private communication (1970).

27. J. J. Regimbal and R. E. Peterson, *Fast Reactor Protection with In-channel Instrumentation,* Trans. ANS 12, 822 (1969).

28. L. Leibowitz, L. W. Mishler, and M. G. Chasanov, *Enthalpy of Solid Uranium Dioxide from 2500°K to its Melting Point*, J. Nucl. Materials, *29*, 356-358 (1969).

29. D. Miller (ANL), private communication.

30. T. G. Theofanous, H. S. Isbin, and H. K. Fauske, *Sodium Bubble Collapse and Pressure Generation*, Trans. ANS *12*, 909-910 (1969).

31. T. G. Theofanous, L. Biasi, H. S. Isbin, and H. K. Fauske, *Nonequilibrium Bubble Collapse - A Theoretical Study*, Paper Presented at the Eleventh National Heat Transfer Conference, AIChE - ASME, Aug. 3-6, 1969. To be published in Chemical Engineering Progress, Symposium Series Heat Transfer.

32. C. E. Dickerman, *Studies on Fast Reactor Core Behavior Under Accident Conditions*, Nuclear Safety *11*, 195-205 (1970).

33. M. H. Fontana (ORNL), private communication (1969).

34. J. F. Marchaterre, R. E. Wilson, and B. M. Hoglund, *Reactor Development Program Progress Report for September 1969*, ANL-7618, pp. 126-128.

35. G. A. Forster (ANL), private communication (1969).

36. P. L. Wattelet et al., *An Appraisal of the FFTF Containment Design Basis Accident*, Draft Report, WARD-BDR-362-33.

37. *Liquid Metal Fast Breeder Reactor Program Plan, Vol. 4, Instrumentation and Control*, WASH-1104 (Aug. 1968).

38. J. F. Boland, *Nuclear Reactor Instrumentation (In-Core)*, Gordon and Breach Science Publishers, New York (1970).

39. K. G. A. Porges, *Fuel-failure Detection in LMFBR Power Plants*, ANL-7533 (Feb. 1969).

40. G. F. Popper and J. M. Harrer, *The Performance of a Counting Mean Square Voltage Channel in EBR-II*, IEEE Trans. Nucl. Sci. NS-15 (1), 22 (1968).

41. D. A. Gwinn and W. M. Trenholme, *A Log N and Period Amplifier Utilizing Statistical Fluctuation Signals from a Neutron Detector*, IEEE Trans. Nucl. Sci. NS-10 (2), 1 (1963).

42. R. A. DuBridge et al., *Reactor Control Systems Based on Counting and Campbelling Techniques*, GEAP-4900 (1965).

43. G. F. Popper, W. C. Lipinski, and J. M. Harrer, *A Wide Range Counting-Campbelling Neutron Flux Detection System*, ANL-7224 (1967).

44. D. P. Roux, *Wide-range Nuclear Channels*, Nucl. Safety *9* (6), 486 (1968).

45. P. Kovanic and K. Wagner, "Reactor Control Systems with Moving Detectors," *Proc. 3rd Intern. Conf. Peaceful Uses of Atomic Energy*, *4*, 227 (1964).

46. K. G. Porges, R. Gold, and W. C. Corwin, "Reactor Power Monitor Based on Cherenkov Radiation Detection," *Proc. IEEE Nucl. Sci. Symposium, October 1969*, IEEE Trans. Nucl. Sci. (in print).

47. J. M. Carpenter and W. K. Lehto, *A Gaseous Cherenkov Power-level Monitor*, Nucl. Appl. *3*, 750 (1967).

48. H. Weiss, "Power Measurement and Automatic Reactor Control by Gamma or Cherenkov Radiation," *Nucl. Electronics, Bombay Conference Proceedings*, Paper No. CN-22/2, p. 461 (IAEA, Vienna, 1966).

49. J. Czaika and W. Kerr, *The Use of a Gamma-sensitive Detector to Measure Thermal Reactor Power*, IEEE Trans. Nucl. Sci. NS-16 (1) (1969).

50. D. P. Roux, D. M. Fry, and J. C. Robinson, *Application of Gamma-ray Detection for Reactor Diagonsis*, ORNL-TM-2144 (1968).

51. D. P. Roux and S. H. Hanauer, *Use of Reactor Gamma Radiation as a Reactor Control and Safety Parameter*, Trans. ANS, *6*. 74 (1963).

52. K. G. Porges and J. Bjorkland, "Gain Stabilization of Analogue Amplifiers in the Nanosecond Regime," *Proceedings of the International Symposium on Nuclear Electronics, Paris, Nov. 25-27, 1963* (European Nuclear Energy Agency, 1964), pp. 811-818.

53. S. J. Rudnick, P. L. Michaud, and K. G. Porges, *Continuous Digital Ratemeter*, Nucl. Instr. Methods *71*, 196 (1969).

54. F. Staub and F. Meier, *Digitale Periodenmeter mit Selbsttatig Gewahlher Optimaler Mittellungszeit*, Neue Technik (Kerntechnik) *B/2*, 48 (1969).

55. W. M. Trenholme and D. J. Keffe, *A Neutron Flux Measuring Channel Covering Ten Decades with a Single Fixed Detector*, IEEE Trans. Nucl. Sci. NS-14 (1), 253 (1967).

56. H. A. Thomas and A. C. McBride, *Gamma Discrimination and Sensitivities of Averaging and RMS-type Detector Circuits for Campbelling Channels*, GA-8035 (1967).

57. A. J. Metz and R. H. Howard, *True Random Ratemeter with Automatic Dead-time Correction for Duty Factors up to 99%*, Rev. Sci. Instr. *40*, 16 (1969).

58. N. R. Campbell, *The Study of Discontinuous Phenomena*, Proc. Cambridge Phil. Soc., *15*, 117 (1909).

59. N. R. Campbell and V. J. Francis, *Random Fluctuations in a Cathode Ray Oscillograph*, Phil. Mag., *37*, 289 (1946).

60. N. R. Campbell and V. J. Harris, *A Theory of Valve and Circuit Noise*, J. Inst. Elec. Eng. (London), III, No. 21, 45 (Jan. 1946).

61. S. O. Rice, "Mathematical Analysis of Random Noise," reprinted from Bell System Technical Journal in *Selected Papers on Noise and Stochastic Processes*, Nelson Wax, Ed., Dover Publications, New York (1954).

62. A. Papoulis, *Probability, Random Variables and Stochastic Processes*, McGraw-Hill Publishing Co., New York (1965).

63. C. Rush, *New Technique for Designing Fast Rise Transistor Pulse Amplifiers*, Rev. Sci. Instr., *35*, 149 (1964).

64. A. DeVolpi, K. G. Porges, and C. Rush, *Subnanosecond RC Risetime from Ionization Counters*, Bull. Am. Phys. Soc., *9*, 46 (1964).

65. K. Porges, W. Corwin, L. Burkel, and E. Lewandowski, *Signal Transmission Line with Low Attenuation and Wide Frequency Passband*, Rev. Sci. Instr., *41*, 138 (1970).

66. John W. Hilborn, *Self-powered Neutron Detectors for Reactor Flux Monitoring*, Nucleonics *22* (6), 69-74 (1964).

67. M. G. Mitel'man, R. S. Erofeev, and Rozenblyum, Soviet J. Atomic Energy *10* (1) (1961).

68. E. G. Linder and P. Rappaport, Phys. Rev. *91*, 202 (1953).

69. J. W. Hilborn and C. W. Joslin, "Chalk River Experience with In-core Flux Detectors,"*Proc. Tripartite Conference on In-core Instrumentation, Harwell* (May 1965).

70. C. N. Jackson, Jr., ^{11}B *Beta Current Thermal Neutron Flux Detector*, BNWL-395 (1967).

71. W. R. Loosemore and G. Knill, "Primary Emission Neutron Activation Detectors for In-pile Neutron Flux Monitoring," *Intern. Symp. In-pile Irradiation Equipment and Techniques, Harwell* (1966).

72. W. R. Loosemore and G. Knill, "Design and Performance of Miniature Primary Emission Neutron Activation Detectors for Spatial Distribution Measurements of Neutrons in Reactors," *Radiation Measurements in Nuclear Power, Institute of Physics and Physics Society Conference*, Berkeley Nuclear Laboratories (Sept. 1966).

73. M. J. Watts, *Results from Hilborn Flux Monitors Installed on X4 Test Section*, EXP-NRX-40911, Atomic Energy of Canada Limited (1965).

74. H. J. Worsham and R. M. Ball, *Experimental Evaluation of Self-powered Neutron Flux Monitors for PWR In-core Use*, Trans. ANS *8* (2), 579 (1965).

75. *Self-powered Flux Detectors*, Reuter-Stokes, Canada Limited, Box 45, Preston, Ontario, Canadian Patent No. 765-917 (Aug. 22, 1967), U.S.A. Patent #3-375-370 (Mar. 26, 1968).

76. K. G. Porges, W. W. Managan, and W. C. Kaiser, "Spatially Continuous Neutron Flux Plotting with Spark Chambers," *Proc. Conf. on Neutron Cross Sections and Technology, March 4-7, 1968, Washington, D.C.*, NBS Special Publication 299, Vol. 1, pp.247-252.

77. G. F. Popper and A. E. Knox, *FARET In-core Instrument Development*, ANL-7161 (July 1966).

78. J. S. Hochheiser, *Liquid Metal Temperature Measurement (Sodium) State-of-Art-Study*, LMEC-MEMO-68-10 (May 1968).

79. R. L. Shepard, *Thermometry for Fast Breeder Reactors*, Reactor Fuel-Process. Technol., *12*, (2), 205-216 (Spring 1969).

80. C. E. Dickerman, R. Purviance, L. E. Robinson, W. Stephany, and F. L. Willis, *Summary and Analysis of TREAT Sodium Loop Experiments on Behavior of Single EBR-II Mark I Pins Under Accident Conditions*, Nucl. Eng. Design, *7*, 442 (1968).

81. *Reactor Development Program Progress Report for January 1970*, ANL-7661, pp. 36-37.

82. *Reactor Development Program Progress Report for March 1970*, ANL-7679, pp. 37-38.

83. S. S. Fam et al., *Ultrasonic Thermometry for LMFBR Systems--Phase I Report*, NYO-3906-4 (Sept. 1968).

84. L. C. Lynnworth et al., *Ultrasonic Thermometry for Nuclear Reactors*, IEEE Trans. Nucl. Sci., NS-16, No. 1, 177-183 (Feb. 1969).

85. G. J. Popper, D. E. Wiegand, and M. C. Glass, *Summary Review of Flow Meters Suitable for Measuring Sodium Flow at Temperatures to 1000°F in the Fast Flux Test Facility (FFTF)*, ANL-7340 (Dec. 1967).

86. R. L. Randall, *Transit Time Flowmeter Employing Noise Analysis Techniques, Part 1, Water Loop Tests*, AI-AEC-12802 (1969).

87. R. L. Randall, *Transit Time Flowmeters Employing Noise Analysis Techniques, Part 2 - 2 in. Sodium Loop Tests*, AI-AEC-12941 (Sept. 1970).

88. J. A. Shercliff, *The Theory of Electromagnetic Flow Measurement*, Cambridge University Press, London, England (1962).

89. D. E. Wiegand, *Summary of an Analysis of the Eddy-current Flowmeter*, IEEE Trans. Nucl. Sci., NS-15, No. 1, 28-36 (Feb. 1968); *The Eddy-current Flowmeter: An Analysis Giving Performance Characteristics and Preferred Operating Conditions*, ANL-7554 (Aug. 1969).

90. C. E. Dickerman, R. P. Purviance, and A. B. Cohen, *Analyses and Significance of Initial EBR-II Mark I Cluster Fast-reactor Safety Integral Loop Experiments in TREAT*, Trans. ANS *10* (2), 698 (1967).

91. M. C. Glass and G. F. Popper, *The Calibration and Stability of a 1200°F Permanent Magnet In-core Sodium Flowmeter*, IEEE Trans. Nucl. Sci., NS-15, No. 1, 37-40 (Feb. 1968).

92. G. F. Popper and M. C. Glass, *The Design and Performance of a 1200°F Magnetic Flowmeter for In-core Application in Sodium-cooled Reactors*, IEEE Trans. Nucl. Sci., NS-14, No. 1, 342-347 (Feb. 1967).

93. D. E. Wiegand and C. W. Michels, *Performance Tests on an Eddy-current Flowmeter*, IEEE Trans. Nucl. Sci., NS-16, No. 1, 192-195 (Feb. 1969).

94. H. W. Slocomb, *Liquid Metal Pressure Measurement (Sodium) State-of-the-Art Study*, LMEC-MEMO-68-7 (Mar. 1968).

95. T. J. Crocker, *FFTF Sodium Service Pressure Measurement: State-of-the-Art Report*, BNWL-882 (Dec. 1968).

96. J. F. Boland, R. D. DeForest, R. O. Ivins, F. S. Kirn, H. Lawroski, and R. C. Liimatainen, *Sensitivity of Pressure Transducers to Transient Neutron and Gamma Radiation*, Trans. ANS, *5*(1), 196 (1962).

97. L. E. Robinson, "Design of the Mark-II Integral Transient Reactor Test (TREAT) Facility Sodium Loop," *Reactor Physics Division Annual Report, July 1, 1965 to June 30, 1966*, ANL-7210, 245 (1966).

98. K. A. Dietz (Ed.), "SNAPTRAN Instrumentation Environmental Testing, Installation and Test Results," *Step Project Quarterly Technical Report, July 1965 - Sept. 1965*, IDO-17165, 28 (1966).

99. V. T. Berta, *SNAPTRAN Experimental Measurements and Instrumentation*, IDO-17205 (1967).

100. C. Michels, H. Wilson, and D. Wiegand, *A Survey and Status Report on Availability of Commercial Vibration Transducers for Immersion in High Temperature Liquid Metal as of August 1968*, to be published.

101. R. F. Saxe, *Detection of Boiling in Water-moderated Nuclear Reactors*, Nucl. Safety, 1, 452-455 (Summer 1966).

102. A. L. Colomb and F. T. Binford, *The Detection of Boiling in a Water-cooled Nuclear Reactor*, ORNL-TM-274 (1962).

103. R. F. Saxe, L. W. Lav, and W. H. Sides, Jr., "Study of Reactor Acoustical Noise," *Instrumentation and Controls Division Annual Report*, ORNL-4091, pp. 155-156 (June 1967).

104. L. C. James, *Experiments on Noise as an Aid to Reactor and Plant Operation*, Nucl. Eng., pp. 18-22 (Jan. 1965).

105. T. T. Anderson and F. H. Just, *Acoustic Boiling Detection in Fast Reactors*, presented at ASM Materials Engineering Congress Civic Center, Philadelphia, Pa. (Oct. 1969).

106. R. F. Saxe, *Considerations Regarding the Acoustical Detection of Boiling in the Presence of Cavitation*, TID-25328 (June 1969).

107. T. J. Marciniak, L. J. Habegger, and H. Greenspan, *Summary Review of Neutronic-noise Techniques for Incipient Boiling Detection in Liquid Metal Fast Breeder Reactors*, ANL-7652 (Jan. 1970).

108. C. Hartwell-Beavis, British Patent 843983 (Aug. 1960).

109. K. W. Cunningham and D. Aliaga-Kelly, British Patent 846497 (Aug. 1960).

110. G. V. Hough, British Patent 836047 (June 1960).

111. K. H. Dent and D. W. Williams, *Burst Cartridge Detection in British Gas-cooled Reactors*, Proc. Inst. M.E., Nuclear Engineering Group, *177*, No. 12, 309 (1963).

112. P. Barr and L. G. Ralfe, *Prediction of the Performance of an Electrostatic Precipitation Wire Machine Using Fission Product Data*, AERE M-593 (Dec. 1959).

113. P. Desneiges and A. Roguin, *Les Solutions Recentes Aux Problemes de Detection des Ruptures de Gaines*, Bulletin d-informations, CEA No. 61, p. 58 (May 1962).

114. A. Roguin, *La Detection des Ruptures de Gaine dans les Piles Nucleaires Refroidies Par Gaz*, CEN, Saclay, CEA R-2784 (1965).

115. J. Graftieaux and A. Roguin, "Development of Fission Product Detectors for the Detection of Burst Fuel Element Cans," *International Conference on Nuclear Electronics, Bombay (1965)*, Paper 22/13.

116. R. R. Smith and C. B. Doe, *Fission Product Monitoring in EBR-I Mark IV*, ANL-6788 (Jan. 1964).

117. W. R. Kritz, *An Automatic Gas Chromatograph for Monitoring of Reactor Fuel Failures, Mark IV Model 2 Design*, DP-668 (Jan. 1962).

118. W. R. Kritz, *Gas Chromatograph Monitors Reactor for Fuel Failures*, Nucleonics *19* (4), 106 (1961).

119. H. Saufferer, *Die Nachweisgrenze von Brennelementschäden in Wassergekühlten Reaktoren*, Kerntechnik, *4*, 453 (1962).

120. D. Okrent (ANL), private communication.

121. K. Porges, *Detection of Transients in Nuclear Surveillance Counting Channels*, ANL-7470 (Nov. 1968).

122. J. J. Lipsett and J. F. Palmer, *Locating Fuel Failures by Fission Product Deposition in CANDU-PHW Reactors*, AECL-2786 (Nov. 1967).

123. K. Porges, "Fuel Failure Detection in Sodium-cooled Reactors," *Proc. Conf. on Safety, Fuels, and Core Design of Large Fast Reactors*, ANL-7120 (Oct. 1966).

124. E. Veleckis, R. Blomquist, R. Yonco, and M. Perin, *The Solubility of Argon in Liquid Sodium*, ANL-7325 (Apr. 1967).

125. E. Veleckis and G. Redding, "Solubility of Helium in Liquid Sodium," *Chemical Engineering Division Annual Report 1969*, ANL-7675, p. 64 (Apr. 1970).

126. F. K. Dhar, *The Solubility of Krypton in Liquid Sodium*, ANL-6900 (1964), p. 125.

127. K. Thormeier, *Zur Löslichkeit von Edelgasen in Flüssigen Metallen*, KFK-964 (EUR 4171d) (Apr. 1969).

128. K. Thormeier, *Löslichkeit von Helium in Flüssigem Natrium*, Atomkernenergie, *14*, 449 (1969).

129. R. Doesch (Karlsruhe), private communication.

130. S. Jacobi, *Panel Report Detection and Location of Failed Fuel Elements*, Vienna, Nov. 13-17, 1967, IAEA (1968).

131. E. Sowa (ANL), private communication.

132. E. Sowa (ANL), private communication.

133. E. Sowa (ANL), private communication.

134. G. J. Bernstein, L. F. Coleman, E. R. Ebersole, W. J. Larson, R. R. Smith, and P. B. Henault, *Identification of Failed Fuel Elements by Xenon Tagging*, Trans. ANS *12* (1), 102 (1969).

135. R. Larsen, R. Meyer, and C. Crouthamel, *Trace Element Analytical Techniques*, ANL-7581, p. 53; ANL-7577, p. 96; ANL-7561, p. 41; ANL-7553, p. 48; ANL-7548, p. 53 (1969).

136. J. A. Buzacott, A. H. Weaving, and T. A. Wesolowski-low, *Quantitative Safety*, Trans. Soc. Instrum. Technol. 60-75 (June 1967).

137. E. R. Volk, D. M. Green, and M. L. Batch, *Design and Capabilities of the Malfunction Detector Analyzer Installed on the Enrico Fermi Fast Breeder Reactor*, APDA-LA-3 (July 1969).

138. N. J. Ackermann, *State of the Art of Subcritical Reactivity Measurements in LMFBR's*, ORNL-TM- (in preparation).

139. M. W. Ashton and P. G. Bentley, "Design Study for On-line Flow Measurement by Transit Time Analysis of Temperature Fluctuations," *Institute of Electrical Engineerings, Conference on Industrial Measurement Techniques for On-line Computers, Conference Publication No. 43*, p. 125 (1968).

140. F. Boonstoppel, B. Veltman, and F. Vergouwen, *The Measurement of Flow by Cross-correlation Techniques*, loc. cit., p. 110.

141. R. L. Randall, *Transit Time Flowmeter Employing Noise Analysis Techniques*, AI-AEC-12802 (1969).

142. C. E. Cohn, *Note on the Packaging of Analog-Digital Converters*, Rev. Sci. Instr., *40*, 532 (1969).

143. P. M. Murphy, D. B. Sherer, and A. S. Gibson, "The Effect of Using Different Safety Criteria and Selected Safety Studies for a 1000 MWe Sodium-cooled Fast Reactor," *Proc. Conf. Sodium Technology and Large Fast Reactor Design*, Nov. 7-9, 1968, ANL-7520.

144. H. Fauske (ANL), personal communication (1970).

145. *1000 MWe Follow-on Report*, Babcock and Wilcox, Vol. 3, BAW-1328 (Feb. 1969).

146. J. B. van Erp (ANL), unpublished (1970).

147. K. G. Porges and G. McGinnis, *Design of the Information Processing Unit of the FERD System of EBR-II*, IEEE Trans. Nuc. Sci. NS-13 (1), 454 (Feb. 1966).